Università degli Studi di Ferrara

PH.D. Course
in
Evolutionary Biology and Ecology

In cooperation with:
Università degli Studi di Parma
Università degli Studi di Firenze

CYCLE XXXII

COORDINATOR Prof. Guido Barbujani

INFLUENCE OF HYDROLOGY AND PRIMARY PRODUCERS ON SILICA CYCLE AND STOICHIOMETRY WITH NITROGEN AND PHOSPHORUS IN FRESHWATER ECOSYSTEMS

Scientific/Disciplinary Sector (SDS) BIO/07

Candidate
Dott. Alessandro Scibona

(signature)

Supervisor
Prof. Pierluigi Viaroli

(signature)

Co-Supervisor
Prof. Daniele Nizzoli

(signature)

Year 2016/2019

Index

1. Introduction

Silicon (Si) is one of the most abundant elements (28.8%) in Earth's crust, second only to oxygen (Wedepohl, 1995). It is present in variable amounts as Si in soils - 5 – 470 mg g^{-1} (Mckeague & Cline, 1963) - aquatic sediments - 0.5 – 800 mg g^{-1}_{DW} (DW = dry matter) (Carter & Colman, 1994; Struyf et al., 2007; Carey & Fulweiler, 2013a; Zhu et al., 2016) - and in the water column of lakes and rivers - 0.01 – 5.9 mg L^{-1} (Schelske et al., 2006; Dürr et al., 2011; Viaroli et al., 2013) - depending on hydro-geological and biological conditions and anthropogenic pressures. Si is an essential element for the growth of many primary producers like terrestrial Poaceans and aquatic siliceous algae, especially diatoms, a key component of phytoplankton and phytobenthos communities (Redfield et al., 1963; Egge & Aksnes, 1992; Schlesinger, 1997). Silicon is also widely used by humans. The anthropogenic component of the Si cycle mainly derives from diatomite mined in lacustrine deposits, or from the production of zeolites and soluble silicates (Breese, 1994; Van Dokkum et al., 2004). Silicon is one of the main components of glass, electronic devices and the most modern solar panels and its compounds can be used in industries for pulp and paper production, water and wastewater treatment, soil stabilization, pharmaceuticals and household products (e.g. zeolites in detergents) and in agriculture as a fertilizer (Sferratore et al., 2006; Dürr et al., 2011; Carey & Fulweiler, 2016). The Si cycle is also closely connected to the carbon cycle as mineral weathering of silicates is an important sink for atmospheric CO_2 (Street-Perrott & Barker, 2008).

Despite the importance of Si, its biogeochemistry in aquatic environments is still poorly understood compared to the amount of knowledge acquired on nitrogen (N) and phosphorus (P). In particular, the interaction between the biological, geological and chemical Si cycles has not received sufficient scientific attention (Struyf et al., 2009; Schoelynck & Struyf, 2016). Recent studies have shown that the knowledge about the biological control of the Si cycle is particularly scarce (Schoelynck et al., 2010; Schaller et al., 2016), limiting the capacity to explain the mechanisms regulating aquatic food webs structure and functioning (Struyf & Conley, 2012; Frings et al., 2014). The low consideration given to the Si cycle so far, compared to N and P, is probably a consequence of the high abundance of Si in nature and to the role played by N and P as limiting elements in the development of the eutrophication process in inland and coastal aquatic ecosystems.

1.1. Nutrient Limitation and Stoichiometry in Freshwater Ecosystems

Silicon is commonly available in high amount in freshwaters as dissolved silica (DSi, Schoelynck et al., 2010), therefore it is assumed not to be limiting the primary productivity. By contrast, eutrophication of aquatic ecosystems is commonly ascribed to the increase of P and N concentrations

(Bennett et al., 2001; Galloway et al., 2003). The N enrichment can trigger blooms of nitrophilous macroalgae while the P excess can stimulate the overgrowth of harmful algae. Recently, the availability of Si has also been taken in account as an essential nutrient for diatoms and as a beneficial element for aquatic macrophytes (Humborg et al., 1997; Serediak et al., 2014; Schoelynck & Struyf, 2016). The availability of DSi, both absolute and/or in relation to the other nutrients, influences how algal communities and the trophic structure of aquatic ecosystems respond to N and P loadings. Therefore Si is also a key player regulating the response of aquatic environments to altered nutrient loads (Schelske & Stoermer, 1971; Hecky & Kilham, 1988; Conley et al., 1993; Turner et al., 1998).

Today it is acknowledged that a controlling mechanism in the evolution of the eutrophication process in fresh and marine ecosystems is the unbalance in the availability of N and P compared to Si (Billen & Garnier, 2007). The current paradigm is that a balanced phytoplankton growth in marine and freshwaters can occur, respectively, at the molar ratio C:N:Si:P=106:16:16:1 (Redfield et al., 1963) and at C:N:Si:P=106:16:40:1 (Dupas et al., 2015). In general, under high N and P concentrations an increased Si load stimulates primary production, especially the growth of diatoms until DSi is depleted. Conversely, the DSi depletion limits diatom production, thus favoring non-siliceous taxa, which may become dominant. Among these taxa, dinoflagellates, coccolithophores and cyanobacteria can prevail with extended blooms. In turn, these blooms can trigger cascading effects through the food web, which cause species loss, harmful algal growth, organic matter accumulation and water deoxygenation (Officer & Ryther, 1980; Struyf et al., 2009; Carey & Fulweiler, 2013b). Despite the emerging awareness about the role of the Si, N, P "nutrient cocktail" in regulating the structure and functioning of aquatic ecosystems, little attention has been paid to the analysis of how these elements are processed together (Duarte et al., 2009; Howarth et al., 2011; Glibert, 2017; Maranger et al., 2018).

1.2. Silica Biogeochemical Cycle, the Importance of Hydrology and "Bio" Component

Si is characterized by a sedimentary biogeochemical cycle. Rivers deliver 80% of Si reaching the costal zones, acting as the main link between terrestrial and coastal ecosystems (Sommer et al., 2006; Tréguer & De La Rocha, 2013). Silicon transport to aquatic ecosystems has been considered for long time a geochemical process, mainly regulated by chemical weathering of silicate minerals and hydrology (White & Blum, 1995). More recently the Si cycle has been described as composed of continental and oceanic sub-cycles, which are connected through the hydrographic network and various reservoirs, in which biological controlling mechanisms have been identified (Frings et al., 2014).

Both terrestrial and aquatic plants are able to take up and store a considerable amount of Si in their tissues (Struyf & Conley, 2009; Frings et al., 2014; Schoelynck & Struyf, 2016). The presence of Si in primary producers covers different functions: it is an essential element for building up frustules by diatoms; it is useful for increasing resistance against wind in terrestrial plants and water drag-flow in macrophytes; it is also able to prevent the assimilation of toxic elements (as Cd^{2+}) and to protect against herbivory (Cooke et al., 2016; Schoelynck & Struyf, 2016; Coskun et al., 2019). In submerged species, Si is taken up as dissolved silicate (DSi = ortho-silicic acid) by roots from pore-water or by shoot from the water column (Broadley et al., 2012). Once transported to stems and leaves, Si is deposited as amorphous silica gel (called also biogenic silica: BSi, $SiO_2 \cdot nH_2O$) in cell walls and phytoliths. BSi deposits can be both intra and extracellular (Sangster, 1970), and the amorphous form can be found in plant cell walls, cell lumens and intracellular spaces. For these reasons, tissues of several aquatic and terrestrial plants may contain up to 10% BSi (Epstein, 1994). Moreover, in 2015 the International Plant Institute (IPNI) recognized Si as a beneficial element for plants (Coskun et al., 2019). Annual fixation of BSi by vegetation ranges between 60 – 200 Tmol yr^{-1}, the same magnitude of Si fixed by the oceanic biogeochemical cycle (240 Tmol yr^{-1}), which is equivalent to 10 – 40% of the DSi export from rivers (Conley, 2002). Therefore, the interaction of primary producers with the Si cycle regulates the DSi load to rivers and to the coastal zone and is a potentially large filter between primary mobilization of DSi from weathering and export to the oceans (Cornelis et al., 2011). A global estimation suggest that 30 – 90% of all DSi fluxes originating in terrestrial systems are linked to accumulation and recycling of BSi pools which are several orders of magnitude more susceptible to dissolution than mineral silicates (Van Cappellen, 2003; Struyf & Conley, 2012). DSi can be recycled by vegetation or released and transported, as BSi, by soil erosion and runoff to aquatic ecosystems (Sferratore et al., 2006; Billen & Garnier, 2007; Street-Perrott & Barker, 2008; Struyf et al., 2009; Struyf & Conley, 2012; Viaroli et al., 2013).

Within the hydrographic network, the DSi loading can be modulated by biologically mediated processes through the synthesis and dissolution of BSi, by interactions with the geosphere and, finally, by hydrology and land use (Struyf & Conley, 2012; Vandevenne et al., 2012). The hydrographic network comprises of a number of cascading subsystems acting as filters and reactors, which strongly regulate Si transport (Meybeck & Vörösmarty, 2005; Dürr et al., 2011). These subsystems include rivers and lentic waters, especially wetlands and lakes, which may have a major effect on Si fluxes (Harrison et al., 2009; Struyf & Conley, 2009; Bouwman et al., 2013; Verburg et al., 2013; Frings et al., 2014). In these systems, the use of silica by primary producers and the accumulation of BSi can act as a sink that regulates Si fluxes (Frings et al., 2014). The role played by primary producers in the

control of Si fluxes has been studied in different environments - like forests, wetlands and grasslands - but information about the role of vegetation in aquatic environments is still scarce (Sommer et al., 2006; Struyf & Conley, 2009; Struyf et al., 2010).

Finally, multiple pressures and impacts due to global change and local human activities are increasingly threatening aquatic ecosystems potentially interfering with nutrient biogeochemistry (Bouwman et al., 2013; Carey & Fulweiler, 2014; Datry et al., 2017b; Maranger et al., 2018). Hydrology in particular is expected to meet deep modifications. Beside changes in precipitation patterns, most water bodies are exploited as water sources to be used for human and animal consumption, irrigation and industrial activities leading to wide fluctuations in river flows and water levels in lakes (Bates et al., 2008; Skoulikidis & Amaxidis, 2009; Grill et al., 2019). The increase in water demand following human needs and societal development is often met with water diversion, construction of large dams, new reservoirs and artificial channels, and with the management of water levels in natural lakes (Grill et al., 2019). All these pressures are causing alterations and even interruption of water flow, with huge impacts on the nutrient supply to downstream waters (Maavara et al., 2015). Reservoirs are increasing noticeably (Lehner et al., 2011) and about 60% of the large river systems are affected by flow regulation for the purpose of exploiting water resources (Nilsson et al., 2005). In addition to the filter capacity of natural lakes, human damming causes an increase of sediment and nutrient retention in parallel with a decrease of water discharge.

1.3. Research Aims

The aim of this PhD research was to improve the knowledge of the Si cycle in aquatic environments and to analyze factors that regulate Si availability in a contest of climate change and increasing anthropogenic pressures. Despite its importance, Si is understudied compared to N and P in freshwater. At the same time, the knowledge of factors regulating Si biogeochemistry requires a comparison with the dynamics of other nutrients, as the ecosystem functioning depends on multiple element processes and stoichiometry. The overarching question of this research is how processes in the hydrographic network interact with the transport - in terms of quantity, availability and mobilization - of Si, N and P. The role of ecosystems as filters in continental Si transport, the role of hydrological alterations, the relative magnitude of the biologically controlled Si cycle compared to basic weathering have been identified as a focus for future research efforts (Struyf & Conley, 2012). Within this contest, three main research themes have been selected.

a) **Estimation of Si loads and fate in a subalpine meromictic lake in relation to N and P.** Lakes and reservoirs are biogeochemical reactors able to regulate the dissolved nutrient inputs, converting them in biomass or transforming them in not reactive chemical species (Ittekkot et al., 2000; Harrison et al., 2009; Verburg et al., 2013; Frings et al., 2014). These processes can greatly differ among elements according to the physico-chemical properties influencing their fate. The occurrence and persistence of thermal stratification and mixing control the in-lake biogeochemical processes and the nutrient retention (Seitzinger et al., 2006; Verburg et al., 2013; Nizzoli et al., 2018) which is expected to increase in meromictic lakes, where water overturn is missing or very infrequent. In this context of persistent water stratification, the Si retention within the water body could change affecting Si delivery and nutrients relative abundances along the hydrographic network. This is an important research theme because deep temperate lakes are undergoing less frequent water turnover, shifting toward holo-oligomictic conditions, with the possible onset of meromixis due to an increment in solutes reaching lentic waters and by the rising atmospheric temperature that cause lake warming, especially surface waters, thus strengthening thermal stratification (Salmaso et al., 2014; Jeppesen et al., 2015; Kraemer et al., 2015; Fenocchi et al., 2017, 2018; Ficker et al., 2017).

b) **Role of different communities of primary producers in littoral zone in the Si accumulation and recycling**. The littoral zone of lakes can be colonized by different communities of primary producers: for this reason, it is considered a biogeochemical hotspot, where a great primary productivity and nutrient recycling take place (Wetzel & Likens, 1991; Den Heyer & Kalff, 1998; Bruesewitz et al., 2012). The littoral zone is also heterogeneous and patchy with bare and soft sediments largely colonized by benthic microalgae, macroalgal aggregates and phanerogam meadows, and with rocky shores and hard-substrates colonized by epilithic algae. Such heterogeneity can influence the magnitude of processes driving Si dynamics and the relative amount of Si relative to N and P. Additionally, the structure and composition of littoral benthic primary producer communities are influenced by human activity and its impact on lake ecosystems, which are mainly concentrated along the shore, influencing directly and indirectly nutrient flows. However, only a few studies have examined the stoichiometry of nutrient fluxes in salt and freshwater marshes (Van Damme et al., 2009; Carey & Fulweiler, 2014), but no research has addressed DSi fluxes and BSi accumulation in the littoral zone of lakes in relation to N and P as yet.

c) **Effect of flow contraction on Si, P and N concentration and mobilization in river sediments during the summer dry period**. Changes in water flow in rivers are particularly exacerbated during the summer period when water diversion and groundwater extraction associated with low precipitation and land-use alteration, decrease water flow. Among the most relevant outcomes of flow reduction there is the increase of the riverbed area exposed to air, flow cessation with the formation of isolated pools or the complete drying of the riverbed (Stanley et al., 1997; Steward et al., 2012; Pekel et al., 2016; Datry et al., 2017a; von Schiller et al., 2017). Such changes affect the transport and retention of nutrients and their stoichiometry (Tzoraki et al., 2007; von Schiller et al., 2011; Arce et al., 2019). However, despite the increasing alteration of river hydrology and the widespread distribution of rivers that cease to flow, few studies have analyzed how these conditions influence Si dynamics in riverbed sediments and its availability in relation to N and P.

2. Silica and Nutrient Loadings and Stoichiometry in a Meromictic Lake (Lake Iseo, Italy)

2.1. Introduction

In last decades human activities have significantly modified the transport of phosphorus (P), nitrogen (N) and silica (Si) across heavily exploited watersheds (Harrison et al., 2009; Baker et al., 2014; Carey & Fulweiler, 2016). Biogeochemical cycles have been deeply altered, shifting processes which control loading formation and transformations from natural to man-managed, the latter being generated by untreated sewages, partially treated wastewaters, agricultural soil runoff and atmospheric deposition (Serediak et al., 2014; Maranger et al., 2018). Furthermore, climatic changes coupled to an altered watershed hydro-geomorphology (e.g. the development of urban areas and infrastructures, excessive crop fertilization and diffuse livestock sources, along with sewer and storm water overflows), might increase the nutrient quantity which is conveyed to aquatic environments (Strayer & Findlay, 2010; Baron et al., 2013).

Nitrogen, phosphorus and silicon are essential to primary production, especially the element which is below the minimum nutritional requirement of a given phytoplankton or vegetal species (Paerl et al., 2016). Since the first OECD report, P has been accounted as the main limiting factor to lake primary productivity (Vollenweider & Kerekes, 1982). Thereafter, also N was assessed as a limiting nutrient, especially in marine ecosystems. A much lower effort was spent for Si, although it was recognized as an essential element for key phytoplankton taxa, like diatoms. Furthermore, Si was acknowledged to play a key role also for several aquatic macrophytes species (Humborg et al., 1997; Serediak et al., 2014; Schoelynck & Struyf, 2016).

More recently, key studies highlighted how eutrophication in coastal waters is a multifactorial issue, depending on both stoichiometry and speciation of N, P and Si (Billen & Garnier, 2007; Glibert, 2017). Nutrient stoichiometry and speciation in coastal ecosystems are affected by the river runoff, which in turn undergoes wide variations and imbalances due to soil uses in the watershed and hydrology and internal processes in the river itself (Elser & Hamilton, 2007; Hillebrand et al., 2014). The P and Si loadings are composed of a relevant particulate fraction, which tends to settle, especially when the river runs at low discharge rates, or is dammed (Ittekkot et al., 2000). By contrast, nitrate is the dominant nitrogen species, which is highly soluble and reactive. Thus, an imbalance of the reactive forms of N, P and Si can occur, which shifts phytoplankton assemblages from diatom-based towards flagellates or coccolithophores dominated communities. Under these circumstances, harmful

algal blooms can take place with detrimental effects on ecosystem suitability for fishing, aquaculture and bathing (Ittekkot et al., 2000; Billen & Garnier, 2007; Seitzinger et al., 2010; Glibert, 2017).

Despite nutrient cycles have been explored individually, little attention was paid to multi-element stoichiometry, thus losing the perception of the complexity of the eutrophication surges and development (Duarte et al., 2009; Howarth et al., 2011; Glibert, 2017; Maranger et al., 2018). Maranger et al. (2018) highlight the importance of the concurrent changes of nutrients along the so-called "freshwater pipe", showing how at the interface between land and ocean, up to ~50% of the expected N and P loadings are missing. The different N and P species are transformed and retained in different ways within freshwater ecosystems. In streams and rivers a molar ratio N:P = 24:1 could indicate an elevated denitrification with N_2 loss to the atmosphere. In lakes, N:P = 62:1 is a symptom of high P sedimentation and burial, and less effective denitrification due to a longer residence time of waters. If few papers take into account N:P stoichiometry (Howarth et al., 2011; Maranger et al., 2018), even fewer consider also Si in nutrient stoichiometry (Cook et al., 2010; Viaroli et al., 2013).

Recently, the hydrographic network has been depicted as a complex system of diverse and interconnected aquatic subsystems which act as reactors and filters, not only transporting, but also transforming nutrient stocks (Meybeck & Vörösmarty, 2005). In this framework, lakes and reservoirs are biogeochemical reactors able to regulate the dissolved nutrient inputs, converting them in biomass or transforming them in not reactive species (Ittekkot et al., 2000; Harrison et al., 2009; Verburg et al., 2013; Frings et al., 2014). These processes can greatly differ among elements, due to their different physical-chemical properties, and metabolic pathways and fate. Furthermore, the element stoichiometry can greatly affect food webs and water quality (Verburg et al., 2013; Serediak et al., 2014). In lake open waters, DSi is continuously assimilated by phytoplanktonic diatoms and few other species to form biogenic silica (BSi) which settles after organism death, accumulating in bottom waters and sediments, where it is partially retained (Hobbs et al., 2010; Frings et al., 2014). Similarly, P retention is due to the assimilation by phytoplankton, along with physico-chemical processes, e.g. adsorption and co-precipitation, especially with metals (i.e. iron, aluminum and calcium), followed by sedimentation and sediment burial (Reynolds & Davies, 2001; Serediak et al., 2014). By contrast, the reactive N mainly occurs as dissolved ammonium (NH_4^+) and, especially, dissolved nitrate (NO_3^-). Both ions can be assimilated by primary producers and undergo sedimentation. Under oxygenic conditions, NH_4^+ can be also oxidized by nitrifying bacteria to NO_3^-, which is highly soluble. Under anoxic conditions, NO_3^- can be reduced via bacterial denitrification to di-nitrogen (N_2) gas, through a multistep reduction including also the formation of the greenhouse N_2O gas (Saunders & Kalff, 2001; Baron et al., 2013). Denitrification takes place mainly in the surficial sediment both in littoral areas and in deep waters (Bruesewitz et al., 2012; Nizzoli et al., 2014, 2018). Under anoxic

condition, anaerobic NH_4^+ oxidation (anammox process) and dissimilative NO_3^- reduction to NH_4^+ (DNRA) can also occurred (Nizzoli et al., 2018). To sum up, N, P and Si undergo different pathways and fate. Si and P have a predominantly sedimentary cycle and are retained in lake sediments. However, the nutrient retention within the lakes is variable and depends on water residence time, temperature, redox potential and trophic status (Seitzinger et al., 2006; Verburg et al., 2013; Nizzoli et al., 2018). The retention is expected to increase in meromictic lakes, where water overturn is missing or very infrequent.

In meromictic lakes, the persistent stratification allows the formation of a deep water layer, the so called monimolimnion, which is usually anoxic and often rich in H_2S (Zadereev et al., 2017). The persistence of deep water stratification can be enhanced by eutrophication and organic matter inputs which can increase the deep water density (Viaroli et al., 2018). In addition to environmental and morphological factors (Boehrer et al., 2017), reducing condition can establish, further amplifying the release of reduced substances and solutes into the water column (Reynolds & Davies, 2001; Siipola et al., 2016; Nizzoli et al., 2018; Viaroli et al., 2018).

To my knowledge, there are no studies on simultaneous N, P and Si cycling and stoichiometry in a meromictic lake. I had the opportunity to carry out a research on these subjects in Lake Iseo, Italy. It is a deep perialpine basin, which is persistently stratified since the early 1970s. The first complete anoxia in the deepest hypolimnion was registered in 1995 (Mosello et al., 2010). Over the last nearly fifty years, the full overturn occurred twice in late winter 2005 and 2006. Afterwards, anoxic condition established rapidly expanding upwards, from the bottom up to 100 m depth (Rogora et al., 2018).

The present study explored Si, N and P mass balances, fluxes, fate and stoichiometry in Lake Iseo over 30 months. Si, N and P loads and their composition in inlet and outlet water were estimated, as well as the molar ratio between them. In addition, mass budgets of each element were estimated in order to assess how meromixis can affect each of them. Finally, the in lake fate of Si was analyzed, always comparing Si to N and P. The hypothesis was that lake stratification could differentially regulate Si, N and P retention, due to their biogeochemical features. Namely, it has been hypothesized that sedimentary elements (Si and P) can be retained much more than N. I also hypothesized that the Si metabolized by diatoms can undergo sedimentation, thus being retained in the monimolimnion, due to the lack of complete overturn. This is a key issue, considering that, in a climate change scenario, the deep perialpine lakes may evolve towards oligomixis and further to meromixis, which is expected to greatly alter nutrient pathways and fate.

Therefore, the specific objectives of this study were: (a) to analyze the loadings and fluxes of Si, N and P under meromictic conditions; (b) to evaluate how, under these conditions, lake controls and

regulates the downstream fluxes of nutrients and their stoichiometry, thus acting as a filter in the hydrographic network.

2.2. Materials and Methods

2.2.1. Study Area

The study was carried out in the deep subalpine Lake Iseo. The lake is located on the southern slopes of the Alps in the central-eastern part of Lombardy region. Lake Iseo is the fourth lake by volume and extension among the deep subalpine lakes (Figure 1, Table 1).

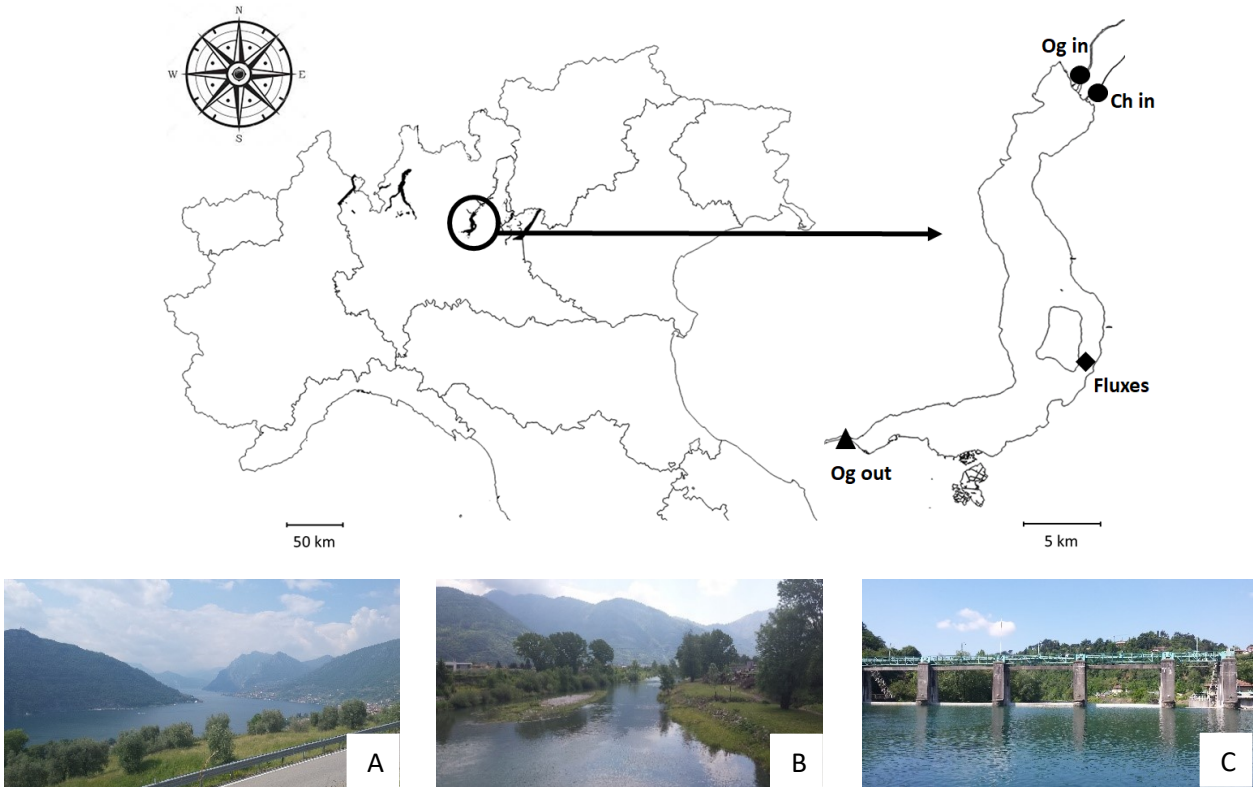

Figure 1. Location of Lake Iseo (left) and detailed map of the lake (right, photo A) showing the three sampling sites for loadings estimation. ● = Oglio inlet and Industrial Channel inlet (photo B, Oglio inlet), ▲= Oglio outlet (photo C), and ♦ = deployment of sedimentation traps and sampling point of deep sediment cores.

The watershed of Lake Iseo has an elongated shape with NE-SO orientation and a total extension of 1842 km^2: 1446 km^2 correspond to the catchment area of the Oglio River and 350 km^2 to the basin of the lake.

The average elevation of the lake watershed is 1429 m a.s.l. Sedimentary rocks mainly characterize the catchment area of the lake, with only the northernmost part presenting crystalline formations (Bini et al., 2007). The 35% of watershed lithology (Lombardy Region – Geological Map 250,000, http://www.geoportale.regione.lombardia.it/download-ricerca) is composed by siliceous formation as quartz phyllites, quartz and tonalite, granites and granodiorites, diorites rhyolites and amphibolites. Population density is 109 ind. km^{-2} and urban wastewater are treated by 50 plants, of which only five serve more than 10,000 equivalent inhabitants each. Agricultural use accounts for 22% of the watershed surface (Table 1), mainly as pastures or rough grazing (21.4%). The main crops are vineyards (11 km^2), chestnut (6 km^2) and corn (3 km^2). The livestock bulk is 418,033 units, which in term of livestock units (1 LSU = 1 adult dairy cow) accounts for 17 LSU km^{-2}. Cattle (18241 LSU), poultry (8145 LSU) and sheep (2307 LSU) are the main farmed groups (ISTAT, 2010, http://dati.istat.it/).

Table 1. Principal watershed features and Lake Iseo main characteristics.

Watershed	
Area, lake included (km^2)	1842
Mean altitude (m a.s.l.)	1429
Siliceous lithological formations*	35%
Agricultural total surface (km^2)	403
Total population (n° ind.)	195914
Lake	
Altitude (m a.s.l.)	185
Volume (km^3)	7.6
Maximum depth (m)	258
Average depth (m)	123
Total Area (km^2)	60.9
Littoral Area (km^2)	5.0
Theoretical renewal time (years)	4.5

* The percentage are referred to quartz phyllites, quartz and tonalite, granites and granodiorites, diorites rhyolites and amphibolites formations and to surficial area (km^2).

Lake Iseo is meromictic since the early 1970s, although complete overturn occurred in 2005 and 2006. The lake is classified as mesoeutrophic due to meromixis and the influence of anthropic activities in the watershed (Salmaso et al., 2018). The oxygen depletion and P accumulation are expanding upwards (Rogora et al., 2018): currently, the water mass is completely anoxic from 100 m depth to the bottom (258 m).

The total water inflow is 4.1 x 10^6 m^3 d^{-1}. The Oglio river is the main natural tributary, which contributes more than 48% of water inflow (Figure 1). The Industrial Channel has a similar discharge and accounts for 50% of the total water inflow. Other minor natural tributaries, like Bagnadore, Borlezza and Rino torrents, represent <2% of the water inflow.

Lake Iseo is man-regulated by a top releasing dam located at Sarnico, at the lake outlet. The dam was built in 1933 and is currently managed by the Oglio Consortium, which regulates the surface water outflow in order to supply water for irrigation and hydroelectric power production and to control the flooding risk. On average the outflow is 3.0 x 10^6 m^3 d^{-1}.

Lake Iseo, like the other southern-alpine lakes, has an elongated shape from North to South (25 km in length), steep banks and a flat bottom in cryptodepression, all characteristics referring to the glacial origin (Ambrosetti et al., 1992). The west shore is steep and rocky, while the eastern side is steep in the northern part but becomes progressively flat towards the south. The surface area of the littoral zone corresponding to the photic layer, between 0 and 10 m depth, is ~5 km^2, i.e. 8.2% of the total lake surface area. The Secchi disk never exceeds 4.5 m depth, limiting the macrophyte growth to about 9 – 10 m depth (Bolpagni et al., 2017). I focused the activities in the depth range 0 – 10 m (see Chapter 3).

2.2.2. Monitoring Inlet and Outlet Nutrient Concentration and Load Estimation

The survey lasted from May 2016 to October 2018. Monthly samplings were conducted on 30 dates at three sites: the Oglio River and the Industrial Channel at the inlet, and the outlet near the Sarnico dam. To take into account the impact of flow variability on water chemistry, the sampling activity was intensified during high flow events on 7 dates. For each sampling date and station, three replicate water samples were collected with a Ruttner bottle and stored in 2 L polyethylene bottles. Samples were filtered (Wathman GF/F) and stored in polyethylene vials: once in the laboratory, samples were stored at 4 °C and analyzed within 24 h to measure dissolved silica (DSi), soluble reactive phosphorus (SRP), ammonium ($N\text{-}NH_4^+$) and nitrate + nitrite ($N\text{-}NO_x$). Finally, the total inorganic nitrogen (DIN) was calculated as DIN = $N\text{-}NH_4^+$ + $N\text{-}NO_x$. Unfiltered samples were analyzed within 48 h for total phosphorus (TP) and nitrogen (TN).

An aliquot of each replicate was filtered on pre-weighed filters (Wathman GF/F, Ø 25 mm, 0.7 μm) for the determination of total particulate phosphorus (PP) and nitrogen (PN). The filters were then placed in an oven at 70 °C for 24h and weighed for determining suspended particulate matter (SPM). A second aliquot of water of each replicate was filtered on polycarbonate (Wathman Nucleopore, Ø 47 mm, 0.4 μm) and frozen for the determination of biogenic silica (BSi). A third water aliquot of each replicate was filtered on Wathman GF/F and the filter was frozen for the determination of chlorophyll-a (Chl-a). The total silica (TSi) was estimated as DSi + BSi.

The annual nutrients and pools loadings from the lake inlets and outlet were calculated as the product of the discharge weighted mean concentration by the mean annual discharge of the 3 years (Quilbé et al., 2006) as follows (1):

$$L = k \frac{\sum_{i=1}^{n} C_i Q_i}{\sum_{i=1}^{n} Q_i} Q_m \qquad (1)$$

where L is the annual loading (t y^{-1}), C_i is the concentration at day i (mg m^{-3}), Q_i is the mean daily discharge at day i (m^3 s^{-1}), Q_m is the mean annual discharge (m^3 s^{-1}) of the three years and k is the factor (31.53 x 10^6) to calculate L on the annual basis.

Si, N and P retention (R, %) in lake was estimated for the three years as (2):

$$R = \frac{L_{in} - L_{out}}{L_{in}} * 100 \qquad (2)$$

where L_{in} is the average Si, N or P loads of the three years (t y^{-1}) estimated with formula (1) in inlet water and L_{out} is the average Si, N or P estimated with formula (1) in outlet waters.

The Iseo Consortium and the Regional Agency for Environmental Protection (ARPA) of Lombardy Region provided the daily average water inflows and outflows, while Paravisio hydro-electrical company provided the discharge of the Industrial Channel. The difference between total discharge and Industrial Channel discharge was accounted as the Oglio River discharge.

Atmospheric N inputs (N_{Dep}) were estimated from wet and dry deposition data of reactive N (N_r) from the Cooperative Programme for Monitoring and Evaluation of the Long-range Transmission of Air Pollutants in Europe (EMEP 2010, http://www.emep.int/). In the Lake Iseo area such N_{Dep} is 9.5 kg N ha^{-1} y^{-1}.

2.2.3. Sediment Traps

In order to quantify sedimentation rates, two multi-trap systems (Hydro-Bios Ltd., Kiel, Germany) were moored to collect total suspended solids at two depths: below the epilimnion (20 m) and near the hypolimnion-monimolimnion interface at 90 m depth (Figure 1). Each trap was equipped with 24 collecting bottles and two cylinders (154 cm^2) for duplicate sampling. The bottle content was preserved with pre-added formalin to prevent decomposition of settled material. The trap was positioned from 8 April 2016 to 5 April 2017 and the time interval of sampling was 31 days. Upon recovery, the bottle content was concentrated and freeze-dried prior the determination of the dry mass by weighing. After removal, samples were immediately brought to the laboratory, stored at 4°C in the dark and processed within two weeks. The trapped material was concentrated in 20 ml vials and dried at 105 °C and then weighted to determine total mass of sedimented suspended solids. BSi, total N and P were estimated on dry material.

The flux rates of sedimentation (expressed as mg m^{-2} d^{-1}) were calculated by multiplying the areal dry mass flux rate times the nutrient content in settled material for each time interval.

2.2.4. Water Column Profiles

The chemical data of water column profile were provided by the Regional Agency for Environmental Protection of the Lombardy Region (ARPA Lombardy), for the period 2001-2017. The following variables were selected: Chl-a, N-NO_x, N-NH_4^+, TN, SRP and TP, all reported as µg L^{-1}; DSi (mg Si L^{-1}) was measured only from 2009 to 2017. The total inorganic nitrogen (DIN) was calculated as DIN = N-NH_4^+ + N-NO_x. The sampling effort of the entire water column (0-258 m) ranged from four (one per season) from 2001 to 2011 to twelve (one per month) from 2012 to 2017.

2.2.5. Benthic Fluxes of Deeper Sediment

Six sediment cores were sampled on 26 October 2018 at 258 m depth in order to analyze the chemical and physical characteristics of the deep surface sediment. The cores were collected with an electronic winch linked to a Plexiglas tube (inner diameter 5 cm, height 30 cm). Once collected, the cores were immediately submerged in anoxic water retrieved at the same depth and closed with a rubber stopper in order to minimize the exposure to atmospheric oxygen, then, they were transported to the laboratory at the University of Parma within 4 hours. Once in the laboratory, sediment cores were housed in a thermostatic room, submerged in an incubation tank (75 L) containing water from

the monimolimnion. The incubation was carried at the same ambient temperature (±1 °C). Anoxia in the tank was assured by covering the incubation tank with a plastic bag and by bubbling the water with N_2. Cores were left to stabilize overnight (~12 hours). The day after sampling, the cores were incubated under dark conditions, mimicking the ambient light of the deep monimolimnion. The incubation lasted 72 h. Water subsamples were withdrawn from each core at the incubation start and after 24, 38 and 72 hours. During maintenance and incubation, the water inside the cores was gently stirred, avoiding sediment resuspension, using magnetic stirrers suspended within each core and driven with a magnet rotated at 40 rpm by an external motor. To begin the incubation, the water level in the tank was lowered below the core edges and the upper opening of the cores was closed with a floating Plexiglas lid. Water samples were collected through a valve in the lid with plastic syringes and filtered through Whatman GF/F glass fiber filters. To determine DSi, $N\text{-}NO_x$ and $N\text{-}NH_4^+$ samples were stored in polyethylene vials, while to measure SRP glass tubes were used. Samples were stored at 4 °C and analyzed within 24 hours. Hourly fluxes of nutrients (mg m^{-2} h^{-1}) were calculated after linear regression of concentration versus incubation time and multiplied by 24 h to obtain daily fluxes (mg m^{-2} d^{-1}).

2.2.6. Analytical Methods

$N\text{-}NH_4^+$ (Koroleff, 1970), $N\text{-}NO_x$ (APHA, 1998), SRP (Valderrama, 1981) and DSi (Golterman et al., 1978) were determined with standard spectrophotometric methods (Perkin Elmer, Lambda 35). An analytical blank that underwent the same procedure as the samples, including filtration, was always analyzed to correct for sample contamination.

The suspended particulate matter was determined by filtration with GF/F filters. Filters were oven-dried at 70 °C for 24h. The dried filters were weighed immediately after being removed from the oven and cooled in a desiccator. Thereafter, they were analyzed to quantify particulate N and P following an alkaline digestion (Maher et al., 2002). Unfiltered samples were processed with the same digestion to determine total N and P. The total dissolved N and P were obtained as the difference between the total and particulate pool of N and P.

The total BSi content of suspended particulate matter and in samples from sedimentation traps was analyzed following DeMaster (1981): 30 mg of dry sediment were digested with 30 ml of 0.1 M Na_2CO_3 in polypropylene bottles for 5 h at 85 °C. Subsamples were collected after 3, 4 and 5 h and analyzed for DSi with the molybdate blue spectrophotometric method (Golterman et al., 1978). Before the analysis, each sample (1 ml of extraction solution) was neutralized with 9 mL of HCl 0.021 M. To correct for the amount of Si resulting from mineral dissolution, the Si content of the

subsamples was plotted against dissolution time. The y-axis intercept of the linear regression line represents the estimated BSi content. All BSi dissolved within the first 3 hours.

On SPM, Chl-a was determined spectrophotometrically according to Lorenzen (1967), after extraction with 10 mL 90% water-acetone. Total N and P content in samples of sedimentation traps were determined at the Leibnitz-Institute of Freshwater Ecology and Inland Fisheries: N was determined using a CHN elemental analyzer (CHNS-O EA 1108 Carlo Erba), while P was determined following Aspila et al. (1976).

2.2.7. Statistical Analysis

Nutrient concentrations data were analyzed with ANOVA to assess difference among sites (inlet and outlet) and season (vegetative and non-vegetative). The relation of nutrient concentrations with the discharges in two sampling sites (inlet and outlet) were further investigated using the Pearson correlation coefficient. Finally, individual regressions were run between the DSi, SRP and DIN concentrations in monimolimnion and the time (year). The slopes of the regressions and the correlation coefficients were used to estimate the annual accumulation (t y^{-1}) of nutrients in the deeper layer of the lake. Statistical analyses were run with the R software v. 3.6.0 (The R Core Team, 2019).

All results in text, figures and tables are presented as mean ± standard error.

2.3. Results

2.3.1. Nutrient Loading to and Nutrient Export from Lake Iseo: Concentrations, Budgets and Stoichiometry

The temporal variations of total, dissolved reactive and particulate forms of Si, P and N, along with water discharge, are reported in Figure 2, Figure 3 and Figure 4, respectively. First of all, discharge rates were greatly variables in the Oglio river tributary, which is under the runoff influence, while they were smoothed in the Industrial Channel, due to the management of the hydroelectric power plant. Also in the lakes outflow, the water discharge was man-regulated, undergoing higher flows in summer, when the water demand was high, and lower flows in late winter when water was accumulated in the lake.

In the Oglio river tributary, TSi was for the most part accounted by DSi, while BSi was on average much lower. However, BSi peaks were detected during flood events at high discharge rates. In the Industrial Channel the TSi and DSi trends nearly coincided, while the BSi pattern differed from

that of the Oglio river tributary, likely due to the different water flow and damming of the channel. On average, in the water outflowing from the lake TSi and DSi concentrations almost coincided, TSi being made for the most part by DSi. Both TSi and DSi followed a seasonal trend, with minimum values in spring-summer, likely due to the lake metabolism.

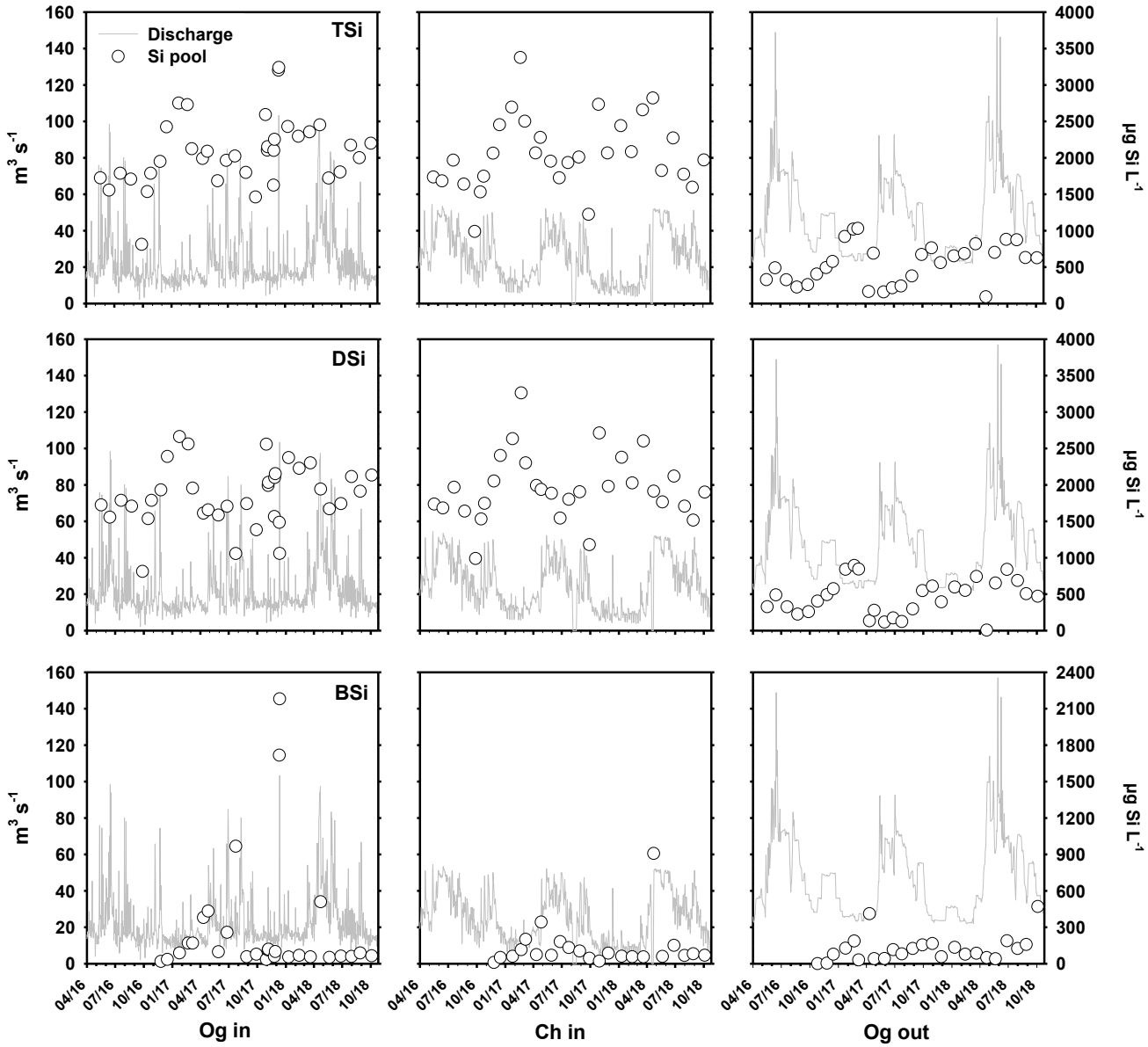

Figure 2. Temporal variations of total (TSi), dissolved (DSi) and particulate biogenic (BSi) silicon concentrations in the inlet and outlet waters of Lake Iseo. Og in = Oglio inlet, Ch in = Industrial Channel inlet, Og out = Oglio river outlet. The water discharge is reported in background.

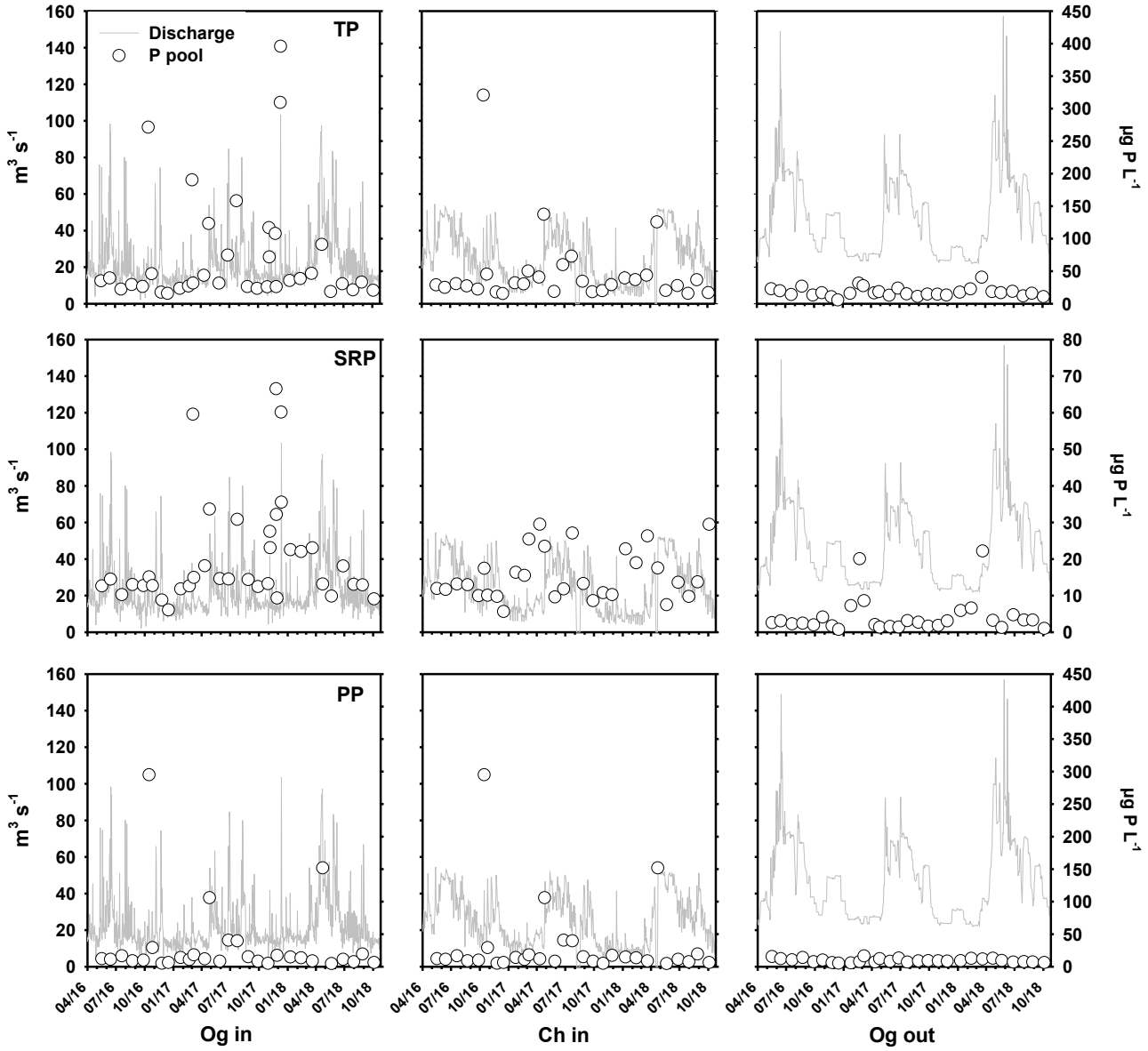

Figure 3. Temporal variations of total (TP), soluble reactive (SRP) and particulate (PP) phosphorus concentrations in the inlet and outlet waters of Lake Iseo. Og in = Oglio inlet, Ch in = Industrial Channel inlet, Og out = Oglio river outlet. The water discharge is reported in background.

In the Oglio river tributary, the TP variability was affected mainly by river discharge: peaks up to 350 µg P L^{-1} were attained during high flow episodes, when also PP attained values up to 250 – 350 µg P L^{-1}. Concurrently, also SRP increased, but at a lower extent, never exceeding 70 µg P L^{-1}. In the Industrial channel, except one date, TP concentrations were lower (<150 µg P L^{-1}) and peaks were attained during high flow periods, coinciding also with the highest PP values, while SRP concentrations oscillated below 30 µg P L^{-1}. In the lake outflow, TP and SRP

were on average <50 μg P L^{-1}, with some seasonality, while PP was retained and close to the detection limit.

Only slight differences were found for TN concentrations among tributaries and emissary, with a weak relationship, i.e. Oglio inlet > Channel inlet > Oglio outlet. This pattern is more evident for DIN, which also underwent some seasonality, depending on water management. Finally, PN concentrations attained some peaks in the Oglio tributary, while they were almost persistently low in both Industrial Channel and Oglio emissary.

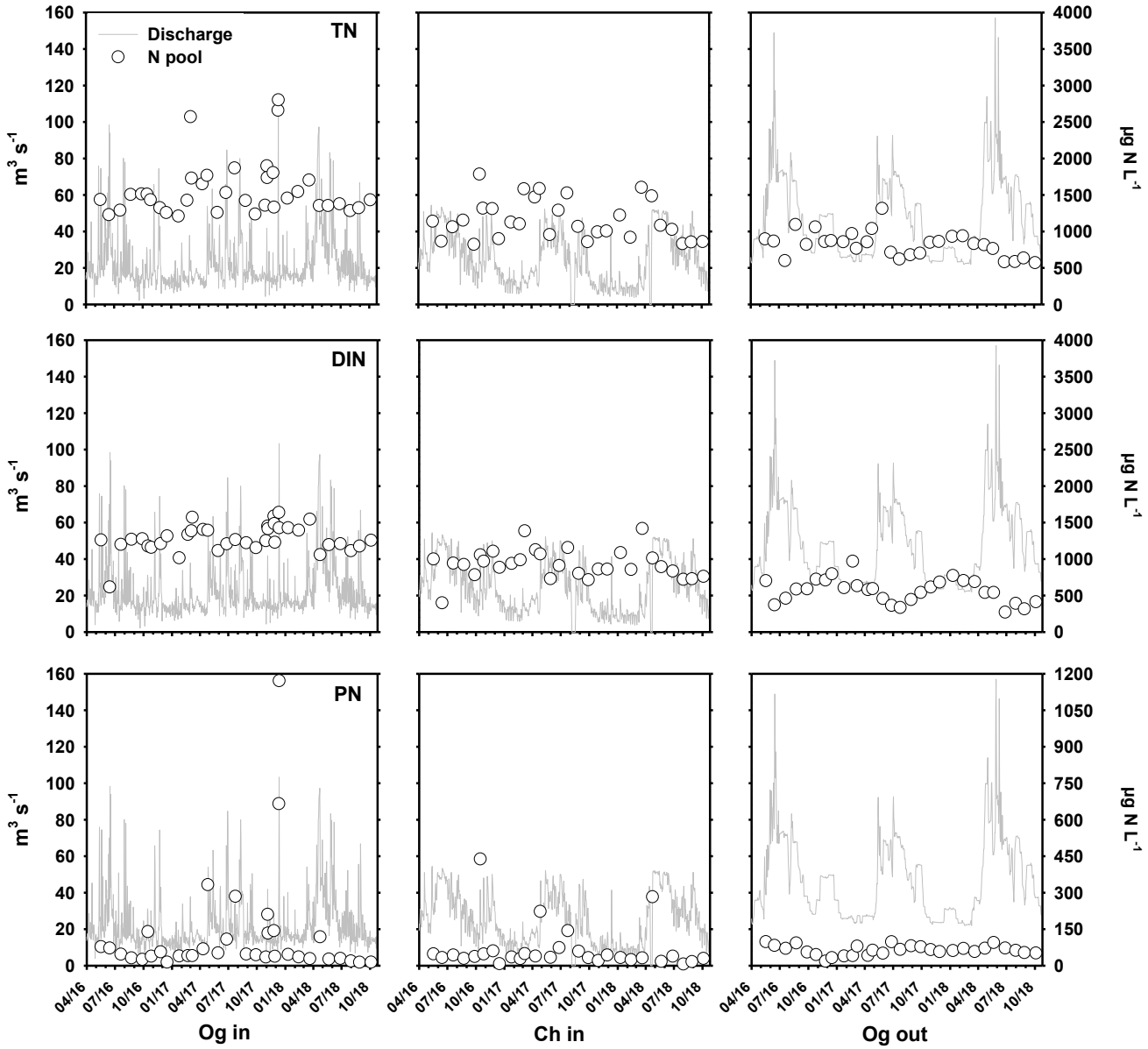

Figure 4. Temporal variations of total (TN), dissolved reactive (DIN) and particulate (PN) phosphorus concentrations in the inlet and outlet waters of Lake Iseo. Og in = Oglio inlet, Ch in = Industrial Channel inlet, Og out = Oglio river outlet. The water discharge is reported in background.

On average, all nutrient concentrations resulted significantly lower in outlet than in inlet waters (ANOVA, $p < 0.001$). DSi decreased from 1899 ± 91 to 462 ± 30 µg Si L^{-1}, DIN diminished from 1126 ± 70 to 567 ± 44 µg N L^{-1} and SRP decreased from 18 ± 5 to 4 ± 2 µg P L^{-1}.

The mean annual loadings of all nutrients resulted lower in outlet than in inlet waters. From inlet to outlet, TSi decreased from 3044 ± 303 t Si y^{-1} to 641 ± 164 t Si y^{-1} (Figure 5), which was equivalent to a 75% Si retention within the lake. DSi and BSi were retained in a similar way - respectively 76% and 75% - but DSi composed the 86% of TSi in both inlet and outlet waters. Total P had a similar behavior to Si, passing from 126 ± 22 t P y^{-1} in the inlet to 26 ± 3 t P y^{-1} in the outlet (Figure 5), with a 79% retention within the lake. SRP (80%) and PP (84%) were similarly retained. In the inlet waters, PP accounted for 73% of TP, whilst its contribution decreased to 56% in the outlet waters. A much lower retention was observed for TN loadings, which decreased from 2117 ± 139 t N y^{-1} (inlet) to 1197 ± 71 t N y^{-1} (outlet) (Figure 5), accounting for only a 45% retention within the lake. Over the whole period considered in this study, DIN was the main N pool in both inflow and outflow, of which more than 90% was accounted by N-NO_x. The contribution and changes of N-NH_4^+ were almost negligible, compared to N-NO_x.

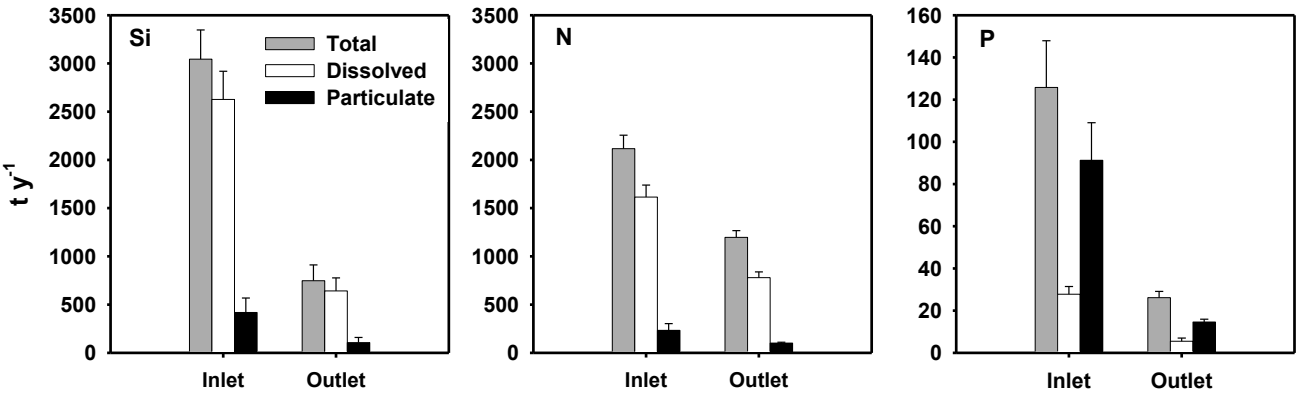

Figure 5. Dissolved silica (DSi), biogenic silica (BSi), total silica (TSi), dissolved inorganic nitrogen (DIN), particulate nitrogen (PN), total nitrogen (TN), soluble reactive phosphorus (SRP), particulate phosphorus (PP) and total phosphorus (TP) loads in the inlet and outlet water. Values calculated as integrated loads of the three years (2016 – 2018). Error bars represent standard error.

The year was partitioned into two periods based on phytoplankton productivity: a vegetative period from April to September (spring and summer), and a non-vegetative one from October to March (autumn and winter). Differences between the two periods were statistically significant only for DSi and DIN concentrations ($p < 0.05$), but only in outlet waters, due to lake metabolism (Figure 6).

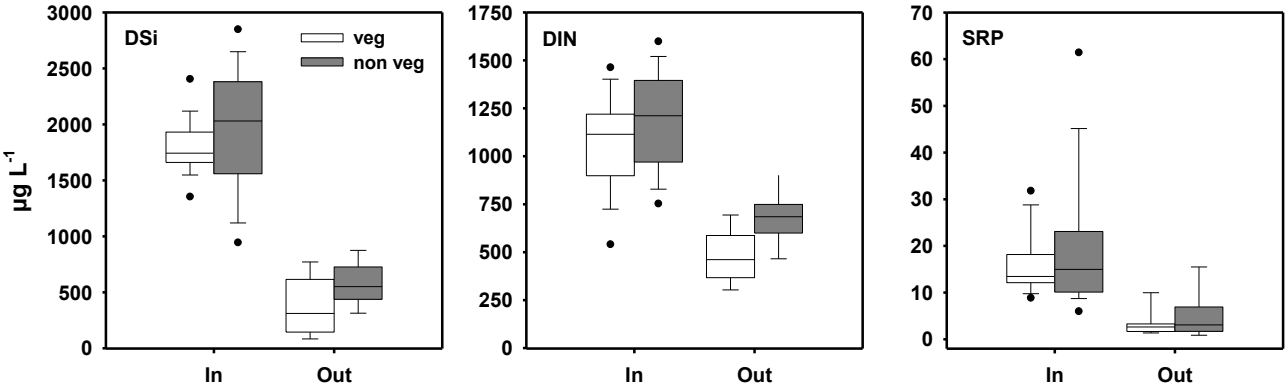

Figure 6. Dissolved silica (DSi), dissolved inorganic nitrogen (DIN) and soluble reactive phosphorus (SRP) concentrations in the inlet and outlet water during vegetative (April – September) and non-vegetative (October – March) periods.

Relationships between water discharge and nutrient concentration were tentatively assessed in both inlet and outlet. The Pearson correlation resulted statistically significant for DIN ($r = 0.50$, $p < 0.01$) and DSi ($r = 0.59$, $p < 0.01$), which were negatively correlated to the discharge in both inflow and outflow (Figure 7). Particulate pools of all nutrients were positively correlated to discharge only in inlets (BSi $r = 0.69$; PN $r = 0.67$; PP $r = 0.61$; $p < 0.001$ for all).

The nutrient retention within the lake influenced the nutrient stoichiometry, which differed between inflowing and outflowing waters. The N:Si ratio increased from 1.36 ± 0.06 in the inlet to 4.57 ± 0.77 in outlet (Figure 8a). This increase was due to both particulate and reactive N and Si species: DIN:DSi increased from 1.25 ± 0.06 in the inlet to 3.11 ± 0.36 in the outlet (Figure 8b), as well as PN:BSi increased from 1.41 ± 0.26 to 2.30 ± 0.70 (Figure 8c). The same pattern was observed for the P:Si ratio which increased from 0.026 ± 0.004 in the inflow to 0.043 ± 0.007 in the lake outflow (Figure 8a). In addition, the P:Si ratio significantly ($p < 0.05$) decreased between vegetative (0.058 ± 0.011) and non-vegetative (0.024 ± 0.003) period in outlet water (Figure 8a). The average value of PP:BSi resulted more than one order of magnitude higher (0.17 ± 0.02) than SRP:DSi (0.009 ± 0.001) in inlet and outlet water (Figure 8b, 8c). During high flow events, especially in autumn and winter, the PP:BSi molar ratio increased up to 0.20 (±0.03), while the lower PP:BSi value (0.13 ± 0.02) was detected during the vegetative period, only in the outlet water (Figure 8c). The molar N:P ratio was lower in inlet (84 ± 5) compared to outlet (116 ± 10) (Figure 8a). Similarly, DIN:SRP and PN:PP were lower in inlet (169 ± 10 and 7.0 ± 0.4 respectively), than in outlet (528 ± 81 and 15.0 ± 0.7, respectively) (Figure 8b, 8c).

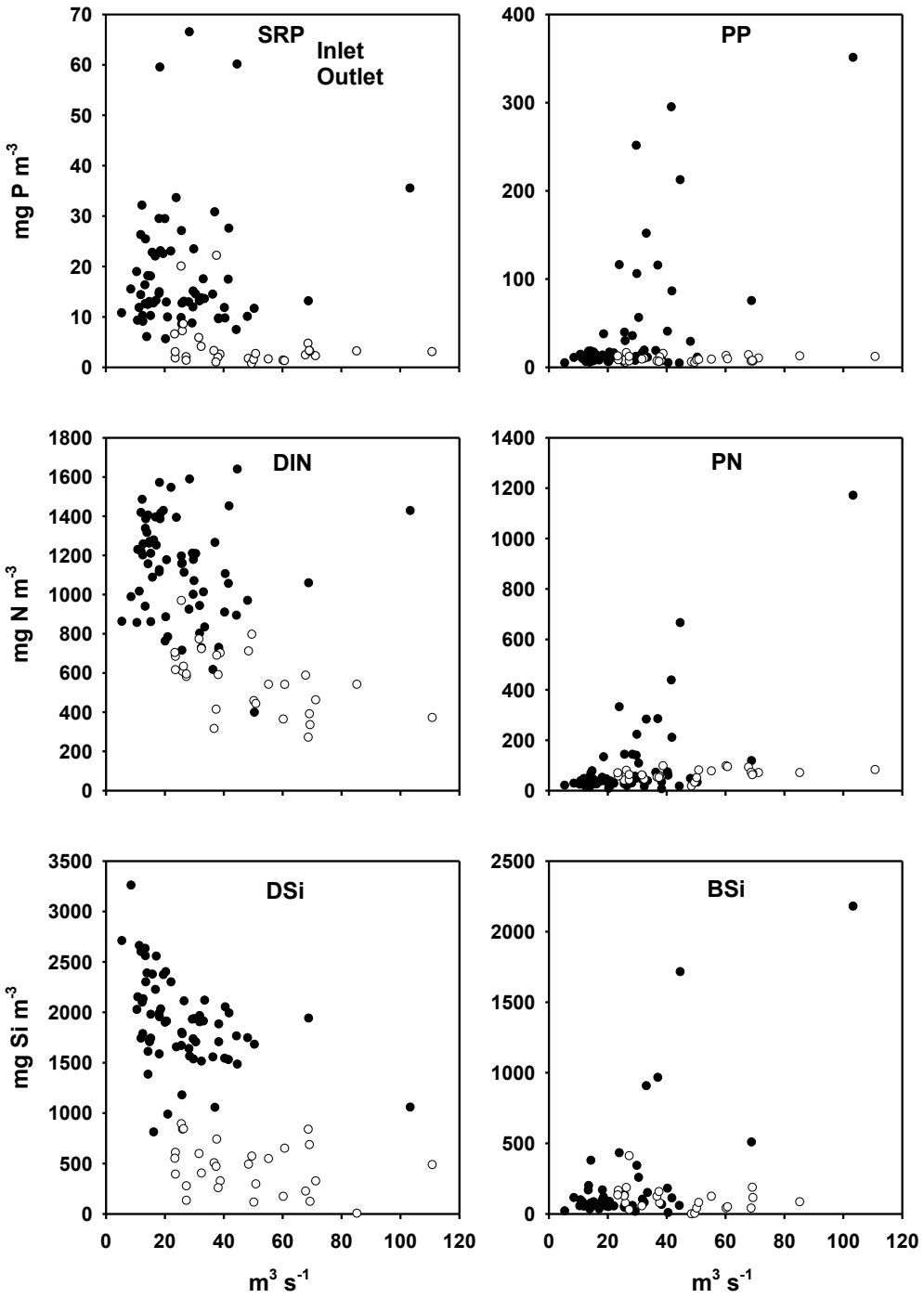

Figure 7. Soluble reactive phosphorus (SRP), particulate phosphorus (PP), dissolved inorganic nitrogen (DIN), particulate nitrogen (PN), dissolved silica (DSi) and biogenic silica (BSi) in inlets (black dots) and outlet (open circles) waters during the monitoring period (May 2016 – October 2018).

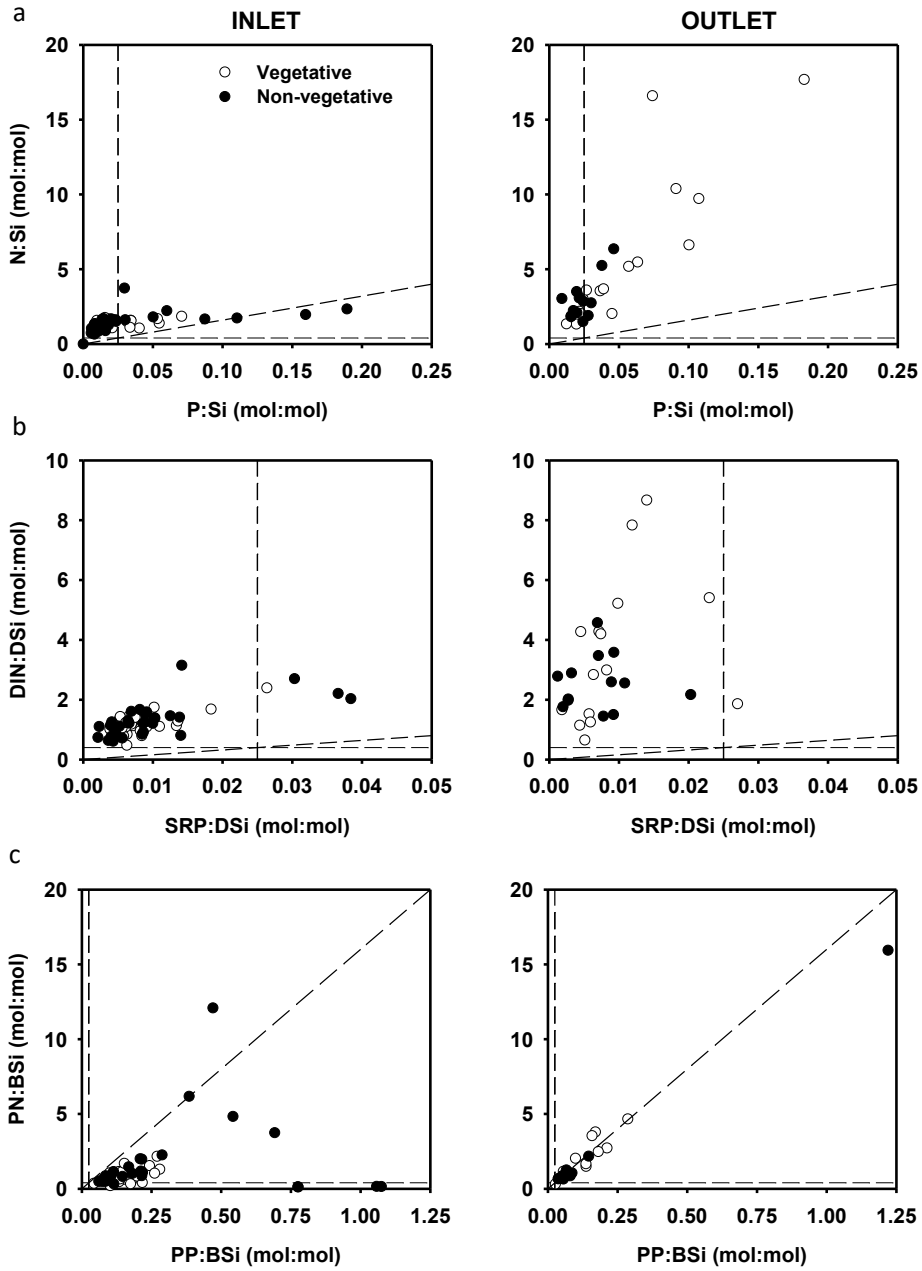

Figure 8. N:Si and P:Si molar ratio in inlet (left panel) and outlet (right panel) during vegetative (open circles) and non-vegetative (black dots) in the period May 2016 – October 2018 for total (a), dissolved (b) and particulate (c) pools. Dashed lines represent the balanced ratios for phytoplankton growth in freshwater (Dupas et al., 2015): N:Si = 0.40, P:Si = 0.025 and N:P = 16.

2.3.2. In Lake Processes and Budgets

Since 2006, Lake Iseo has been persistently stratified, with a stable monimolimnion. Both particulate and dissolved nutrients are affected by this lake condition, but with different behavior of P and Si compared to N (Figure 9).

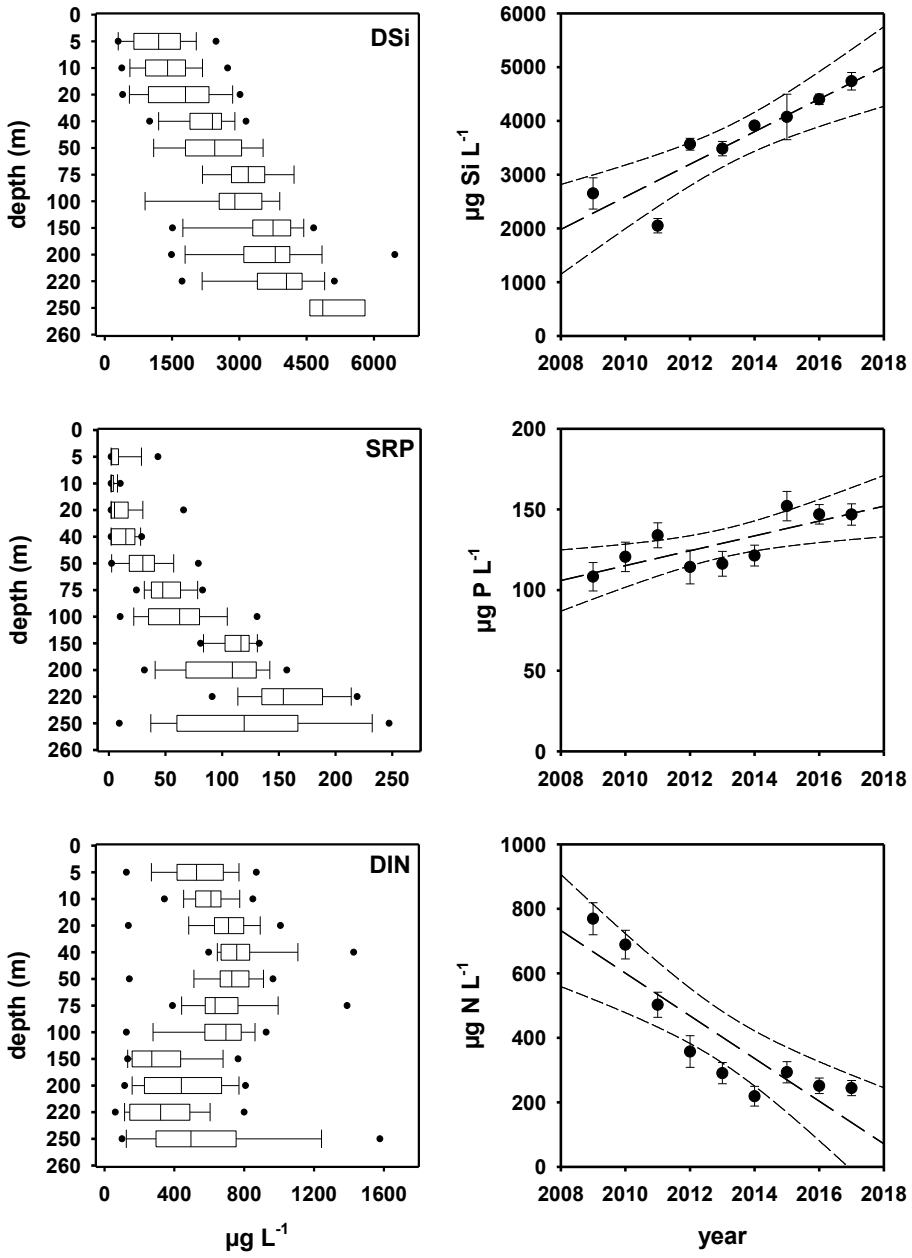

Figure 9. Concentration of dissolved silica (DSi), soluble reactive phosphorus (SRP) and dissolved inorganic nitrogen (DIN) along the water column (left panel, data reported as boxplot) and in monimolimnion along the years (right panel, data reported as mean annual value and standard error). Data provided by ARPA Lombardy from 2009 to 2017 and expressed as µg L^{-1}.

DSi concentration increased more than three times from epilimnion (1330 ± 170 µg Si L^{-1}) to monimolimnion (3649 ± 290 µg Si L^{-1}) and SRP grow more than forty times from 2.7 (± 0.4) µg P L^{-1} in epilimnion to 123.3 (± 5.8) µg P L^{-1} in monimolimnion. On the contrary, DIN average concentration in epilimnion resulted higher (621 ± 30 µg N L^{-1}) compared to monimolimnion (373 ± 72 µg N L^{-1}) (Figure 9, left panels).

The DIN composition varied with depth. In the surface waters N-NO_x contributed on average by 90%, while in the monimolimnion N-NH_4^+ accounted on average for 20% of DIN. Moreover, N-NH_4^+ contribution progressively increased from 7% in 2012 to 49% in 2017, which is a result of anoxia and reducing conditions in the monimolimnion. In parallel, with a linear regression of concentrations vs time I estimated that from 2009 to 2017 DSi increased by 303 µg Si $L^{-1}y^{-1}$ (R^2 = 0.82, p <0.001) and SRP increased by 4.6 µg P $L^{-1}y^{-1}$ (R^2 = 0.60; p <0.001). Contrariwise, DIN concentration decreased by 66 µg N $L^{-1}y^{-1}$ (R^2 = 0.78, p <0.001) (Figure 9, right panels).

The DIN:DSi molar ratio decreased with depth from 1.1 ± 0.2 in epilimnion to 0.2 ± 0.1 in monimolimnion, while the SRP:DSi molar ratio slightly increased from 0.002 ± 0.003 in the epilimnion to 0.032 ± 0.004 in the monimolimnion. Based on these ratios, in the epilimnion, DSi is potentially limiting in comparison to SRP but not to DIN, while DSi is in excess with respect to DIN but not to SRP in the monimolimnion (Figure 10).

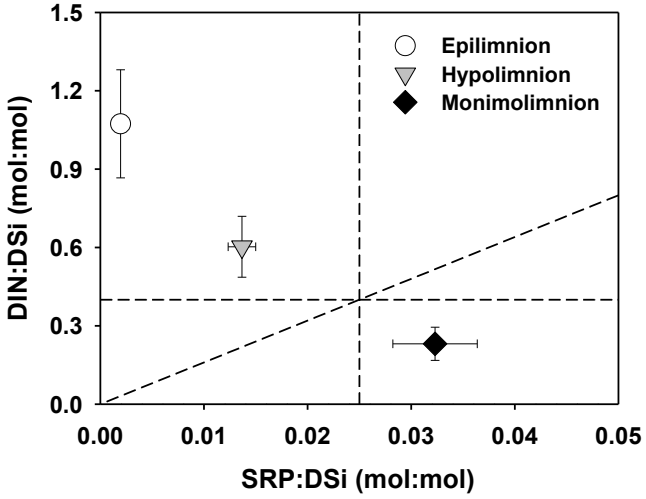

Figure 10. DIN:DSi and SRP:DSi molar ratios in epilimnion, hypolimnion and monimolimnion. Dashed lines represents the value of the ratio in freshwater (Dupas et al., 2015): N:Si = 0.40, P:Si = 0.025 and N:P = 16. Data are expressed as mean values and standard errors (error bars).

The composition of the settling SPM was analyzed at two depths, i.e. 20 m in the epilimnion and 90 m in the hypolimnion. The settled SPM had a mean BSi content of 109 ± 10 mg Si g^{-1}, but with significant differences (p <0.05) between vegetative and non-vegetative periods at the two depths. In the latter BSi was 140 ± 3 mg Si g^{-1} at 20 m and 155 ± 10 mg Si g^{-1} at 90 m depth, while in vegetative period it was 77 ± 15 mg Si g^{-1} at 20 m and 104 ± 11 mg Si g^{-1} at 90 m depth. PP was on average 2.2 ± 0.1 mg P g^{-1} and during non-vegetative period decreased from 2.7 ± 0.2 mg P g^{-1} at 20 m depth to 2.1 ± 0.1 mg P g^{-1} at 90 m depth. PN was on average 21 ± 2 mg N g^{-1} and decrease from

23 ± 2 mg N g^{-1} at 20 m depth to 14 ± 1 mg N g^{-1} at 90 m depth during non-vegetative period. By contrast, there was an accumulation of PN at 90 m during vegetative period (19 ± 2 mg N g^{-1}).

The average sedimentation rate was 108 ± 12 mg Si m^{-2} d^{-1} for BSi, 19 ± 1 mg N m^{-2} d^{-1} for PN and 2.5 ± 0.6 mg P m^{-2} d^{-1} for PP. The nutrient stoichiometry of settled matter was affected by both depth and periods (Figure 11).

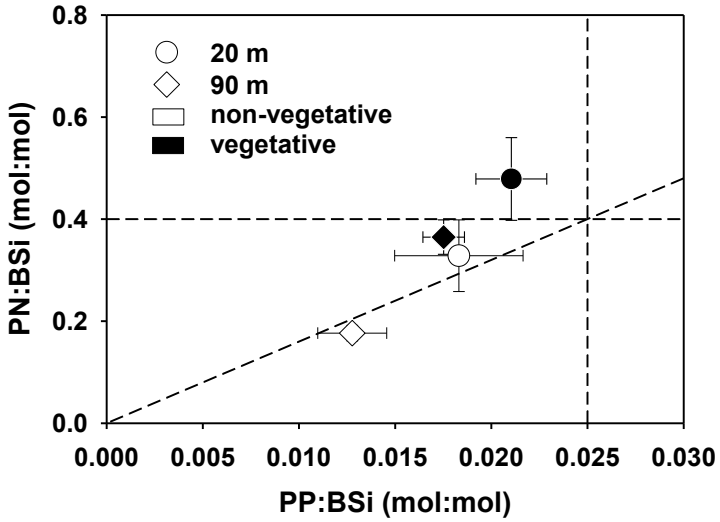

Figure 11. PN:BSi and PP:BSi molar ratios of settled matter collected in the sedimentation traps at 20 m (circle) and 90 m (diamond) during non-vegetative (open symbol) and vegetative periods (black symbol). Dashed lines represent the balanced ratio for phytoplankton growth in freshwater (Dupas et al., 2015): N:Si = 0.40, P:Si = 0.025 and N:P = 16. Data are expressed as mean values and standard errors (error bars).

PN:BSi ratio was on average 0.32 ± 0.04. At 90 m depth, PN:BSi increased from 0.18 ± 0.02 in non-vegetative to 0.36 ± 0.03 in vegetative period. In the same way, PN:PP ratio increased at 90 m depth from 15.3 ± 0.7 in non-vegetative period to 21.0 ± 1.0 in the vegetative one. This pattern was verified also at 20 m depth for PN:PP, increasing from 18.7 ± 1.1 in non-vegetative to 26.3 ± 1.9 in vegetative periods. The PP:BSi ratio showed a decreasing trend from 20 to 90 m, especially in non-vegetative period (Figure 11).

In order to achieve a better understanding of processes which regulate in lake fluxes and inherent stoichiometry of Si, N and P benthic fluxes were compared in the deep and littoral sediments. Nutrient dynamics in the littoral zone are discussed in details in Chapter 3. DSi fluxes were greater in the littoral zone (47.1 ± 19.3 mg Si m^{-2} d^{-1}) than in deeper sediments (36.4 ± 4.5 mg Si m^{-2} d^{-1}). By contrast, SRP was mainly released both from bottom (2.31 ± 0.85 mg P m^{-2} d^{-1}) and littoral sediments

(0.04 ± 0.33 mg P m^{-2} d^{-1}), but flux rates were greater in the deepest sediments. DIN was taken up in the littoral zone (-15.0 ± 6.5 mg N m^{-2} d^{-1}) and recycled into the water column in the deepest sediment layer (21.7 ± 1.1 mg N m^{-2} d^{-1}).

Benthic fluxes in littoral zone highlighted a greater Si release in comparison to N uptake and very low P fluxes (Figure 12). The DIN uptake was accounted for mainly by N-NO_x removal, which was likely due to reduction pathways, e.g. denitrification. The N-NH_4^+ removal was much lower, partly due to nitrification in the oxic water layers.

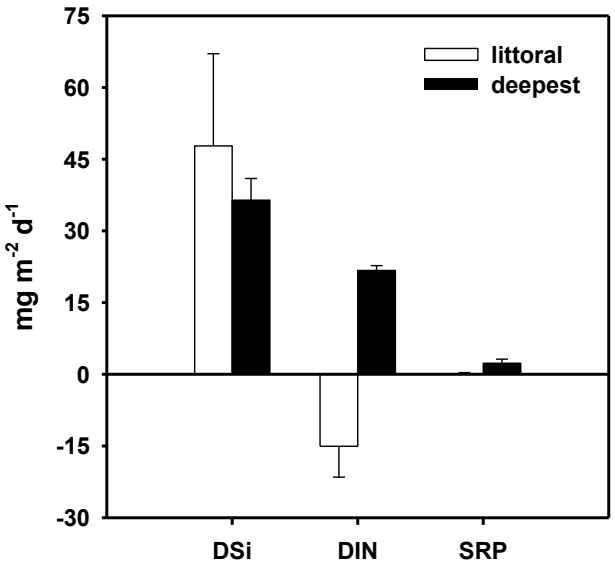

Figure 12. Comparison of benthic fluxes of dissolved silica (DSi), dissolved inorganic nitrogen (DIN) and soluble reactive phosphorus (SRP) in the littoral zone and in deepest sediments of Lake Iseo. Error bars represent standard error (n = 33 in littoral zone sediment; n = 6 in deepest sediment). Data of littoral zone from Chapter 3.

Compared to epilimnetic waters, in the monimolimnion nutrient stoichiometry of benthic fluxes underwent some imbalance, with P (P:Si = 0.06 ± 0.03) and N (N:Si = 1.26 ± 0.15) in excess of Si. DIN was released from bottom sediments as N-NH_4^+, while N-NO_x was likely a residual from the last complete overturn. In terms of budget, N-NH_4^+ tended to become dominant due to its efflux from sediment, while N-NO_x was consumed. Contrariwise, in the littoral zone DIN was almost entirely composed by nitrate, whilst the ammonium release from sediments was much less relevant.

2.4. Discussion

This study aimed at analyzing how and to which extent a deep lake can regulate nutrient fluxes, acting as a nutrient filter in the hydrographic network (see for definition Meybeck & Vörösmarty, 2005). As far as I know, this is the first study addressing multi-element dynamics and stoichiometry in lakes, comprising Si and its biogenic pool. Lakes are recognized as biogeochemical reactors, able to retain and store nutrients as Si, N and P depending also on their depth (Harrison et al., 2009; Frings et al., 2014; Maranger et al., 2018). Less is known about the relationships among elements and their stoichiometry. Many lakes are undergoing a less frequent water overturn, and they are shifting towards oligomixis and even meromixis (Salmaso et al., 2018). In meromictic lakes, due to the permanent and stable stratification of the water column, the deeper water mass (monimolimnion) can become a sort of nutrient storage, excluding nutrient from the upwelling during water overturn.

The first cause of reduction of complete overturn events in Lake Iseo has been attributed to salinity on vertical density distribution and the consequent deoxygenation of the deep water (Ambrosetti & Barbanti, 2005). Meromixis is made more stable by the warming of the water column, which amplifying the thermal differences between surface and bottom waters, thus strengthening the stratification (Valerio et al., 2015).

2.4.1. Nutrient Retention in Lake and the Role of Meromixis

The extent of the retention of external Si, N and P loadings within Lake Iseo is reported in Table 2. The retention of TSi and TP was nearly twofold the TN one. This is clearly due to the sedimentary features of Si and P cycles (Ruttenberg, 2003; Teodoru et al., 2006). Instead, the N cycle was dominated by dissolved reactive forms, especially nitrates that are easily soluble.

Table 2. Summary of the retention in Lake Iseo of total (TSI) and dissolved silica (DSi); total (TN) and dissolved inorganic nitrogen (DIN); total (TP) and soluble reactive phosphorus (SRP). Data are expressed as mean values and standard errors in parenthesis.

	TSi	**DSi**	**TN**	**DIN**	**TP**	**SRP**
Inlet (t yr^{-1})	3044 (303)	1899 (292)	2174 (139)	1614 (124)	126 (22)	28 (4)
Outlet (t yr^{-1})	747 (164)	641 (135)	1197 (71)	779 (60)	26 (3)	6 (2)
Retention (%)	**75**	**76**	**45**	**52**	**79**	**80**

The retention capacity depends also on other factors, especially lake morphology and hydrology. A wick positive regression between relative retention of inflowing Si and water residence time (R^2 = 0.12) was found for other lakes (Frings et al., 2014). Lake Iseo features, i.e. TSi loading retention of 75% and water residence time of 4.5 years, fitted well with this regression, especially considering lakes features only (Figure 13). Taking in account the lake surface, Si retention was 37.7 g m^{-2} y^{-1}, a value slightly higher compared to other lakes worldwide (19.7 ± 22.6 g m^{-2} y^{-1}) (Harrison et al., 2012; Frings et al., 2014). Possible causes of this higher value could be the morphological characteristic of the lake (i.e. high depth and restricted littoral zone) and the presence of meromixis, both concurring to the increase of Si retention.

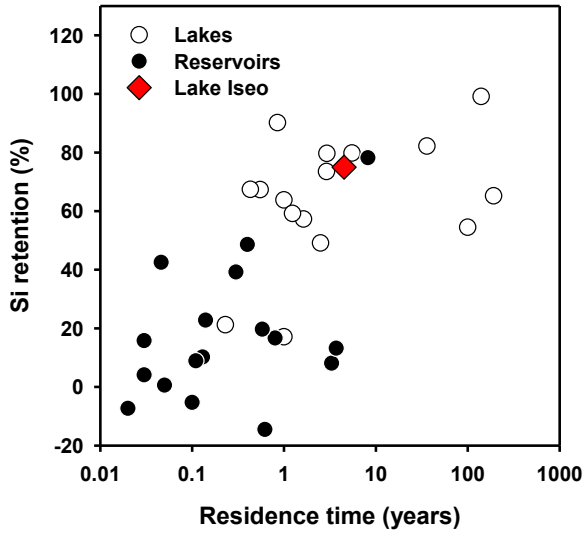

Figure 13. Residence time (years in a log scale) and retention capacity of Si (in %) in different lentic bodies worldwide, both natural lakes (open circles) and reservoirs (black dots). Data available in Frings et al. (2015). Red diamond represents Iseo Lake.

Total P retention in Lake Iseo was comparable to other lakes (Reynolds & Davies, 2001; Cook et al., 2010; Verburg et al., 2013). In Lake Idro, which is about 50 km northwards, a retention between 9 and 35% was estimated in different years (Viaroli et al., 2018). This could be due to different causes. Volumes and depths of lakes are different. On average Lake Iseo is deeper (mean depth = 123 m, maximum depth 258 m) than Lake Idro (mean depth = 77 m, maximum depth 124 m) and the water residence time is much less in Lake Idro (0.9 years). The water level of both lakes is man regulated, but level oscillations are greater in Lake Idro. Land use in the watersheds are different, being Lake Idro watershed (Viaroli et al., 2018) less exploited than Lake Iseo basin (Table 1). In Lake Iseo, TN retention was lower (45%) than what predicted by reference predictive retention model for reactive N (Seitzinger et al., 2006). DIN retention (52%) resulted similar to the 31% retention estimated for

Lake Idro (Nizzoli et al., 2018). Under meromictic conditions, the complete overturn is much less frequent or does not occur at all, thus causing oxygen depletion and anoxia in the deepest water layer. The 40% of the benthic system in Lake Iseo was anoxic. As a consequence, $N\text{-}NO_x$ depleted and extreme reducing conditions favored N recycling rather than denitrification (Nizzoli et al., 2018). This condition can induce the $N\text{-}NO_x$ consumption in the monimolimnion. This imbalance of nutrient loadings could depend on the removal pathway of Si and P, which is mainly sedimentary, compared to N, which is mainly biological, e.g. primary productivity and denitrification. Furthermore, there is an excess of N, e.g. both from atmospheric inputs and agriculture and livestock.

The differential retention of N, P and Si is confirmed by molar ratios which clearly changed from inlet to outlet. In outlet water, N:Si and N:P resulted higher than in the inlet, confirming a stronger retention of Si and P compared to N. An increase of N:P and N:Si ratio in outlet water has already been described, even though with little values due to a lower retention of Si and P (Cook et al., 2010). The N:P ratio of Lake Iseo, with the only exception of outlet waters during the non-vegetative period (134 ± 19), is in agreement with the range of value found in American lakes, ranging from 34 – 110 (Maranger et al., 2018). The Si depletion, which is regulated mainly by natural processes, is contrasted by P and N replenishment by anthropogenic activities (Cook et al., 2010), which often results in the increase of flagellate and cyanobacteria blooms along with the concurrent decrease of diatoms in coastal waters (Humborg et al., 2000) and in freshwater (Glibert, 2017).

Nutrient regulation undergoes different pathways, following the evolution of phytoplankton productivity in the water column. DSi is regulated by primary production in early spring when diatoms grow, while DIN decreases in summer due also to denitrification as demonstrated in other lakes (Nizzoli et al., 2018). This could be also explained by the shift of primary producers assemblages from diatom dominated in early spring to cyanobacteria dominated in summer (Havens, 2008). The DSi to DIN stoichiometry suggests a stronger DSi limitation in outlet water.

The higher retention of Si and P is reflected in the annual increase of DSi and SRP in monimolimnion, respectively 1089 ± 17 t Si y^{-1} and 17 ± 1 t P y^{-1} (Table 3). In Lake Idro, a comparable accumulation of 8 t P y^{-1} was found (Viaroli et al., 2018). From 2009 to 2017 the N:Si and N:P ratio decreased in the monimolimnion, suggesting a progressively unbalanced of stoichiometry. The N:Si decrease from 0.58 to 0.10 ($R^2 = 0.77$) remarking the progressively N loss in deep water of Lake Iseo. The same trend was found for N:P ratio, decreasing from 16 in 2009 to 4 in 2017 ($R^2 = 0.82$), while P:Si remained stable in the monitored period (0.034 ± 0.004), confirming the similar fate that connects P and Si cycling.

Table 3. Regression of concentration (µg L^{-1}) versus time (year) of dissolved silica (DSi), dissolved inorganic nitrogen (DIN), nitrate and nitrite ($N\text{-}NO_x$), ammonium ($N\text{-}NH_4^+$) and soluble reactive phosphorus (SRP) in Lake Iseo monimolimnion from 2009 to 2017.

Nutrient	Slope (µg L^{-1} y^{-1})	R^2	p
DSi	303.0 (4.7)	0.82	<0.001
DIN	-66.2 (3.3)	0.78	<0.001
$N\text{-}NO_x$	-72.7 (9.1)	0.91	<0.001
$N\text{-}NH_4^+$	6.6 (0.3)	0.20	n.s.
SRP	4.6 (0.3)	0.60	<0.001

2.4.2. Fluxes from and to Sediments

The nutrients retention in Lake Iseo was due to the balance between settling SPM downwards and the regeneration upwards the water column. Stocks and fluxes of N, Si and P are depicted in Figure 14. Overall, sedimentation rates in Lake Iseo were much lower than in other studies, referring to both natural lakes and reservoirs. Usually, reservoirs drain larger catchments area than lakes, thus receiving a greater runoff (Maranger et al., 2018). In addition, the lower residence time and the higher settling velocities of reservoirs can speed up processes (Harrison et al., 2009; Clow et al., 2015). Nonetheless, the annual BSi load to bottom sediment in Lake Iseo (Figure 14) resulted only slightly lower than those found by Teodoru et al. (2006) for reservoirs.

From late spring to late summer of 2017, the littoral zone of Lake Iseo appeared to perform as a DSi source, as a weak SRP source and as a DIN sink (see Chapter 3). The N removal resulted similar to the N assimilation of 9 – 38 t N y^{-1} reported for Lake Idro (Nizzoli et al., 2018). All fluxes from sediment to water resulted lower than sedimentation rates in the 20 m shallow zone, suggesting that nutrient retention occurred not only in the deepest sediments but also in the shallow coastal zone of the lake. The settled material underwent a nitrogen shortage during the non-vegetative period, probably due to a diatom bloom in autumn and a summer cyanobacteria growth (Havens, 2008).

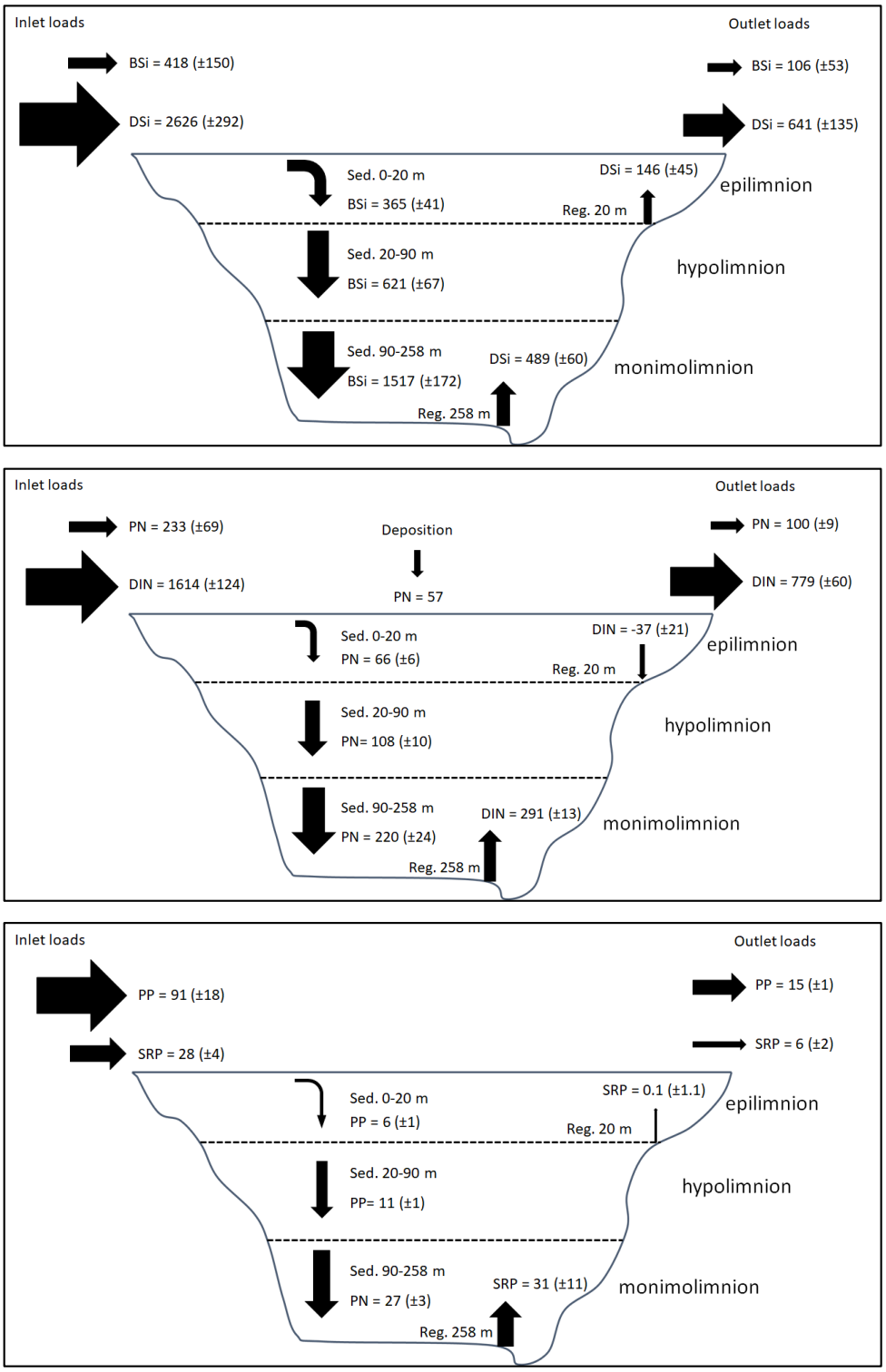

Figure 14. Main fluxes and pathways of Si, N and P as dissolved and particulate pool in Lake Iseo. In addition to inlet and outlet nutrient pools, nutrient sedimentation in epilimnion (Sed. 0-20 m, trap at 20 m depth), hypolimnion (Sed. 20-90 m, average between the 2 traps) and monimolimnion (Sed. 90-258 m, trap at 90 m depth), nutrient regeneration from littoral zone (Reg. 20 m) and deep sediment (Reg. 258 m) are reported. Fluxes are reported as t y^{-1}. Standard error in parenthesis. Arrows size is proportional to flux rates.

Phosphorus resulted always in excess in comparison to Si but not to N at both sediment trap depths. All nutrients were regenerated from bottom sediments at 258 m depth to the water column, with more N than Si. Nonetheless, in monimolimnion N was deficient compared to Si, likely due nitrate consumption, e.g. through denitrification (Table 3), which was not compensated by N regeneration from sediment. At the same time, the N:P ratio was unbalanced towards P in monimolimnion. Overall, Si, P and N-NH_4^+ increased in time, due to the lack of a complete water mixing. This nutrient bulk is made unavailable to the photic zone while the stratification persists. In other words, this system looks like a 'time bomb' which can be only triggered by full water mixing, making high nutrient concentrations available to phytoplankton into the photic zone (Viaroli et al., 2018). Similar events occurred in 2005 – 2006, when SRP concentrations in the epilimnion attained up to 75 μg P L^{-1} (Salmaso et al., 2014; Rogora et al., 2018).

The differences between input and output loadings of Si, P and N do not match well with changes accounted by in lake processes (sedimentation and sediment fluxes, Figure 14). For Si, the difference between the process within the lake and the mass budget is missing 60 t y^{-1} of Si, which could be due to some external source or to atmospheric deposition over the lake. Conversely, P and N in lake processes and P and N mass budgets had relevant differences. The high contribution of PP in inlet water (76% of total load) may suggests a strong deposition immediately after the lake inlets. This could explain the 54 t P y^{-1} missing. The N mass balance was missing 31% of the inlet load which was not accounted by fluxes. This difference could be explained by the denitrification. The denitrification is an important process occurring in anoxic condition (Bruesewitz et al., 2012; Nizzoli et al., 2014, 2018) which, for example, in the close Lake Idro represents ~10% of the inlet load (Nizzoli et al., 2018).

2.5. Conclusions

This study analyzed how and to which extent a meromictic deep lake acts as a Si filter in the hydrographic network and compared Si retention and pathways with those of the more extensively studied dynamics of N and P. This is an understudied but important issues in inland waters, as it can provide new insight to understand the role of lake ecosystems to regulate Si fluxes and its availability relative to N and P. Additionally, the fact that Lake Iseo is experiencing a meromictic phase would help to understand how infrequent to no mixing can influence in lake nutrient dynamics.

The results confirm previous findings that lakes behave as biogeochemical reactors which retain and accumulate nutrients. In addition to previous work, it was evidenced that the retention of Si (75%)

and P (79%) are comparable and both are higher than N (45%) retention. As such, the lake has the potential to alter the relative amount of nutrients along the hydrographic network with outflowing waters more enriched in nitrogen compared to silica and phosphorus than inflowing waters.

The Si and P retention capacity is likely exacerbated by meromixis. Si and P dynamics are mainly governed by sedimentation of particulate forms that are either buried in the sediment or recycled through the water column as dissolved forms. Si and P and $N\text{-}NH_4^+$ accumulate in the monimolimnion due to the absence of water mixing, making unavailable these nutrients to the photic zone, while the stratification persists. To better understand the overall processes and nutrients mass balances, further researches are needed to explore the Si deposition from atmosphere dust, P speciation in the monimolimnetic sediments and denitrification extent, especially in the chemocline.

In conclusion, the meromixis promotes Si and P retention and likely P limitation in epilimnetic waters, leading to a possible and temporary drop of the eutrophication risk, but at the same time cause a nutrient disequilibrium in the river emissary. In the long run such an unbalance in favor of N could affect the structure of primary producer community in downstream ecosystems as it can favor flagellate bloom along with the concurrent decrease of diatoms. These conditions are likely to become more severe in the future - exacerbated by the concurrence of eutrophication and climate changes - and therefore it seems very important to study the dynamics regulating silica and the other nutrients in lakes that are experiencing a reduction of mixing frequency, as well as it is pivotal to explore the origin of external nutrient loads, forcing those systems.

3. Silica Storage, Fluxes, and Nutrient Stoichiometry in Different Benthic Primary Producer Communities in the Littoral Zone of a Deep Subalpine Lake (Lake Iseo, Italy)

3.1. Introduction

Lake functioning depends on size and morphology, with a first distinction being between shallow and deep lakes. In shallow lakes, there is a prevalence of either microphytobenthos (MPB) or submerged aquatic vegetation (SAV), which control both primary productivity and biogeochemical cycles (Scheffer, 1997). Large, deep lakes are dominated by phytoplankton communities, in which siliceous algae play a major role in primary productivity and control of nutrient cycling (Salmaso et al., 2018). However, with regard to deep lakes, a distinction should be made between holomictic lakes and oligomictic and meromictic lakes. In the last two categories, water stratification can persist over decades, thus increasing Si retention in the deepest water mass, as was found for other elements (Nizzoli et al., 2018; Viaroli et al., 2018). The persistent stratification of the water mass can also impede "benthic-pelagic coupling", i.e., avoidance of recycling of the DSi regenerated from sedimentary BSi and amorphous silica to the photic layer (Chapter 2).

Studies on Si retention by lakes have been mainly concerned with mass balances, taking into account input-output differences over a consistent time scale (Frings et al., 2014). This approach assumes that lakes are mixed reactors dominated by open waters, but the role of other sub-system components are not considered separately, such as the littoral zone. This land-water interface is shallow, allowing light to penetrate to the bottom so that benthic primary producers develop (Vadeboncoeur & Steinman, 2002; Strayer & Findlay, 2010; Zohary & Ostrovsky, 2011). Here, helophytes and macrophytes synthesize and accumulate BSi, thus controlling both stocks and fluxes of DSi (Struyf & Conley, 2009, 2012). Helophytes and macrophytes take up DSi from pore-water and transform it into BSi, which concentrates in plant tissue for up to 3% of the total dry weight (Schoelynck et al., 2010). Once fixed in plant biomass, BSi is gradually released back into the abiotic environment as DSi through grazing and biomass decay (Meybeck & Vörösmarty, 2005; Struyf & Conley, 2009). Fluxes and export of DSi can be enhanced by fungal and microbial activity, which stimulates BSi mineralisation and DSi release from detritus (Alfredsson et al., 2016). In the littoral zone, such Si filtering by primary producers is thought to affect the rate of DSi exchange across the water-sediment interface, with DSi being transported towards open water (Borrelli et al., 2011; Struyf & Conley, 2012). DSi retention also depends on seasonal factors, especially the seasonality of growth and decay of littoral primary producers (Struyf & Conley, 2009; Carey & Fulweiler, 2013a). In bare

sediments, DSi fluxes are controlled by benthic diatoms and bioturbation driven by benthic fauna (Bartoli et al., 2003; Nizzoli et al., 2007). DSi is assimilated to BSi by diatoms in light conditions, with the benthic system acting as a net DSi trap. In dark conditions, on the other hand, photosynthesis does not occur; the diatom filter is inactive, so the DSi is released back to the water column from sediments (Bartoli et al., 2003). Exchanges from sediment to the water column can be further accelerated by benthic fauna bioturbation (Nizzoli et al., 2007).

The littoral zone, either with MPB or SAV and helophytes, is a biogeochemical hotspot, where a greater amount of primary productivity and nutrient recycling takes place, together with faster rates of mineralization, when compared to the contiguous pelagic and terrestrial areas (Wetzel & Likens, 1991; Den Heyer & Kalff, 1998; Bruesewitz et al., 2012). The littoral zone, however, is heterogeneous and patchy. In fact, there is a mosaic of diverse conditions underlying multiple and differentiated ecological functions on account of the substrate structure, the physical and chemical conditions in the sediment and water column, disturbance regimes, and inputs of organic matter and nutrients, which change radically over time and space (Strayer & Findlay, 2010). Whereas bare and soft sediments are largely colonized by benthic microalgae, macroalgal aggregates and phanerogam meadows, rocky shores, and hard-substrates host epilithic algae, depending on light penetration and nutrient availability. The magnitude of processes driving Si dynamics is thought, therefore, to vary in different microhabitats colonized by different primary producers.

As far as I know, there are very few lake studies regarding the direct measurements of BSi accumulation and DSi fluxes across the water-sediment interface, all focusing on bare sediments colonized by MPB (Kelderman et al., 1988; Spears et al., 2008), while further research on SAV and epilithic macro- and microalgae (EA) needs to be carried out. In littoral areas of lakes, a major focus on the magnitude of DSi exchange is not only necessary given its general importance in ecosystem functioning, but also because of its influence on N:P:Si stoichiometry, as Si shortage can shift phytoplankton composition towards communities dominated by noxious or harmful algae (Glibert, 2017). Unlike other phytoplankton taxa, diatoms and a few other microalgae, such as Crysophyceans, require proportionally more Si relative to N and P, with Si becoming a frequent factor in growth limitation (Redfield et al., 1963; Egge & Aksnes, 1992). Only a few studies have examined the stoichiometry of nutrient fluxes in salt and freshwater marshes (Van Damme et al., 2009; Carey & Fulweiler, 2014), but no research has analyzed DSi fluxes and BSi accumulation in the littoral zone of lakes in relation to N and P.

This study focuses on BSi and DSi storage and fluxes in the littoral zone of Lake Iseo, a deep sub-alpine lake located in the north of Italy (Salmaso et al., 2018). The purpose of this research is twofold. First, the aim was to analyze stocks, transformations, and fluxes of BSi and DSi during the

growth phase of benthic vegetation in different habitats of the littoral zone colonized by diverse primary producer communities. The second aim is to analyze and compare the stoichiometry of stocks and fluxes in order to understand how different benthic vegetation communities influence N:P:Si ratios. The postulate of this work was that the littoral zone of lakes is a natural filter, where DSi is assimilated as BSi by macroalgae and microphytobenthos from the water column, and by rhizophytes from pore-water. More specifically, the hypothesis is that such BSi and DSi transformations can significantly modify the relationships between the reactive forms of Si, N, and P, thus affecting their stoichiometry and, ultimately, the responses of primary producer communities. Consequently, the main objectives of this study were: (a) to estimate the extent of BSi accumulation in the biomass of the most representative primary producers at the local level; (b) to compare BSi accumulation in sediments colonized by different benthic vegetation; (c) to quantify DSi fluxes across the water sediment interface in relation to the dominant primary producers; and (d) to evaluate how heterogeneity affects Si dynamics and stoichiometry relative to reactive N and P.

3.2. Materials and Methods

3.2.1. Study Area

The study was carried out in Lake Iseo, the fourth largest lake in the Alps for its surface and volume (60.9 km^2, and 7.6 km^3, respectively; Figure 15, Table 1). The lake's main inlets are the River Oglio and the Industrial Canal, which contribute ~49% and ~51% of the water inflow (4.1×10^6 m^3 d^{-1}), respectively.

Agricultural use accounts for 22% of the watershed surface, mainly as pastures or rough grazing (21.4%). Population density is 109 ind. km^{-2}, while livestock units (1 LSU = 1 adult dairy cow) account for 17 LSU km^{-2}. Cattle (18,241 LSU), poultry (8145 LSU) and sheep (2307 LSU) are the main farmed livestock (ISTAT, 2010, http://dati. istat.it/). Lake Iseo is meromictic; its trophic status is meso-eutrophic due to meromixis (Salmaso & Mosello, 2010) and the influence of anthropic activities in the watershed. The water mass is currently completely anoxic, from 100 m depth to the bottom (258 m).

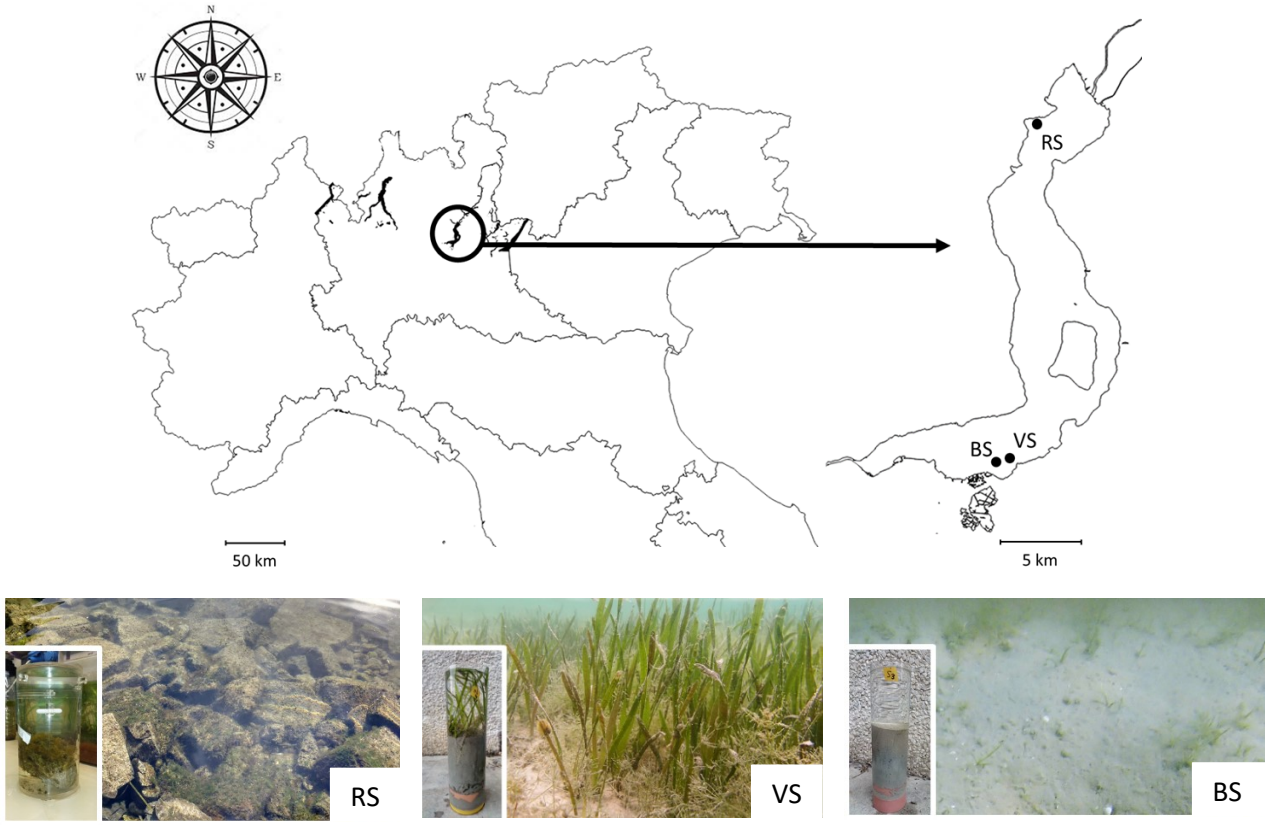

Figure 15. Location of Lake Iseo (left), and a detailed map of the lake (right) showing the three sampling sites (RS = rocky shore; VS = vegetated sediment; BS = bare sediment).

The west shore is steep and rocky, while the eastern side is steep in the northern part but becomes progressively flat towards the south. The surface area of the littoral zone is ~5 km^2, i.e., 8.2% of the total lake surface area. The Secchi disk never exceeds the 4.5 m of depth, limiting the macrophyte growth to about 9 – 10 m of depth (Bolpagni et al., 2017). Accordingly, we focused our activities in the depth range 0 – 10 m. The coastal morphology is a driver for different benthic primary producer communities. Specifically, in the north-west part of the lake, the benthic substrate is composed of rocks and pebbles (>90%), which are colonized by epilithic macro- and microalgae (site RS, Figure 15). The south-east flat coastal area is characterized by a soft bottom substrate, mostly covered by meadows of *Vallisneria spiralis* L. and, to a lesser extent, *Najas marina* L. (site VS, Figure 15). Here, large patches of bare and soft sediment are also colonized by microphytobenthos (site BS, Figure 15).

3.2.2. Monitoring Design and Sampling

Three sites were compared (RS, VS and BS), each with a different community of benthic primary producers: epilithic diatoms and filamentous macroalgae on hard substrate (EA) at the RS site;

submerged phanerogams (SAV; *V. spiralis* and *N. marina*) at the VS site; and microphytobenthos (MPB) at the BS site.

The following sampling period was chosen in order to capture the seasonal growth phase of each primary producer assemblage: 12 April, 27 June, and 28 August 2017 at RS; 30 May, 31 July, and 3 October 2017 at VS and BS. Sampling dates are collectively reported in tables, figures and text as Early (late spring – early summer), Mid (midsummer) and Late (late summer – early fall) phases of the life cycle of the main components of the benthic primary producer community.

At the RS site, six stones colonized by periphyton were collected on each sampling date. After harvesting, the stones were immediately transferred into six distinct small Plexiglas microcosms (inner diameter 10 cm, height 20 cm) with water collected from the site. At the VS site, six sediment cores were sampled with Plexiglas tubes (inner diameter 10 cm, height 40 cm) on each date, while at the BS site, six cores (inner diameter 8 cm, height 30 cm) were also collected on the same dates. Simultaneously, at both VS and BS, five additional sediment cores (inner diameter 4 cm, height 20 cm) were sampled to establish the chemical and physical characteristics of the surface sediment. During sampling, extra care was taken to not disturb the superficial sediment. All samples between −1 and −4 m were manually collected by scuba diving. To ensure the maintenance and incubation of stones and cores in the laboratory, approximately 100 L of water were taken from each site.

Once collected, both cores and microcosms were placed in thermal containers, submerged in water from the sampling site, and transported within 4 h to the laboratory at the University of Parma. Here, sediment cores and stones were housed in a thermostatic room, placed inside aerated incubation tanks (75 L) containing lake water from each site, and maintained at the same ambient temperature (±1 °C).

Water temperature and conductivity were determined in situ with a multiparametric probe (YSI 556). Three water samples were also collected from each site at ~50 cm above the sediment surface. Water samples were filtered (Whatman GF/F) and analyzed within 24 h to measure dissolved silica (DSi), ammonium ($N\text{-}NH_4^+$), nitrate and nitrite ($N\text{-}NO_x$), and reactive phosphorus (SRP). Finally, total inorganic nitrogen (DIN) was calculated as $DIN = N\text{-}NH_4^+ + N\text{-}NO_x$.

3.2.3. Benthic Fluxes and Benthic Metabolism

In the laboratory, cores and microcosms were immediately left to stabilize ~12 h in lake water with the upper end open and completely submerged. During maintenance and incubation, the water inside the cores and microcosms was gently stirred, avoiding sediment resuspension, using magnetic stirrers suspended within each core, and driven with a magnet rotated at 40 rpm by an external motor. The temperature of the water was maintained at the same ambient temperature of the sampling sites.

The day after sampling, the cores were first incubated in darkness and, subsequently, in light to measure water sediment fluxes. To begin the incubation, the water level in the tank was lowered below the core edges and a water sample was taken from each core to determine the initial chemical characteristics. In order to start the incubation process, the upper opening of the cores was closed with a floating Plexiglas lid. At the end of the incubation, the cores were opened and the water was sampled from each core to determine final chemical characteristics. Fluxes of oxygen and nutrients were paired for dark and light incubation –i.e., measured on the same cores. Following the dark incubation, the incubation tanks were re-filled with water from the site, the cores re-submerged and left uncapped for one hour to re-equilibrate prior to start light incubations. Light conditions were obtained with adjustable halogen lamps; light intensity (400–600 μE m^{-2} s^{-1}) was set on the basis of the average daily radiation of the sampling day recorded with a PAR quanto-photo-radiometer (Delta OHM, model HD 9021, Padova, Italy). Incubation time for both dark and light conditions ranged between 2 and 5 h. Based on previous incubations, the time was set in relation to water temperature and the dominant primary producer community inside the cores in order to obtain an oxygen variation of <20% of the initial concentration.

Water samples were collected with plastic syringes. Subsamples were transferred into glass tubes (Labco Exetainer©, Lampeter, Wales) to which Winkler reagents were added to determine dissolved O_2. The remaining water was filtered through Whatman GF/F glass fiber filters: to determine DSi, N-NO_x and N-NH_4^+ samples were stored in polyethylene vials, while to measure SRP, glass tubes were used. Analyses for O_2 determination were performed immediately after collection; samples for determination of SRP and N-NO_x were stored at 4 °C and analyzed within 24 h, while samples for DSi and N-NH_4^+ were frozen and subsequently analyzed. Fluxes of O_2 and nutrients were quantified as the change over time of the concentration of each parameter using the formula (3) (Nizzoli et al., 2014):

$$F_x = \frac{(C_f - C_0) \times V}{A \times \Delta t} \qquad (3)$$

where, F_x is the flux of the x chemical species (mg m^{-2} h^{-1}), C_f is the final concentration of x (mg L^{-1}), C_0 is the initial concentration of x (mg L^{-1}), V is the volume of the water column (L), Δt is the incubation time (h) and A is the sediment surface area inside the core (m^2).

As a result of the irregular shape of the stones, the surface area of each rock was carefully measured using the foil-wrapping technique (Maasri et al., 2008). In short, the surface of each rock was wrapped with close-fitting aluminum foil, trimming any excess, and then weighing the foil wrap.

A regression equation based on the weight and area relationship of aluminum foil (n = 10) was used to convert rock foil wrapping weights to areas.

Net daily sediment–water fluxes were calculated as the sum of the light and dark rates multiplied by the average light and dark phase duration.

3.2.4. Primary Producer Biomass and Sediment Features

At the end of incubation, the biomass of the primary producers from each intact core and microcosm was quantified.

Filamentous algae and epilithic material were removed from each stone with tweezers and brushes. Filamentous algae were rinsed and cleaned to remove epiphyte slime, placed in pre-weighed aluminum dishes, and fresh weighed. Subsequently, the algae were oven-dried at 70 °C for two days. The dried samples were weighed immediately after being removed from the oven and cooled, then ground up and homogenized. The dried biomass was analyzed for BSi, N, and P content. Sediment deposited on rocks at the RS site was also collected by carefully scraping the stone surface with a spoon and then both fresh and dry weighed, with the dry sediment retained for OM, BSi, N and P analysis.

Cores with macrophytes (site VS) were extracted, flushed with tap water, and filtered through a 2-mm mesh sieve. The collected plants were further washed with deionized water and sorted by species. From each specimen, leaves and roots were separated, rinsed, and cleaned to remove debris, epiphytic algae and macro-invertebrates; then placed in pre-weighted aluminum dishes and fresh weighed. Subsequently, the material was oven-dried at 70 °C for two days. The dried samples were weighed after removal from the oven, cooled, and then ground up, homogenized, and analyzed for BSi, N, and P content.

In the laboratory, cores for sediment characterization were extracted and the upper 0 – 2 and 2 – 5 cm sediment horizons were retained for subsequent analysis. Microphytobenthos (MPB) biomass at the BS and VS site was determined as chlorophyll-a (Chl-a). Phaeopigments (Pha) were also determined as a proxy for degraded MPB biomass. The BSi, N and P fixed by MPB were then estimated, based on the conversion factor BSi:Chl-a = 14.3:1 g g^{-1} (Sigmon & Cahoon, 1997) and C:Chl-a = 30 g g^{-1}, and converted to N assuming a molar C:N ratio of 9 and to P assuming a molar C:P ratio of 158 (de Jonge, 1980; Kahlert, 1998; Sundback et al., 2000). The remaining sediment slurry from VS and BS sites was analyzed for OM, BSi, N, and P content.

3.2.5. Analytical Methods

Dissolved oxygen was determined using the Winkler method (APHA, 1998). $N\text{-}NH_4^+$ (Koroleff, 1970), $N\text{-}NO_x$ (APHA, 1998), SRP (Valderrama, 1981), and DSi (Golterman et al., 1978) were determined with standard spectrophotometric methods (Perkin Elmer, Lambda 35). An analytical blank that underwent the same procedure as the samples, including filtration, was always analyzed to correct for sample contamination.

Chl-a and Pha were determined spectrophotometrically according to Lorenzen (1967) from 1 cm^3 sediment slurry extracted with 10 mL 90% water-acetone.

Organic matter was determined as loss on ignition at 550 °C with a standard procedure (Azzoni et al., 2015). Total N content was determined using a CHN elemental analyzer (CHNS-O EA 1108 Carlo Erba), while organic P was determined following Aspila et al. (1976).

The BSi content of primary producers was analyzed according to Struyf et al. (2005). In short, 30 mg of dry plant tissue were digested with 30 mL 0.1 M Na_2CO_3 in polypropylene (PP) bottles. During the extraction, samples were constantly shaken for 4 h at 150 rpm in a shaking water bath at 85 °C. Before the analysis, each sample (1 mL of extraction solution) was neutralized with 9 mL of 0.021 M HCl and analyzed using the molybdate blue spectrophotometric method (Golterman et al., 1978).

The total BSi content of sediments was analyzed following DeMaster (1981), by digesting 30 mg of dry sediment with 30 mL of 0.1 M Na_2CO_3 in polypropylene bottles for 5 h at 85 °C. Subsamples were collected after 3, 4 and 5 h and analyzed using the molybdate blue spectrophotometric method (Golterman et al., 1978). Before the analysis, each sample (1 mL of extraction solution) was neutralized with 9 mL of HCl 0.021 M. To correct for the amount of Si resulting from mineral dissolution, the Si content of the subsamples was plotted against dissolution time. The *y*-axis intercept of the linear regression line represents the estimated BSi content. All BSi dissolved within the first 3 h.

3.2.6. Statistical Analyses

Flux data were analyzed with three-way generalized least square (GLS) models, which were run with condition (light and dark), site (RS, VS, BS), and sampling date (Early, Mid, Late) as the main fixed factors (interaction included). To deal with observed heteroscedasticity, it was used the argument "weights" within the function *gls*, and the function *varident* to specify variance models. An *a posteriori* comparison of the means was performed using a post hoc Tukey test. Statistical analyses

were run with the *nmle* (Pinheiro et al., 2016) and *emmeans* (Lenth et al., 2018) packages in R software v. 3.6.0 (The R Core Team, 2019).

All results in text, figures and tables are presented as mean ± standard error.

3.3. Results

3.3.1. Water and Sediment Characteristics

The temperature of the littoral waters of Lake Iseo ranged from 15 °C in April to 28 °C in midsummer. The chemical characteristics of near-bottom waters differed between sites (Table 4).

Table 4. Dissolved silica (DSi), soluble reactive phosphorus (SRP), ammonium ($N\text{-}NH_4^+$), nitrate and nitrite ($N\text{-}NO_x$) and dissolved inorganic nitrogen (DIN) concentration and DSi:DIN, DSi:SRP and DIN:SRP molar ratios in the water column at the three investigated sites (RS = rocky shores; VS = vegetated sediments; BS = bare sediments). All data represents the mean of three replicates (standard error in parenthesis).

Water	**RS**			**VS**			**BS**		
Characteristics	**Early**	**Mid**	**Late**	**Early**	**Mid**	**Late**	**Early**	**Mid**	**Late**
DSi	57	130	225	404	400	494	137	238	490
($\mu g\ Si\ L^{-1}$)	(1)	(5)	(24)	(20)	(39)	(13)	(10)	(10)	(13)
SRP	2	5	2	4	4	2	5	5	2
($\mu g\ P\ L^{-1}$)	(0)	(1)	(0)	(1)	(0)	(0)	(1)	(1)	(0)
$N\text{-}NO_x$	592	509	538	426	376	442	497	420	485
($\mu g\ N\ L^{-1}$)	(4)	(3)	(6)	(7)	(2)	(8)	(8)	(6)	(8)
$N\text{-}NH_4^+$	56	85	63	100	94	89	74	55	54
($\mu g\ N\ L^{-1}$)	(4)	(3)	(3)	(4)	(6)	(3)	(4)	(3)	(5)
DIN	648	595	601	526	470	531	571	476	539
($\mu g\ N\ L^{-1}$)	(5)	(4)	(6)	(4)	(6)	(9)	(9)	(6)	(10)
DSi:DIN	0.04	0.11	0.19	0.39	0.42	0.47	0.12	0.25	0.46
(mol:mol)	(0.00)	(0.00)	(0.02)	(0.02)	(0.04)	(0.01)	(0.01)	(0.01)	(0.01)
DSi:SRP	38	31	109	148	155	309	36	65	262
(mol:mol)	(3)	(4)	(13)	(20)	(26)	(29)	(5)	(5)	(32)
DIN:SRP	863	293	596	395	348	664	307	262	564
(mol:mol)	(88)	(38)	(42)	(55)	(44)	(57)	(40)	(18)	(56)

DSi concentrations were highest at the VS site and lowest at the RS site. While DSi concentrations were constant at the VS site, they increased throughout the season, reaching the same level as those at the BS site, and to a much lesser extent at the RS site. SRP concentrations were <5 μg P L^{-1} and no differences were found between sites. DIN concentrations and their seasonal trends were similar in the three sites, and were mainly driven by N-NO_x which accounted for more than 80% of DIN on average. The DSi:DIN and DSi:SRP ratios conformed to the DSi concentration pattern, the ratios being VS>BS>RS. At both BS and RS, DSi:DIN and DSi:SRP increased throughout the season. At BS, values attained those measured at VS, while at RS, values remained nearly two times lower. On average, molar ratios DSi:DIN = 0.28, DSi:SRP = 132 and DIN:SRP = 37 evidenced that DSi concentrations in the water column were low compared to DIN. SRP was deficient with respect to both DIN and DSi, especially at RS.

The surface sediment was similar at the VS and BS sites - soft and homogenous - although OM, N, and P were slightly greater at VS than at BS (Table 5).

The percent of OM and nutrient content was comparatively higher at station RS, where the sediment was probably enriched by the biomass growing on stones. Accordingly, the average sedimentary BSi concentration was higher at RS (1.00 ± 0.17%) compared to VS (0.79 ± 0.03%) and BS (0.46 ± 0.02%). Similar patterns were also found for total N (0.50 ± 0.08% at RS, 0.33 ± 0.01% at VS, and 0.21 ± 0.00% at BS), and organic P (ranging from 0.11% at RS to 0.01% at both VS and BS). The BSi:N:P stoichiometry highlighted how BSi, when compared to N and P, accumulated preferentially in sediments at VS and BS rather than at RS. While the variation in the BSi:N molar ratio exhibited a narrow range (from 0.72 to 1.38 at all sites), the N:P molar ratio was approximately 10 times lower at RS compared to VS and BS. BSi:P ratios were also higher at VS and BS than at RS, though to a lesser extent.

Table 5. Content of organic matter (OM), biogenic silica (BSi), total nitrogen (N), organic phosphorous (P), chlorophyll a (Chl-a), and phaeopigments (Pha) and BSi:N, BSi:P and N:P molar ratios in sediment at the three investigated sites (RS = rocky shores; VS = vegetated sediments; BS = bare sediments). All data represents the mean ± standard error (standard error in parenthesis), n.a. = not available.

Sediment	RS			VS			BS		
characteristics	Early	Mid	Late	Early	Mid	Late	Early	Mid	Late
OM (% DW)	n.a.	7.23 (0.33)	8.72 (0.27)	4.46 (0.04)	4.00 (0.15)	4.30 (0.05)	2.57 (0.23)	2.57	2.78
BSi (% DW)	n.a.	0.78 (0.02)	1.08 (0.03)	0.89 (0.04)	0.72 (0.05)	0.82 (0.06)	0.54 (0.01)	0.46 (0.02)	0.41 (0.03)
P (% DW)	n.a.	0.10	0.12	0.01 (0.00)	0.01 (0.00)	0.01 (0.00)	0.01 (0.00)	0.01 (0.00)	0.01 (0.00)
N (% DW)	n.a.	0.42	0.58	0.32 (0.01)	0.31 (0.00)	0.35 (0.00)	0.21 (0.01)	0.20 (0.01)	0.21 (0.01)
BSi:N (mol:mol)	n.a.	0.98	0.72	1.37 (0.01)	1.16 (0.08)	1.16 (0.06)	1.27 (0.03)	1.19 (0.05)	0.98 (0.05)
BSi:P (mol:mol)	n.a.	9.07	7.49	77 (1)	66 (4)	67 (3)	91 (4)	79 (2)	56 (6)
N:P (mol:mol)	n.a.	9.23	10.35	57 (2)	58 (2)	58 (2)	72 (4)	66 (1)	57 (3)
Chl-a (mg m^{-2})	n.a.	21 (3)	42 (7)	141 (5)	190 (23)	196 (22)	193 (34)	220 (15)	288 (12)
Pha (mg m^{-2})	n.a.	5 (1)	7 (1)	146 (1)	97 (10)	136 (12)	55 (9)	40 (3)	79 (4)

On the areal basis, the total quantity of OM, N, and P in the 0–2 cm sediment horizon was almost constant within each site, but with differences between sites, with VS > BS >> RS (Table 6). The BSi bulk decreased from early to late phases at both VS (33.4 to 23.8 mg Si m^{-2}) and BS (25.9 to 20.2 mg Si m^{-2}), whereas it increased at RS (0.5 to 0.8 mg Si m^{-2}) (Table 6).

Table 6. Features of organic matter (OM), biogenic silica (BSi), organic nitrogen (N), organic phosphorous (P), chlorophyll a (Chl-a) and phaeopigments (Pha) and BSi:N, BSi:P and N:P molar ratios in the 0-2 cm sediment horizon at the three investigated sites (RS = rocky shores; VS = vegetated sediments; BS = bare sediments). All the data are mean ± standard error (standard error in parenthesis), n.a. = not available.

	RS			VS			BS		
	Early	Mid	Late	Early	Mid	Late	Early	Mid	Late
OM ($g\ m^{-2}$)	n.a.	767	1500	539 (30)	479 (23)	500 (15)	329 (18)	333 (5)	358 (23)
BSi ($g\ m^{-2}$)	n.a.	0.47 (0.06)	0.75 (0.09)	33 (1)	25 (1)	24 (1)	26 (1)	24 (1)	20 (1)
P ($g\ m^{-2}$)	n.a.	0.06 (0.01)	0.11 (0.01)	0.48 (0.00)	0.43 (0.01)	0.39 (0.01)	0.32 (0.02)	0.34 (0.01)	0.41 (0.03)
N ($g\ m^{-2}$)	n.a.	0.24 (0.03)	0.52 (0.06)	4.86 (0.14)	4.39 (0.13)	4.10 (0.20)	4.08 (0.03)	4.04 (0.09)	4.22 (0.15)
BSi:N (mol:mol)	n.a.	0.98	0.72	1.37 (0.01)	1.16 (0.08)	1.16 (0.06)	1.27 (0.03)	1.19 (0.05)	0.98 (0.05)
BSi:P (mol:mol)	n.a.	9.07	7.49	77 (1)	66 (4)	67 (3)	91 (4)	79 (2)	56 (6)
N:P (mol:mol)	n.a.	9.23	10.35	57 (2)	58 (2)	58 (2)	72 (4)	66 (1)	57 (3)
Cha ($mg\ m^{-2}$)	n.a.	21 (3)	42 (7)	140 (5)	190 (23)	196 (22)	193 (34)	220 (15)	288 (12)
Pha ($mg\ m^{-2}$)	n.a.	5 (1)	7 (1)	146 (1)	97 (9)	136 (12)	55 (9)	40 (3)	79 (4)

3.3.2. Primary Producer Biomass and Elemental Composition

The benthic community at RS was dominated by filamentous epilithic macroalgae (EA), specifically by *Cladophora glomerata* (Linnaeus) Kützing in late spring to early summer, and by *Spirogyra* spp. in late summer (Table 7). To sum up, the total biomass of filamentous algae decreased from early (63 ± 19 g $_{DW}$ m^{-2}) to late summer (39 ± 22 g $_{DW}$ m^{-2}). At the VS site, SAV biomass followed a clear seasonal pattern with the highest values in midsummer (Table 7). The SAV was mainly composed of *Vallisneria spiralis* and, to a lesser extent, of *Najas marina*. *Chara globularis* Thuiller, *Lagarosiphon major* (Ridl.) Moss, *Myriophyllum spicatum* L., *Ceratophyllum demersum* L., and *Elodea nuttallii* (Planch.) H. St. John occurred occasionally, contributing up to a maximum of 25% of the total biomass. At the BS site, the bare sediment was colonized by MPB, with Chl-a values ranging from 193 to 288 mg m^{-2} (Table 5). Here, rare and small individuals of *C. globularis* were also detected, but with negligible biomass. Microalgae also colonized hard substrata and sediment at RS and VS, attaining Chl-a concentrations from between 21 (RS) and 196 (VS) mg m^{-2} (Table 5).

The Pha content, a proxy for degraded vegetal biomass, clearly decreased from macrophyte covered to bare sediments and hard substrates in the order VS > BS > RS (Table 5).

Table 7. Biomass (B, g $_{DW}$ m^{-2}), biogenic silica (BSi, %), nitrogen (N, %) and phosphorus (P, %) content and BSi:N, BSi:P and N:P molar ratios in filamentous algae and macrophytes (leaves and roots). All data represents mean ± standard error (standard error in parenthesis), n.a. = not available.

Primary producer		Seasonal phase	B	BSi	N	P	BSi:N	BSi:P	N:P
Filamentous algae		Early	62 (19)	3.36 (1.03)	0.86 (0.26)	0.07 (0.02)	0.98	62	63
		Mid	48 (21)	1.41 (0.40)	0.23 (0.06)	0.01 (0.00)	1.54	141	91
		Late	30 (22)	0.75 (0.20)	0.19 (0.05)	0.01 (0.00)	0.98	106	108
Vallisneria spiralis	Leaves	Early	99 (36)	0.72	3.64	0.22	0.10	4	37
		Mid	206 (16)	1.00	2.35	0.13	0.21	9	40
		Late	117 (11)	0.91	2.45	0.10	0.19	10	54
	Roots	Early	60 (22)	0.48	2.92	0.16	0.08	3	40
		Mid	125 (9)	0.50	2.61	0.17	0.10	3	34
		Late	70 (13)	0.33	3.32	0.16	0.05	2	46
Najas marina	Leaves	Early	4	n.a.	n.a.	n.a.	n.a.	n.a.	n.a.
		Mid	97 (27)	0.64	2.82	0.27	0.11	3	23
		Late	54 (17)	0.85	1.95	0.15	0.22	6	29
	Roots	Early	n.a.	n.a.	n.a.	n.a.	n.a.	n.a.	n.a.
		Mid	15 (4)	0.61	1.83	0.12	0.17	6	34
		Late	n.a.	n.a.	n.a.	n.a.	n.a.	n.a.	n.a.

The BSi content was greater in the biomass of *C. glomerata* and *Spirogyra* ssp. (up to 5.5%) compared to the content recorded in *V. spiralis* and *N. marina* (up to 1.1%). In *V. spiralis*, the BSi content was higher in leaves than in roots, and was greater than in *N. marina*, in which roots and leaves exhibited a similar content (Table 7). In contrast, N and P content in filamentous algae were

1.7 – 3.0 times lower than in macrophytes, attaining values from 2.3 to 3.6% (N) and from 0.10 to 0.22% (P) in the above ground biomass of *V. spiralis,* and from 1.9 to 2.8% (N) and from 0.15 to 0.27% (P) in the above ground biomass of *N. marina*. In the same way, N and P content in belowground biomass were similar to those recorded above ground (Table 7). As a consequence the BSi:N:P stoichiometry in plant biomass differed between sites. At RS, the BSi:N molar ratio of macroalgae ranged from 2.0 to 3.1 and the BSi:P molar ratio ranged from 56 to 127, both attaining maximum values in midsummer.

Concurrently, the N:P molar ratio increased from 29 in spring to 49 in late summer. At VS, both BSi:N and BSi:P in macrophytes biomass were much lower, i.e., 0.06 to 0.19 (BSi:N) and 2.5 to 9.2 (BSi:P). Furthermore, the BSi:P ratio was greater in the leaves than in the roots of *V. spiralis*.

The standing stocks of BSi, N and P (Figure 16) retained by primary producer biomass varied between sites and throughout the season. The BSi stock was greater at RS than at VS. At RS, BSi underwent an abrupt decrease in midsummer, attaining a value similar to VS in late summer. In contrast, at the BS site, BSi associated with MPB progressively increased and was much greater than at RS and VS, especially from midsummer onwards.

At the VS site, BSi was mostly retained by the leaves, while only a small fraction accumulated in the roots. Both N and P stocks followed a different pattern, i.e., VS > BS > RS. However, while biomass-N decreased throughout the summer at both RS and VS, it remained steadily constant at BS. In addition, at VS, the nitrogen decrease was mainly accounted for by leaves, while it accumulated in roots in late summer. The P stocks accounted for by the different primary producer assemblages was always low and often negligible, when compared to BSi and N.

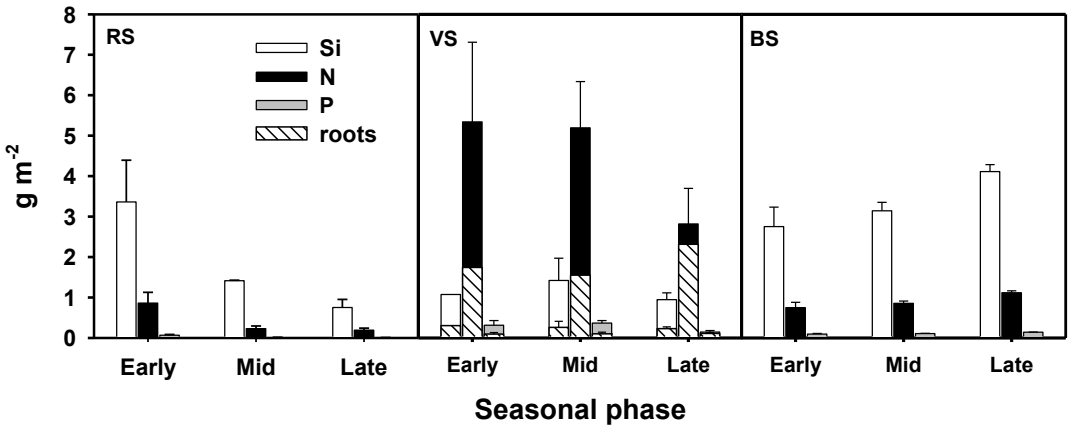

Figure 16. Biogenic silica **(**BSi), nitrogen (N), and phosphorus (P) stocks in the primary producer biomass in the three sampling periods. Error bars represent standard error (n = 6). Legend: RS = rocky shores; VS = vegetated sediments; BS = bare sediments. At site BS, BSi, N, and P were estimated from sedimentary Chl-a.

3.3.3. Oxygen Fluxes and Gross Primary Production

Oxygen fluxes differed significantly between light and dark conditions, among sites, and throughout the season (Figure 17, Table 8). At RS, both light and dark oxygen fluxes, as well as the resulting gross primary production (GPP), decreased from the early phase to the late seasonal phase. In contrast, at VS and, to a lesser extent, at BS, both dark and light fluxes and GPP peaked in midsummer.

Table 8. Summary of the results of two-way generalized least square (GLS) models of benthic oxygen (O_2), dissolved silica (DSi), soluble reactive phosphorus (SRP), nitrate and nitrite ($N\text{-}NO_x$), ammonium ($N\text{-}NH_4^+$) and dissolved inorganic nitrogen (DIN) fluxes. Significant (p <0.05) outcomes are highlighted in bold.

Source of Variation	DF	**O_2**	**DSi**	**SRP**	**$N\text{-}NO_x$**	**$N\text{-}NH_4^+$**	**DIN**
Site	2	**<0.001**	**<0.001**	**<0.050**	**<0.001**	**<0.001**	**<0.001**
Condition	1	**<0.001**	0.182	0.811	0.224	**<0.001**	**<0.001**
Sampling date	2	0.210	0.185	0.263	**<0.001**	**<0.001**	0.109
Site*Condition	2	**<0.001**	0.703	0.304	0.699	0.067	0.601
Site* Sampling date	4	**<0.001**	**<0.001**	0.467	0.346	**<0.001**	0.946
Condition* Sampling date	2	**<0.001**	0.108	0.587	0.488	**<0.001**	**<0.010**
Site*Condition* Sampling date	4	**<0.001**	0.550	0.533	**<0.001**	0.879	**<0.050**

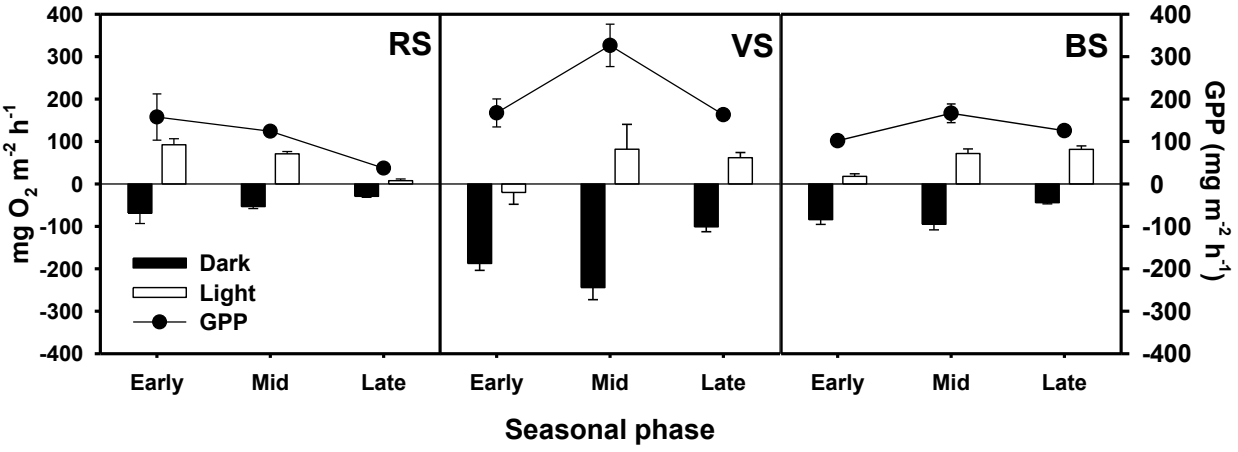

Figure 17. Light and dark oxygen fluxes (O_2) and gross primary production (GPP) measured in the three sampling sites in the different sampling dates. Error bars represent standard error (n = 6). Legend: RS = rocky shores; VS = vegetated sediments; BS = bare sediments.

At VS, the daily net oxygen flux was always negative, with a minimum in early summer (−2156 ± 417 mg O_2 m^{-2} d^{-1}). On the contrary, the net daily oxygen flux was positive at RS in the early phase at its peak (834 ± 269 mg O_2 m^{-2} d^{-1}) and in midsummer (582 ± 42 mg O_2 m^{-2} d^{-1}), becoming negative only in the late phase (−185 ± 67 mg O_2 m^{-2} d^{-1}). At BS, a slightly positive trend occurred during the sampled period: daily oxygen fluxes oscillated from a negative value in early summer (−590 ± 144 mg O_2 m^{-2} d^{-1}) to a positive value in late summer (322 ± 96 mg O_2 m^{-2} d^{-1}).

3.3.4. Nutrient Fluxes across the Water Sediment Interface

Differences in dissolved silica (DSi) fluxes were statistically significant between sites, but showed no evident difference between light and dark conditions or between dates (Figure 18; Table 8). The interaction between sites and seasonal phases was probably due to the steep decrease of DSi fluxes from late spring to mid-summer at the VS site. At the RS site, DSi fluxes were steadily negative from spring to fall, indicating a consistent uptake, although on average the extent of the flux was low. Dark silica fluxes were always positive at VS, while under light condition, they decreased from a marked release in late spring to a small uptake in late summer.

Over the time span of this study, daily fluxes of DSi were on average negative at the RS site (−20 ± 6 mg Si m^{-2} d^{-1}), which indicates uptake by epilithic algae and sediment. Conversely, they were positive at the VS site (121 ± 49 mg Si m^{-2} d^{-1}) and the BS site (34 ± 19 mg Si m^{-2} d^{-1}), highlighting a net DSi release, even in late summer, when a small uptake was detected under light conditions.

Fluxes of soluble reactive phosphorus (SRP) were low and exhibited a large amount of variability, ranging from −0.5 to 0.7 mg P m^{-2} d^{-1} (Figure 18). Only the differences between sites were statistically significant (Table 8). However, weak seasonal patterns were also identified at BS, where uptake under light decreased from the early to the late phase, whereas SRP release from sediment to the water column simultaneously increased. At the VS site, SRP was mainly released from sediment to the water column, with the only exception of a slight uptake in midsummer, when GPP peaked.

N-NO_x fluxes were statistically different between sites and dates (Table 8). At the RS site, they were negligible, exhibiting a large amount of variability, while at VS and BS, uptakes up to almost −10 mg N m^{-2} h^{-1} were detected in early summer (Figure 18). Patterns of N-NH_4^+ fluxes were almost specular to N-NO_x, as N-NH_4^+ was steadily released from the sediment to the water column. Differences between sites and with relation to light and dark conditions were also clearly evidenced (Figure 18, Table 8).

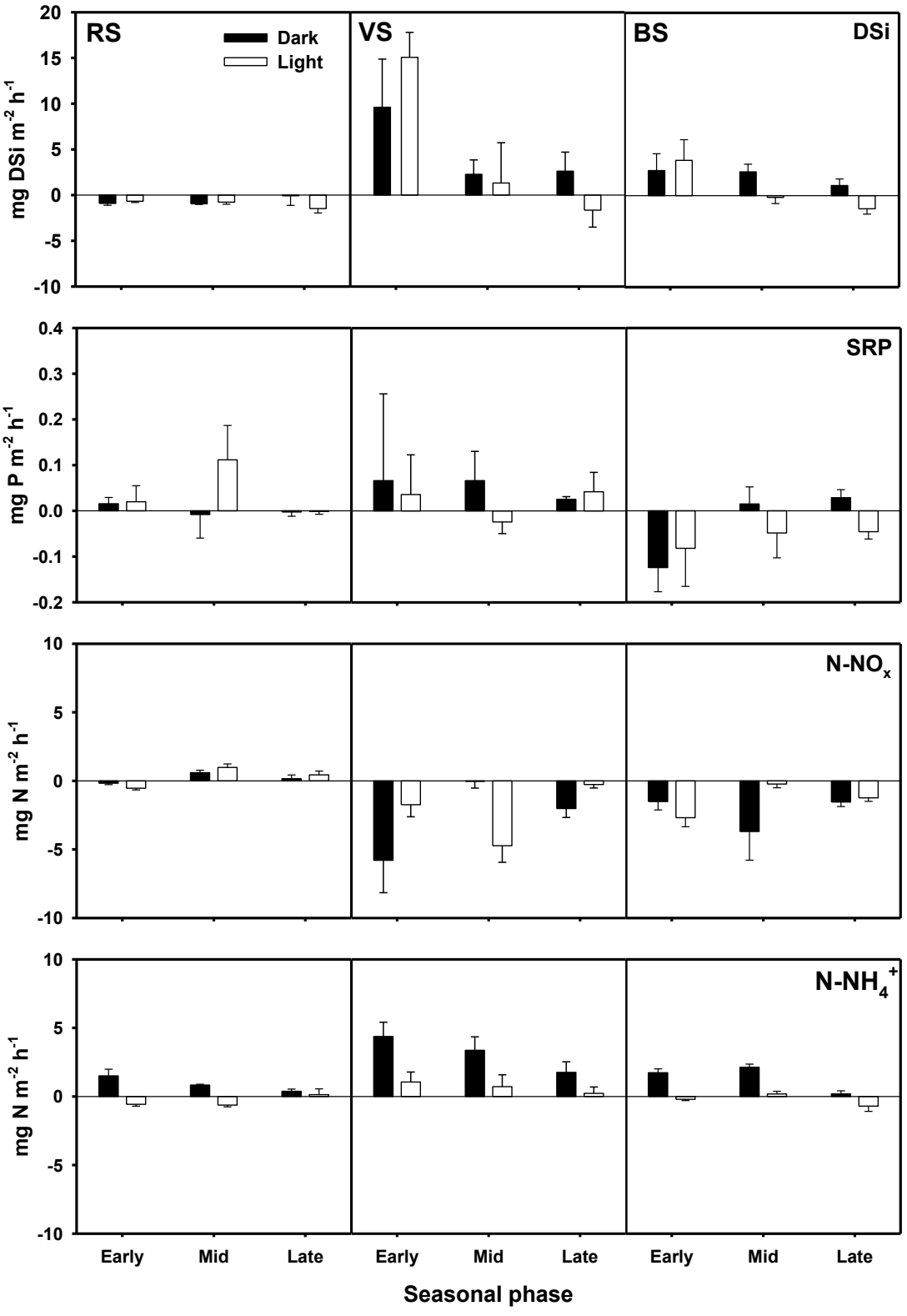

Figure 18. Light and dark fluxes of dissolved silica (DSi), soluble reactive phosphorus (SRP), nitrate and nitrite ($N\text{-}NO_x$), and ammonium ($N\text{-}NH_4^+$) measured in the three sampling sites at the different dates. Error bars represent standard error (n = 6). Legend: RS = rocky shores; VS = vegetated sediments; BS = bare sediments.

To some extent, the benthic system was a net sink of dissolved inorganic nitrogen (DIN) under light conditions at VS and BS, while dark flux data was strongly affected by spatial and temporal heterogeneity. In contrast, the benthic system was a small DIN source (0.6 ± 0.2 mg N m^{-2} h^{-1}) at RS. Differences between sites were also revealed by the stoichiometry of DSi, DIN, and SRP fluxes, with RS behaving in a much more diverse way than BS and VS (Figure 19).

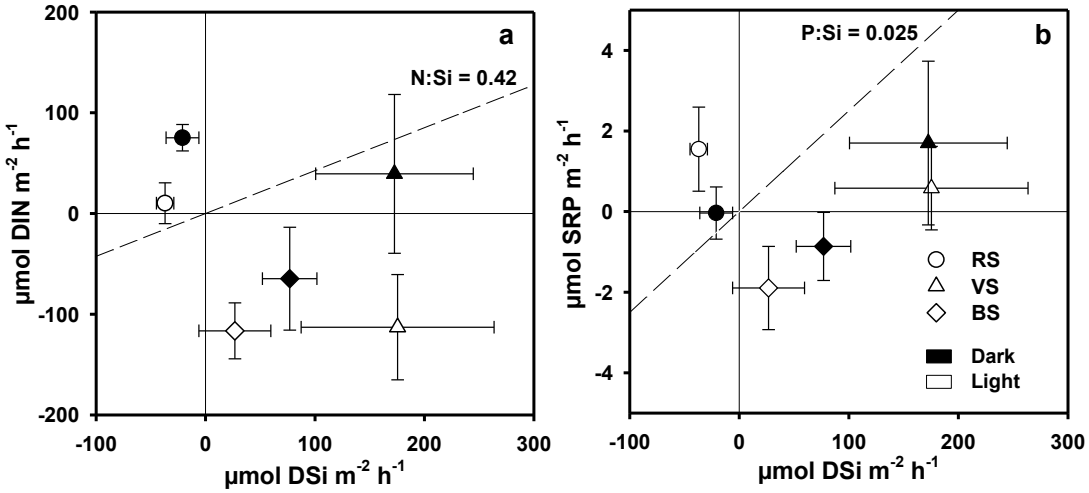

Figure 19. Average DSi:DIN (**a**) and DSi:SRP (**b**) ratios of benthic fluxes under light and dark conditions in the three sampling sites. Error bars represent standard error (n = 18). Legend: RS = rocky shores; VS = vegetated sediments; BS = bare sediments.

3.4. Discussion

In this work, Si accumulation and recycling was assessed with respect to N and P in the littoral zone of Lake Iseo. These issues are little studied but of relevance given the importance of Si for primary producer growth, as they can provide new insights into the role of benthic processes that regulate DSi bioavailability. Several papers focus on DSi fluxes in similar systems, i.e., shallow brackish and freshwater ecosystems, but less is known about the BSi content of surface sediments, EA, and SAV biomass. Overall, while DSi fluxes measured in the present study fall within the ranges reported in the literature (Table 9), comparisons are less reliable for sedimentary BSi, since there is scarce data available.

Table 9. Sedimentary DSi fluxes (μg Si m^{-2} h^{-1}) and BSi content (%) in sediments of different aquatic ecosystems. Legend: MPB = microphytobenthos, bare = bare sediment, algal = benthic macroalgae.

Reference	System	Depth (m)	Condition	DSi Flux (mg Si m^{-2} h^{-1})	BSi (%)	Method *
(Newberry & Schelske, 1986)	lake		Bare	2.3 – 4.6	10.2 – 15.9	1
(Kelderman et al., 1988)	lake	3	MPB	−1.6 –11.5		
(Conley et al., 1988)	lake		Bare	2.6 – 11.8	1.0 – 22.0	2
(House et al., 2000)	river		Bare	1.0 – 4.0		
(Bartoli et al., 2003)	coastal lagoon		MPB	light −0.01 ± 0.08 dark 1.40 ± 0.20		
(Friedrich et al., 2003)	coastal lagoon	2 – 4	Bare	1.2 – 29.9		
			Uptake	3.8 – 28.7		
(Ferris & Lehman, 2007)	lake	5 – 10	Bare	3.1 ± 0.3	1.7	1
(Spears et al., 2008)	lake	3.9	MPB	light −2.3 – 21.9 dark −2.0 – 15.13		
(Hobbs et al., 2010)	lake	20	Bare	0.05	0.4 – 1.5	1
(Trachsel et al., 2010)	lake		Bare	0.1 – 3.4	0.2 – 1.4	1
(Tallberg et al., 2013)	coastal	33	Algal	0.28 – 3.36		
(Aigars et al., 2015)	coastal	44 – 45	Bare	1.1 – 2.9		
(Tallberg et al., 2017)	costal	2 – 7	Bare	0.7 – 5.7		

* Method used to analyze BSi: Na_2CO_3 (1) and NaOH (2).

The littoral zone is a filter between terrestrial and aquatic ecosystems, which can retain or release DSi, DIN, and SRP through primary production, grazing, detritus decomposition and mineralization, etc. (Wetzel & Likens, 1991). In general terms, the results identify the components of the benthic communities that primarily account for the filtering capacity of lakes and lentic waters. In addition, lentic waters are key components of fluvial filters, which can selectively remove, retain, or release nutrients and chemical elements into outflowing waters (Ittekkot et al., 2000; Meybeck & Vörösmarty, 2005).

The comparative contribution of SAV, MPB and EA to BSi storage and DSi fluxes is shown in Figure 20. Surprisingly, despite the fact that the primary producers considered in this study accumulated BSi, the littoral zone was on average a DSi source to the water column, especially the SAV meadow. However, the littoral zone was heterogeneous and patchy with two contrasting features that depend on hydro-morphology – i.e., flat, soft sediments and steep, hard (rocks and pebbles)

substrates – which in turn shape the dominant community. On account of these differences, process rates and DSi outcomes were variable between the littoral communities due to the fact that the primary producers colonizing each area exhibited a distinct preference for Si. The SAV meadows and MPB patches were a net DSi source, while only EA assemblages on rocky substrates were a net sink.

3.4.1. BSi Storage in Primary Producer Biomass and Surficial Sediment and BSi, N, and P Stoichiometry

Submerged vegetation in the littoral zone accumulated Si, but differences among species were observed. As far as I know, this study is the first to report data on BSi content in *Vallisneria spiralis*, since previously published data gathered from Lake Maggiore by Gommes & Muntau (1981) did not distinguish between BSi and other Si forms. In addition, only a single value was found (BSi = 0.02%) for *Najas marina*, which grew in a turbulent, turbid, and presumably light-limited aquatic system (Xing et al., 2013). The BSi content of SAV species measured in this study falls in the lower range of values (0.7 – 2.8%) detected for phanerogam species in shallow freshwater ecosystems, including running waters (Schoelynck et al., 2010; Schaller et al., 2016; Schoelynck & Struyf, 2016). Usually, macrophytes are expected to have a lower BSi content in lakes than in rivers, since physical stressors, e.g., current velocity and turbulence, can stimulate BSi assimilation, thus conferring resistance against drag forces (Schoelynck et al., 2012).

In *N. marina,* the Si, N, and P stoichiometry in the above- and below-ground biomass was similar. On the contrary, *V. spiralis* tended to accumulate more BSi in its leaves, also with respect to N and P, than in its roots. The difference between species can be explained by the ability of *V. spiralis* to exploit deep sediment layers, thanks to its long roots. Studies in the same area of Lake Iseo demonstrate that DSi concentrations are greater in pore waters of bare sediments than in sediments colonized by *V. spiralis* (Racchetti et al., 2011). SAV species can, therefore, increment the transport of Si from sediment to the water mass. This capacity to take up DSi is reduced by organic enrichment of sediment, as demonstrated for N and P (Soana et al., 2015).

In rocky shores, the strong dominance of diatoms and the high Si:N and Si:P ratios in macroalgae tissues can account for Si accumulation, exceeding N and especially P uptake, despite a lower plant biomass (Bartoli et al., 2003; Carrick & Lowe, 2007; Malkin et al., 2009; Cao et al., 2019). It was found that the P content in epilithic biomass was close to or below the lower limit of the optimal range for growth (0.01 – 0.02%) reported for epilithic primary producers (Müller, 1983; Riber et al., 1983; Swift & Nicholas, 1987; Grimshaw et al., 1993). The actual molar C:N:P = 443:23:1 at RS also evidenced a P and, to a lesser extent, N shortage, when compared to the optimal ratio for periphyton growth, i.e., C:N:P = 119:17:1 (Hillebrand & Sommer, 1999). In contrast with what was found at the

RS site, SAV species at VS efficiently accumulated N and P. These elements exhibited a seasonal pattern similar to the BSi one, with a peak in the early phase and a sharp decrease in the later part of the season (Figure 16). Such a pattern can be explained by both leaf detachment (Pinardi et al., 2009; Ghirardi et al., 2019) and element translocation from leaves to roots and rhizomes. Both processes usually occur at the end of the vegetative growth phase.

The BSi stock was high at VS and less high at RS, but values were comparable with those of other studies (Malkin et al., 2009; Schoelynck et al., 2010, 2012; Carey & Fulweiler, 2013a; Schaller et al., 2016; Schoelynck & Struyf, 2016). In these analysis, the BSi bulk was on average 24 – 33 g Si m^{-2} in the SAV meadow, of which 6 – 12% was accounted for by MPB and by SAV fresh detritus, while in bare sediments at BS, BSi was 20 – 25 g Si m^{-2}, of which 11–20% was from MPB (Table 6). In contrast, the BSi stock at RS was one order of magnitude lower than VS and BS sites and comprised between 2 – 4 g Si m^{-2}, of which 60 – 80% was from epilithic macro- and microalgae. Accumulated debris at the rocky site contributed only 0.47 – 0.75 g Si m^{-2}. The nutrients stored in the biomass were relevant compared to the nutrient content in the overlying water. At RS and BS sites, BSi in primary producers resulted one order of magnitude higher than DSi in overlying water, while at the VS site, it was four times higher than DSi in overlying water (Figure 20).

In this study, it was not quantify the amount of Si retained in the biomass of epiphytes growing on SAV leaves and filamentous macroalgae. Previous studies reported that epiphyte biomass on macrophytes varies greatly, from a negligible amount up to the same quantity as the host biomass, and depends on plant morphology, light, nutrient availability, and allopathic effects (Toporowska et al., 2008; Pettit et al., 2016). The BSi stocks in SAV and EA communities in this study should, therefore, be considered as a conservative estimate, since the microalgal epilithic community is commonly depicted as being very efficient in storing and retaining nutrients (Vadeboncoeur & Steinman, 2002). Additionally, diatoms are an important component of the epiphytic communities (Burkholder & Wetzel, 1989; Cattaneo et al., 1998; Malkin et al., 2009) and accumulate a large quantity of BSi. For example, epiphytic diatoms on *Cladophora glomerata* can store up to ~15% BSi, a larger amount than the BSi content stored by *C. glomerata* itself (Malkin et al., 2009).

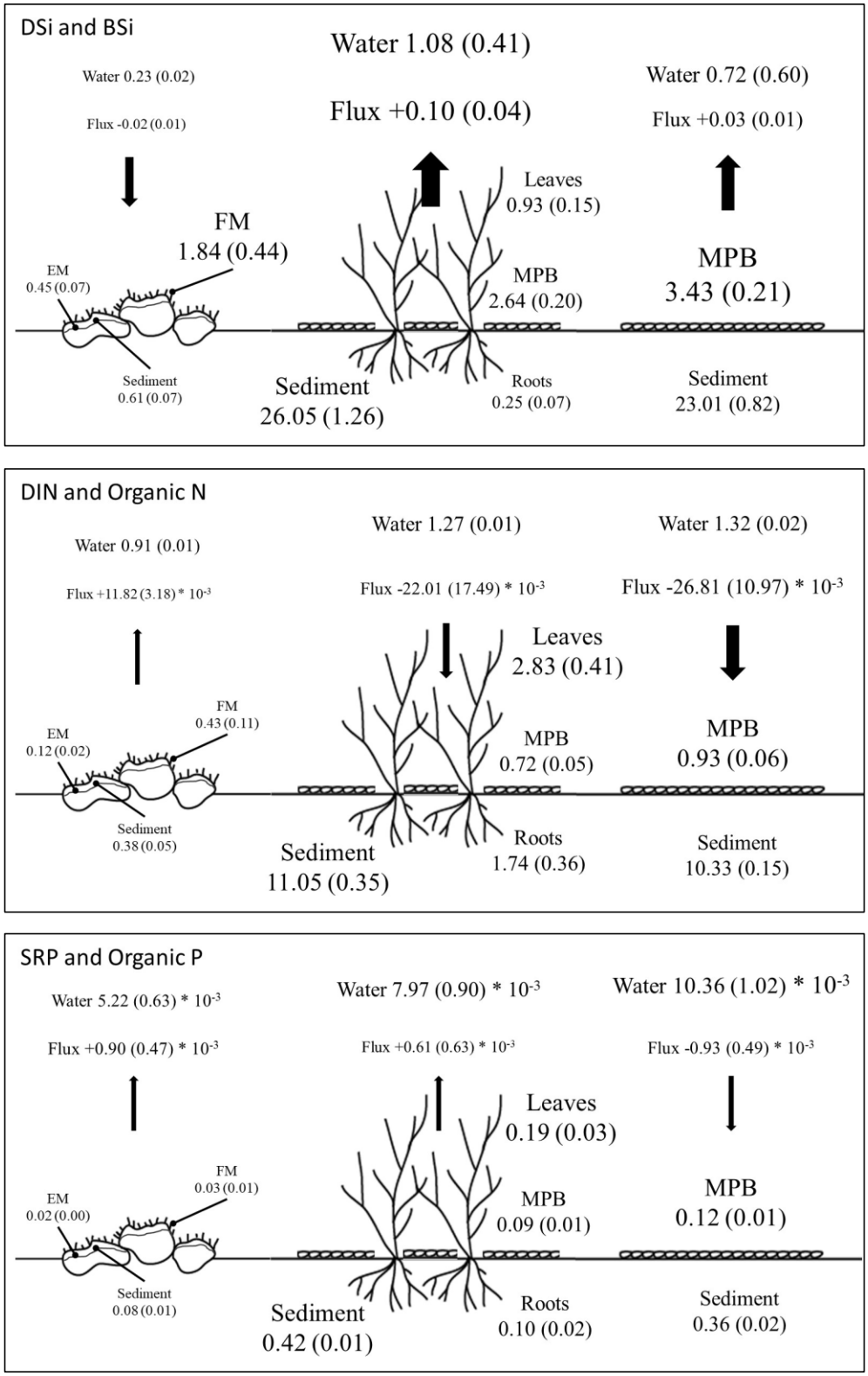

Figure 20. Average water column concentrations, main fluxes, and compartments of Si, N, and P. Fluxes are reported as g m^{-2} d^{-1}, while water concentrations, sediment, microphytobenthos (MPB), epilithic matter (EM), filamentous matter (FM), leaves and roots contents are reported as g m^{-2}. Standard error is shown in parenthesis. The size of numbers and letters is proportional to flux and stock extent.

3.4.2. DSi, DIN, and SRP Fluxes across the Water Sediment Interface

Over ~4 months, from June to September, in the 0 – 2 cm sediment horizon in *V. spiralis* meadows, an average BSi decrease of 9.6 g Si m^{-2} was estimated, representing the difference between the initial and final areal BSi concentrations (Table 6). In the same site, the average DSi release from sediment to the water column obtained from net daily fluxes integrated over the same time span (Figure 20) was 12.8 g Si m^{-2}. At the BS site in the bare sediment, the BSi loss from the 0 – 2 cm horizon calculated in the same way was 5.7 g Si m^{-2}, while the net DSi efflux for the same period was 3.9 g Si m^{-2}. The concordance between the decrease of sedimentary BSi bulk and fluxes demonstrates how both vegetated and bare sediments were a net source of DSi, probably resulting from BSi dissolution, with the DSi efflux from the SAV meadow being almost three times greater than in bare sediment. These findings corroborate the hypothesis that SAV can mediate the DSi transport from pore water to the water column. Otherwise, silica fluxes were important when compared to overlying water: the DSi released at BS and VS sites represented 4.2% and 9.3% of DSi in the water column.

At both the VS and BS site, BSi decreased mainly during the early part of the season, with a negligible amount of efflux from sediment in late summer. Furthermore, the sedimentary DSi flux under both light and dark conditions was related to the sedimentary areal BSi (Figure 21). This pattern was probably due to the fast decay of detrital BSi from different sources, primarily SAV and its epiphytes, which are known to have a short half-life of just a few weeks (Spears et al., 2008). It is likely that part of the lost BSi was taken up and retained by SAV, but then exported from the meadow as detached leaves (Ghirardi et al., 2019). The Si assimilation by MPB accounted for a slight BSi increase at the BS site (Figure 16) but, at <1 g m^{-2}, it was not sufficient to compensate for the total BSi loss. In contrast, the rocky site accumulated BSi and the DSi flux was always directed from the water column to the epilithic algal community. DSi uptake at this site can be explained by the higher Si demand of the EA community, as evidenced by the higher BSi content in macroalgal tissues. However, despite the higher BSi tissue concentration, the total BSi bulk at this site was one order of magnitude lower than in SAV meadows and bare sediments as a consequence of lower plant biomass and sediment accumulation on rock surfaces.

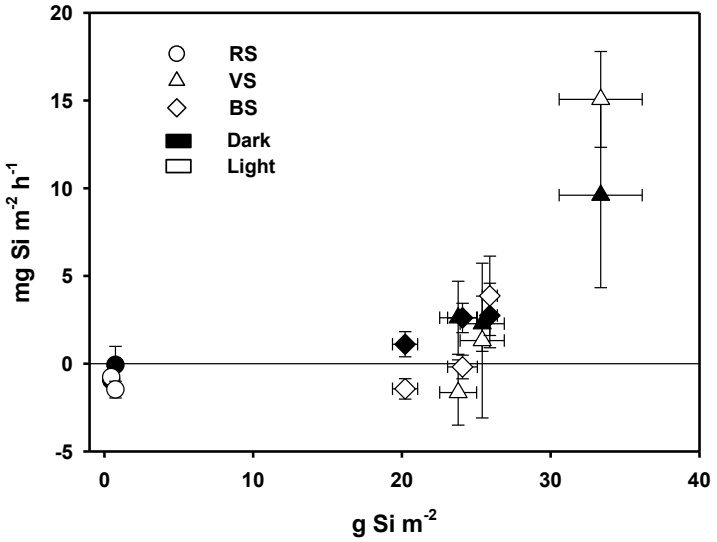

Figure 21. Average Si content in sediments and Si benthic fluxes under light and dark conditions in the three sampling sites. Error bars represent standard error.

To sum up, from late spring to late summer, the soft bottom in the littoral zone of Lake Iseo appeared to perform as a DSi source and, comparatively, as DIN and SRP sink, whereas the steep, rocky shore behaved as a DSi sink and DIN and SRP source. Such DIN and SRP patterns are not unexpected because in shallow and soft organic sediments, nitrate can be denitrified (Nizzoli et al., 2014, 2018), while SRP can be either assimilated or co-precipitated (Moore et al., 1998; Reynolds & Davies, 2001; Pinardi et al., 2009). Moreover, the high Si:N and Si:P ratios in macroalgal tissues can explain the Si consumption in RS, which exceeds N and especially P uptake.

3.4.3. The Fate of DSi in the Littoral Zone in Relation to Submerged Aquatic Vegetation

Human activity and its impact on lake ecosystems is mainly concentrated along the shore, where the coupling of terrestrial and aquatic systems is particularly evident (Francis et al., 2007). Urban development, fluctuation of water levels, tourism, and pollution from diffuse or point sources contribute to the direct or indirect impairment of the structure and composition of benthic primary producer communities. The results of this work pose the question of whether modification of the littoral zone alters its filtering capacity and ultimately the availability of DSi in the water column.

The filtering capacity of littoral zones can be impaired by eutrophication and degenerative processes resulting from organic enrichment (Viaroli et al., 2008; Soana et al., 2015). Like many other littoral zones, the southern part of Lake Iseo is under the influence of coastal runoff (Barone et al., 2019). Such stressors can affect the health status of the extensive SAV meadows, which also

undergo a great inter-annual variability (Ghirardi et al., 2019). Here, in soft, shallow sediments, meadows of *V. spiralis*, and to a much lesser extent *N. marina*, can produce dense biomass covering up to 100 ha, while zones with sparse SAV usually spread over an additional 300 – 400 ha (Ghirardi et al., 2019). In eutrophic waters, *V. spiralis* develops a large leaf mass, which is known to detach and drift due to waves and currents (Donnermeyer & Smart, 1985; Pinardi et al., 2009). In the River Mincio, close to Lake Iseo, during the maximum growth phase, a very rapid leaf renewal was reported with plastochrone intervals of ~3 days (Pinardi et al., 2009). Under these conditions, the standing biomass is affected by a consistent leaf loss, resulting in a floating mass, which can also be detected in satellite images (Ghirardi et al., 2019). In addition, *V. spiralis* often undergoes uprooting, which exposes bare sediments to microphytobenthos colonization. Uprooting can be triggered by the organic enrichment of sediment, which stimulates oxygen consumption, exceeding the capacity of *V. spiralis* to supply oxygen to the rhizosphere (Soana et al., 2015). The oxygen balance in the rhizosphere can be also impaired by epiphytes growing on leaves as they settle, thus accreting organic deposits on the surface sediment (Viaroli et al., 1996). Simultaneously, the epiphyte cover can limit light accessibility to *V. spiralis*, negatively affecting photosynthesis and oxygen transport to roots, which triggers a negative feedback loop leading to plant dieback (Viaroli et al., 2008; Soana et al., 2015). In 2017, in the littoral meadows of Lake Iseo, a bare sediment zone up to 67 ha was exposed as a result of uprooting, and was probably replaced by MPB (Ghirardi et al., 2019). In the light of this development, the question arose as to how this large-scale loss of SAV communities alters Si cycling at the land–water interface. When SAV was active, the DSi flux towards the water column was 12.8 g Si m^{-2} during the entire summer, while in the same zone and during the same period, the bare sediment released only 3.9 g Si m^{-2}. The disappearance of pristine SAV communities could, therefore, potentially decrease DSi recycling and its availability in the water column, with direct repercussions on phytoplankton species composition, as Si shortage strongly impacts phytoplankton, driving the communities towards ones dominated by noxious or harmful algae (Glibert, 2017).

3.5. Conclusions

One of the main findings of this study is that macro- and microalgae communities on rocky substrates behave as a DSi sink and are a source of inorganic nitrogen and phosphorus for the water column. In contrast, littoral sediments colonized by submerged aquatic vegetation and microphytobenthos behave as a DSi source for the water column and as a sink for inorganic nitrogen and phosphorus. *Vallisneria spiralis*, in particular, can transfer DSi from pore-water to the overlying water column through BSi synthesis and mineralization. This pathway can be a relevant DSi source,

compensating or at least contrasting Si losses due to sedimentation and segregation in the deeper water mass as shown and discussed in Chapter 2. This is a key issue for oligomictic and, especially, meromictic lakes, which do not completely overturn.

The capacity of SAV to simultaneously control both Si and N and P cycling depends on the health status of the community. This aspect should not be ignored when considering the anthropogenic impact from watersheds and lake surroundings. Recent studies have demonstrated that SAV meadows can suffer deterioration and leaf detachment at a greater rate than the expected physiological one, with even uprooting events taking place. A challenging issue is to assess what the fate of such organic matter bulk is, and how this can contribute to self-sustain lake deterioration.

4. Speciation and Stoichiometry of Silica, Nitrogen and Phosphorus in Riverbed Sediments in Relation to Hydrological Variability

4.1. Introduction

Multiple pressures and impacts due to climate change and local hydrological and morphological alterations are increasingly threatening aquatic ecosystems (Bouwman et al., 2013; Carey & Fulweiler, 2013a; Datry et al., 2017b; Maranger et al., 2018). In particular, lotic ecosystems have been recognized as extremely sensitive (Sala et al., 2000; Hotaling et al., 2017). Hydrology is expected to meet deep modifications, with many riverine systems experiencing altered flow regimes, marked by higher occurrence of extreme events (floods and droughts) in terms of frequency, intensity and unpredictability (Cooper et al., 2013; Acreman et al., 2014; Acuña et al., 2014). These modifications influence abiotic features, biotic community structure, ecosystem functioning and service provision (Schimel et al., 2007; Bonada & Resh, 2013; Arce et al., 2014; Abril et al., 2016). Changes in water flow are particularly accentuated during the summer period when water diversion and groundwater extraction, associated with low precipitation and land-use alteration, decrease water flow. Among the most relevant effects of flow decrease there is the loss of lateral and longitudinal connectivity, the reduction of the submerged portion of the riverbed and the increase of the riverbed sediments exposed to air (Stanley et al., 1997; Pekel et al., 2016; von Schiller et al., 2017). Under the more extreme conditions of water scarcity, typically occurring from late spring to summer, the contraction of the river flow can be followed by flow cessation with the fragmentation of the watercourse and the formation of isolated pools or the complete drying of the riverbed (Steward et al., 2012; von Schiller et al., 2015). Currently, more than half of the global river network length is represented by systems that cease to flow at some point in time and space (Acuña et al., 2014; Datry et al., 2014). In this context, an interesting case is represented by temperate streams of Northern Italy, which are currently facing a “Mediterraneization” process due not only to global change but also to increasing local anthropogenic pressures, e.g. intensification of water captations and land-use alteration.

Flow contraction results in the formation of patches in space and time, characterized by changes of water velocity, light, temperature, quantity and quality of settling material, availability of allochthonous or autochthonous organic substrates, physical and chemical characteristics of water, diversity and abundance of aquatic biota (e.g. diatoms, macrophytes, macroinvertebrates and fish) and availability of colonizable surfaces by primary producers and benthic fauna (Dodds & Whiles, 2010; Dodds et al., 2018). Such changes are in turn tightly linked to biogeochemical processes such

as carbon and nutrient processing (Arnell & Gosling, 2013; Datry et al., 2017a; Bernhardt et al., 2018; Tonkin et al., 2018) and therefore can influence the amount and timing of Si availability and downstream transport (Wagener et al., 1998; von Schiller et al., 2011; Bernal et al., 2013). In the latest years, the awareness of the importance of flow reduction on C, N and P availability and transport raised in the scientific community (von Schiller et al., 2011, 2015; Merbt et al., 2016; Datry et al., 2018; Arce et al., 2019; Shumilova et al., 2019) and studies on sediment biogeochemistry under contraction and fragmentation phases and laboratory experiments on re-flooding processes have been encouraged (Skoulikidis et al., 2017; Arce et al., 2019). Accumulation and recycling of BSi pools are important factors that regulate DSi availability in aquatic environments, but controlling factors are still poorly understood. However, despite the increasing alteration of river hydrology and the widespread distribution of rivers that cease to flow, there are no studies that analyze how these conditions influence Si dynamics and its availability in relation to N and P in riverbed sediments. Si was studied only by Skoulikidis and coworkers (2017), who highlighted a Si, P and NO_3^- reduction in water during the summer period and an increase during the first flood event.

The amount and forms of dissolved inorganic nutrients accumulated in riverbeds are strongly influenced by the alternation of wet and dry phases, by the highly variable hydrological connections among subsystems within the river and between the river and the surrounding terrestrial environment (McClain et al., 2003; von Schiller et al., 2015; Boulton et al., 2017). Exposure to sunlight and intense desiccation alter the physico-chemical properties of the accumulated organic matter while the progressive reduction of moisture content limits decomposition and nutrients mineralization rates (Tzoraki et al., 2007; Bernal et al., 2013; Merbt et al., 2016). Additionally, exposure to air induces cell lysis during drying and modifies sediment properties by increasing oxygen penetration which favors the oxidation of reduced ions determining a progressive increase in redox potential (De Groot & Van Wijck, 1993).

Such extremely different conditions can modify the availability and mobility of inorganic Si, N and P by affecting the activity of microbial communities, by influencing sediment sorption properties, by exposing redox-sensitive metals to oxygen or by changing their mineral forms (Attygalla et al., 2016; Lehtimäki et al., 2016; Merbt et al., 2016). For example, oxygen availability in sediment influences rates of microbial nitrification that oxidize ammonium to nitrate under oxic conditions and denitrification that reduces nitrate to N_2 under anoxic conditions (Galloway et al., 2003; Burgin & Hamilton, 2007). High NO_3^- concentrations in drying riverbeds (Tzoraki et al., 2007; Arce et al., 2014; Merbt et al., 2016) are promoted by the increased nitrification and by low denitrification (Gómez et al., 2012; Merbt et al., 2016). P content and mobility within the sediments are also affected by the oxidation state and availability of Fe and Al (Attygalla et al., 2016; Siipola et al., 2016).

The sediment biogeochemistry of Si is poorly studied if compared to N and P, and with contrasting results. Studies on soils indicate that Si accumulates under climates in which a distinct dry season is recognized (Sommer et al., 2006) and Si leaching results low in Mediterranean and dry tropical climates (Cornelis et al., 2011). In addition, higher Si uptake results in both dry and humid temperate grasslands compare to other climates, as temperate forest ecosystem (Blecker et al., 2006). The assimilated Si is stored into primary producers as phytoliths, characterized by a greater dissolution than mineral weathering (Alexandre et al., 1997; Fraysse et al., 2006). In aquatic sediments anoxia has been shown to both increase (Hartikainen et al., 1996) or decrease the concentrations of the more mobile Si forms (Siipola et al., 2016). On the other hand, hypoxic and anoxic conditions seem to increase the dissolution of the accumulated BSi, causing an accelerated destruction of diatom frustules (Danielsson, 2014; Siipola et al., 2016) and increasing DSi availability. Beside oxygen, BSi dissolution is also influenced by its age, origin and physiological condition of the primary producers making difficult to predict its recycling in aquatic environments (Lehtimäki et al., 2016). Therefore, more studies are needed to unravel the behavior of Si and its availability in relation to N and P.

The aim of this study was to quantify the concentration of Si in riverbed sediments and its stoichiometry relative to N and P under two contrasting hydrological phases and evaluate how their spatial and temporal variability relate with sediment drying and organic matter accumulation. In order to achieve these goals, Si, P and N pools were quantified and a rewetting experiment was conducted in submerged and exposed river sediments collected from three rivers at the beginning and at the end of the summer period. The overall hypothesis is that the concentration of the more mobile forms of inorganic Si, P and N, their relative amounts and the potential of nutrients release when water returns were different in relation to the severity of river flow contraction and fragmentation during the summer period.

4.2. Materials and Methods

4.2.1. Study Area

The study was conducted in the piedmont section of three rivers – Trebbia, Taro and Enza – that drain the Apennine side of the Po river watershed in northern Italy (Figure 22). The Po river watershed belongs to a warm temperate climate according to Koppen climate classification with humid summers, but it is changing towards a temperate climate with hot, dry summers (Mediterranean

climate) (Rubel et al., 2017). For this reason, the three studied rivers experienced summer flow reduction and riverbed contraction and fragmentation in recent years (Figure 22, Table 10).

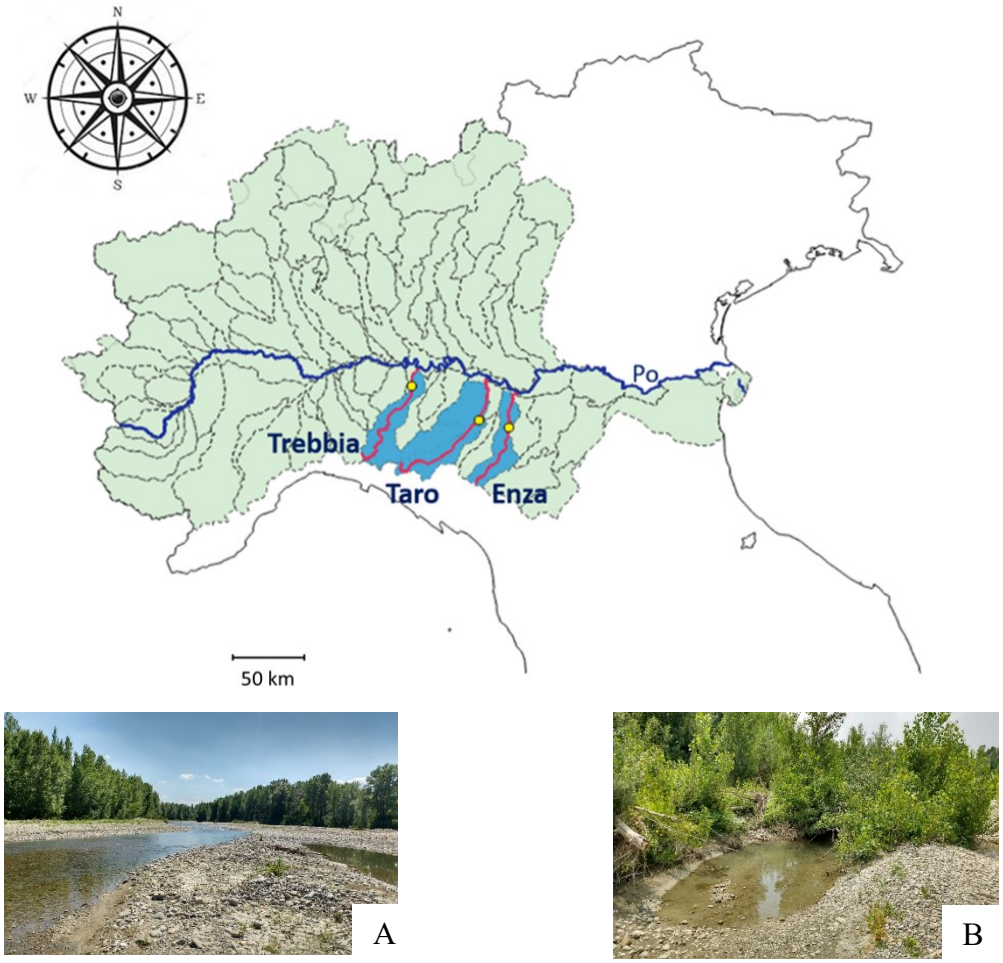

Figure 22. Trebbia, Taro and Enza location in Po River watershed and sampling points (yellow dots) (Trebbia 0546848E, 4979431N; Taro 0592709E, 4954907N; Enza 0613369E, 4950323N. Coordinates reference system WGS84/UTM zone 32N). Example of hydrological phases: A) contraction phase; B) fragmentation phase with isolated pools formation.

The Trebbia River originates from the Ligurian Apennines at about 800 m a.s.l. and its watershed covers 1.5% of the total area of the Po river basin (Figure 22, Table 11). The Trebbia hydrological regime is torrential with a median flow of 11 $m^3 s^{-1}$ (Table 10). The main channel in the piedmont section has a branched bed with an average width of the active floodplain in the sampling site of 484 m. The riverbed is mainly composed of cobbles but with depositional silty and sandy areas.

The watershed of the Taro River accounts for 2.9% of the total area of the Po river watershed (Table 11), with 77% of mountain areas. The course of the Taro river is characterized by a first stretch of fast waters flow due to the high slope, characterized by pebbles and debris transport and soil

erosion. In the piedmont section, the riverbed becomes more permeable with a branched bed, marked by a high width (500 – 600 m) and a modest incision of the banks (2.0 – 2.5 m). From 1992 to 2013, the median discharge was 16 $m^3 s^{-1}$, but during the summer the water flow was almost absent (Table 10). The average width of riverbed in the sampling area is 462 m and is mainly composed of cobbles but with depositional silty and sandy areas.

Table 10. Frequency distribution of Trebbia, Taro and Enza average daily discharges ($m^3 s^{-1}$) measured in the closing station of the watershed from 1992 to 2013 (Viaroli, 2017).

	Trebbia	**Taro**	**Enza**
Min	0	0	0
25° quartile	4	4	0
50° quartile	11	16	4
75° quartile	25	35	13
Max	624	1813	479

The watershed of the Enza river accounts for 2.9% of the total area of the Po river watershed (Table 11), with 64% of mountain areas. The flow of the Enza River has a torrential regime with flood events in autumn and spring, low-flow in winter and is almost dry in summer. From 1992 to 2013, the median flow rate was 4 $m^3 s^{-1}$ but the flow was zero for about 25% of the year (Table 10). The average width of the riverbed in the sampling area is 115 m and is mainly composed of cobbles but with depositional silty and sandy areas.

Table 11. Trebbia, Taro and Enza morphometric and climatic characteristic (from Regional Agency for Environmental Protection of Emilia-Romagna Region (ARPAE): www.arpae.it)

River	**Length (km)**	**Watershed (km^2)**	**Rainfall (mm y^{-1})**	**Winter-Summer Temperature (°C)**	**Active floodplain (m)**
Trebbia	118	1.070	800 – 2000	3.8 – 23.4	484
Taro	126	2.030	800 – 1000	3.7 – 23.3	462
Enza	93	899	700 – 2000	3.5 – 23.5	115

4.2.2. Monitoring Design and Sampling

Each river was sampled on 17 May 2017 (spring) and 2 August 2017 (summer). At each sampling date surficial sediment samples (1 cm depth, 50*50 cm area) were collected in 5 different sites. At each site 3 samples were collected: one from the submerged portion of the riverbed; one at the interface between the active channel and the exposed sediment; and one from the dry and exposed portion of the riverbed. All samples were collected in an area extending 10 m outward from the middle of the active channel, for a total amount of 15 sediment samples each river and each sampling date (Figure 23) covering an area of 3.75 m^2. Immediately after collection the sediment was homogenized and 50 ml transferred in polyethylene vials. Additionally, 2 liters of site water were collected using polyethylene bottles. Sediment and water samples were maintained under dark and refrigerated conditions in a cool box upon return to the laboratory. Once in the laboratory water samples were filtered (Wathman GF/F, Ø 47 mm, 0.7 µm) and analyzed within 24 hours to measure dissolved silica (DSi), ammonium ($N\text{-}NH_4^+$), nitrate and nitrite ($N\text{-}NO_x$) and soluble reactive phosphorus (SRP). Sediment samples were processed for sediment characterization and quantification of Si, N and P pools and for rewetting experiments.

Figure 23. Example of distribution of sediment samplings in rivers on the main channel (on the left) and on isolated pool (on the right).

4.2.3. Sediment Characterization

5 ml of sediment were oven dried at 60 °C for 24h in order to determine moisture content, porosity, and density. Organic matter (OM) and BSi content were also determined on the oven dried sediment.

2 ml of sediment were weighted and put in a Falcon vial (50 ml) for subsequent sequential extraction of nutrients following the SEDEX method (Ruttenberg, 1992; Ruban et al., 1999; Anderson & Delaney, 2000). Originally, the method was developed for the extraction of different species of P

with different mobility and is based on four sequential extractions which exploits the different reactivity of the P pool components in relation to different extracting solutions: P exchangeable or loosely adsorbed (P-exc), P bound to iron (P-Fe), P bound to authigenic calcium (P-auth) and P bound to detritus calcium (P-detr) (Table 12). In this work, the method was also used to extract Si with the main focus on the first two pools (exchangeable and iron bound) (Tallberg et al., 2009) and to extract the first pool of N (exchangeable) (Table 12). After extraction, samples were centrifuged for 13 minutes at 3500 rpm and the P, N and Si were determined as SRP, $N\text{-}NO_x$, $N\text{-}NH_4^+$ and DSi. To correct for any extracting solution and filter interferences, calibration curves have been built using nutrient standard solutions specific for each extracting solution (Braga et al., 2014; Scibona et al., 2015).

Table 12. Pools, extraent solutions, time extractions and features of extracted pools used for sequential extraction procedure (SEDEX) (Ruttenberg, 1992; Ruban et al., 1999; Anderson & Delaney, 2000).

Step	Pool	Extraent solution	Time extraction	Features of extracted pool
1	P-exc Si-exc $N\text{-}NO_x$ -exc $N\text{-}NH_4^+$-exc	$MgCl_2$ 1M (pH=8)	2h	Weakly reactive P absorbed to particulate sediment.
2	P-Fe Si-Fe	CBD* (pH=7)	6h	Iron, Mn e Al P bound. Pool sensitive to redox conditions.
3	P-auth	Acetate buffer 1M (pH=4)	2h	Authigenic carbonate fluorapatite, biogenic apatite, calcium carbonate associated to P. Pool sensitive to pH conditions.
4	P-detr	HCl 1N (pH=1)	16h	Detritic apatite. Almost non-reactive pool in environmental conditions.

*CDB: 0.22M Sodium Citrate + 0.033M Sodium Dithionite + 1M Sodium Bicarbonate.

Step 1 was obtained after two extractions of two hours each with 20 ml of $MgCl_2$ 1M at pH 8 and a rinsing phase with 20 ml of distilled water. Step 2 was obtained by extraction in succession with 10 ml of CDB for 6 hours, 10 ml of $MgCl_2$ 1M for 2 hours and then rinsed with 20 ml of distilled water. Pool of step 3 was extracted with 20 ml of 1M acetate buffer (pH 4) for 2 hours and with 2 washes with 20 ml of $MgCl_2$ 1M and 20 ml distilled water. Finally, pool of step 4 was extracted with 20 ml of HCl 1N for 16 hours.

4.2.4. Rewetting simulation

An aliquot of 4 ml of homogenized sediment was taken from each sampling point and transferred into 250 ml plastic bottle darkened with aluminum paper. Then 100 ml of filtered river water (Wathman GF/F, Ø 47 mm, 0.7 µm) were added. Bottles containing sediments and the filtered water were capped and shacked (100 rpm) at room temperature (20 °C) for 4 h. The selected duration reflects the time when most of the dissolved substances are leached and minimizes microbial modification of leachates upon rewetting (Blackwell et al., 2013; Shumilova et al., 2019). At the end of the extraction, samples were centrifuged (13 minutes at 3500 rpm) and then the supernatant was collected with plastic syringes and filtered through Whatman GF/F glass fiber filters. Samples were stored at 4 °C in polyethylene vials for DSi, N-NO_x and N-NH_4^+ determinations and in glass tubes for SRP determination. Samples were analyzed within 24 hours.

The concentration of DSi, N-NH_4^+, N-NO_x, SRP in leachates were used to calculate the net released amounts per gram of dry substrate using the following formula (4):

$$C_x = \frac{C_f - C_i}{DW} \qquad (4)$$

where, C_x is the concentration of the x chemical species (µg g^{-1} $_{DW}$), C_f is the final concentration of x (µg L^{-1}), C_0 is the initial concentration of x (µg L^{-1}) and DW is the dry weight of the incubated sediment (g $_{DW}$). A positive value of C_x indicates a net release of the target compound to the water column while a negative value indicates a net resorption of the target compound. The initial concentration corresponds to the concentration of stream water.

4.2.5. Analytical Methods

N-NH_4^+ (Koroleff, 1970), N-NO_x (APHA, 1998), SRP (Valderrama, 1981) and DSi (Golterman et al., 1978) were determined with standard spectrophotometric methods (Perkin Elmer, Lambda 35) in water, extraction solution and rewetting water. An analytical blank that underwent the same procedure as the samples, including filtration, was always analyzed to correct for sample contamination.

Moisture, porosity and density were determined following Pansu & Gautheyrou (2007). Organic matter was determined as loss on ignition at 550 °C with a standard procedure (Azzoni et al., 2015). The total BSi content of sediments was analyzed following DeMaster (1981), by digesting 30 mg of dry sediment with 30 ml of 0.1 M Na_2CO_3 in polypropylene bottles for 5 h at 85 °C. Subsamples were

collected after 3, 4 and 5 h and analyzed using the molybdate blue spectrophotometric method (Golterman et al., 1978). Before the analysis, each sample (1 ml of extraction solution) was neutralized with 9 mL of HCl 0.021 M. To correct for the amount of Si resulting from mineral dissolution, the Si content of the subsamples was plotted against dissolution time. The *y*-axis intercept of the linear regression line represents the estimated BSi content. All BSi dissolved within the first 3 hours.

4.2.6. Statistical Analysis

Data were analyzed with generalized least square (GLS) models, which were run with river (Trebbia, Taro, Enza) and season (Spring, Summer) as the main fixed factors and with moisture as covariate. To deal with observed heteroscedasticity, it was used the argument "weights" within the function *gls*, and the function *varident* to specify variance models. An *a posteriori* comparison of the means was performed using a post hoc Tukey test. Statistical analyses were run with the *nmle* (Pinheiro et al., 2016) and *emmeans* (Lenth et al., 2018) packages in R software v. 3.6.0 (The R Core Team, 2019).

All results in text, figures and tables are presented as mean ± standard error.

4.3. Results

4.3.1. Hydrological Conditions, Nutrient Concentrations in Water Column and general Sediment Features

Hydrological conditions were different between the two seasons in the three rivers in particular during summer. Annual discharge in 2017 ranged from 1.4 to 401 $m^3 s^{-1}$ in the Trebbia river with an average of 12.9 $m^3 s^{-1}$ (ARPAE). In spring, the discharge was similar to the annual average (15.6 $m^3 s^{-1}$), while in summer it decreased to 1.9 $m^3 s^{-1}$. In the Taro river, the annual discharge in 2017 comprised between 0.1 and 1280 $m^3 s^{-1}$ and the average was 17.3 $m^3 s^{-1}$ (ARPAE). In spring, the discharge was similar to the annual average (15.8 $m^3 s^{-1}$), while in summer it decreased drastically to 0.2 $m^3 s^{-1}$. The Enza river had the lowest discharge with an annual average of 7.0 $m^3 s^{-1}$ in 2017, ranging between 0 and 248 $m^3 s^{-1}$ (ARPAE). The discharge was similar to the annual average in spring (5.9 $m^3 s^{-1}$), while in summer the flow resulted interrupted and only some sparse pools remained on the riverbed.

The Trebbia river active channel width resulted the highest and was on average 23 m, passing through 31 m in spring to 14 m in summer. The Taro river active channel width was on average 18 m, passing from 23 in spring to 18 in summer forming many river branches. Finally, the Enza river active channel width resulted the lowest and was on average 8 m, decreasing from spring (10 m) to summer (5 m), in which isolated pools formed.

On average, DSi concentration in water slightly increased from spring to summer (Table 13), with the exception of Trebbia river in which the concentration slightly decrease in summer.

Table 13. Dissolved silica (DSi), dissolved inorganic nitrogen (DIN), nitrate ($N\text{-}NO_x$), ammonium ($N\text{-}NH_4^+$) and soluble reactive phosphorus (SRP) concentrations in water column and N:Si, P:Si and N:P molar ratio in spring and summer season for each river. Concentrations are reported as $\mu g\ L^{-1}$, while stoichiometry ratio as mol:mol. Standard error are shown in parenthesis.

		DSi	**DIN**	**$N\text{-}NO_x$**	**$N\text{-}NH_4^+$**	**SRP**	**N:Si**	**P:Si**	**N:P**
Spring	Trebbia	2691 (194)	391 (34)	349 (36)	42 (3)	10.6 (3.8)	0.68 (0.05)	0.0051 (0.0024)	86 (21)
	Taro	2528 (271)	210 (17)	160 (11)	50 (12)	3.6 (0.4)	0.18 (0.03)	0.0016 (0.0003)	116 (15)
	Enza	2762 (508)	1815 (8)	1783 (9)	32 (2)	5.1 (1.5)	1.56 (0.44)	0.0014 (0.0004)	1159 (116)
Summer	Trebbia	2267 (52)	230 (9)	216 (8)	13 (4)	2.3 (0.9)	0.20 (0.01)	0.0009 (0.0003)	172 (19)
	Taro	2708 (252)	157 (2)	154 (2)	3 (1)	3.1 (0.2)	0.12 (0.01)	0.0011 (0.0002)	113 (8)
	Enza	3104 (119)	933 (7)	929 (7)	4 (1)	14.2 (5.8)	0.60 (0.03)	0.0050 (0.0019)	252 (79)

Conversely, on average, SRP, $N\text{-}NO_x$ and $N\text{-}NH_4^+$ concentrations decreased from spring to summer (Table 13), with the exception of SRP in Enza river in which the concentration increase in summer. $N\text{-}NO_x$ concentrations contributed between 65 and 100% to the DIN. The average N:Si

molar ratio resulted 0.49 ± 0.13 and decreased from spring to summer in each river (Table 13). The average P:Si molar ratio (average value 0.0024 ± 0.0006) decreased in Trebbia river and increased in Enza river from spring to summer (Table 13). Conversely, N:P molar ratio was 323 ± 87 and changed from spring to summer: the ratio increased in Trebbia river and decreased in Enza river between seasons.

4.3.2. Sediment Characterization and Nutrient Sequential Extraction

Sediment moisture content varied substantially (0.1% – 90.7%) across samplings within the three rivers in the two seasons with an average value of 27%.

Organic matter content (OM) in riverbed sediment was on average 2.8 ± 0.3%, but it evidenced a great variability ranging between 0.02% to 18.36% with both values measured in Trebbia river. Average OM increased from spring (1.2 ± 0.1%) to summer (4.3 ± 0.6%) and resulted on average higher in the Enza river (Figure 24).

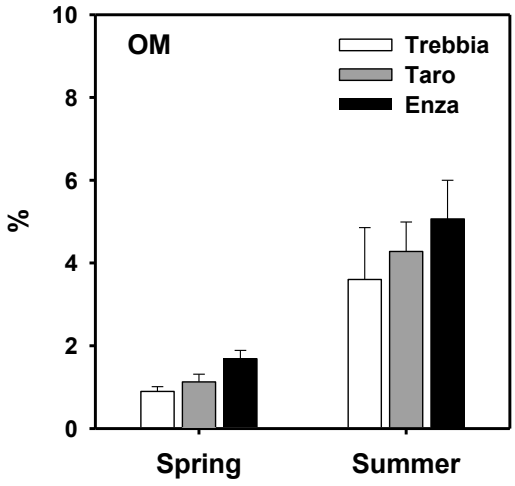

Figure 24. Sediment content of organic matter (OM) measured in the three rivers at the different seasons. Error bars represent standard error (n = 15).

Moisture content is related with the organic matter content (Table 14) but the net effect depends on the river. In the Taro and Enza rivers sediment organic matter content decreased with sediment drying while in the Trebbia river OM content decreased with increasing sediment moisture.

Average sedimentary TSi (biogenic silica + exchangeable silica + iron bound silica) concentration was 3780 ± 732 μg Si g^{-1}_{DW} and resulted 4 times higher in summer

(6161 ± 1371 µg Si g^{-1}_{DW}) compared to spring (1399 ± 171 µg Si g^{-1}_{DW}). The three analyzed Si pools contributed differently to the total amount of Si in sediments: exchangeable silica contributed the 1.3 ± 0.2%, iron bound silica contributed the 7.3 ± 1.2%, while biogenic silica represented the greatest Si fraction (91.4 ± 1.4%).

Table 14. Summary of the results of two-way generalized least square (GLS) models of exchangeable silica (Si-exc), iron bound silica (Si-Fe), biogenic silica (BSi), exchangeable phosphorus (P-exc), iron bound phosphorus (P-Fe), authigenic calcium bound phosphorus (P-auth), detritic calcium bound phosphorus (P-detr), exchangeable nitrate and nitrite (N-NO_x-exc) and exchangeable ammonium (N-NH_4^+-exc) concentrations. Only significant p level ($p < 0.05$) are reported.

Source of Variation	DF	OM	Si-exc	Si-Fe	BSi	P-exc	P-Fe	P-auth	P-detr	N-NO_x-exc	N-NH_4-exc
Moisture	1	<0.01	<0.05	<0.001	<0.001	<0.001	<0.001	<0.001		<0.01	<0.001
Season	1	<0.001	<0.001	<0.05	<0.05	<0.001	<0.001	<0.001	<0.05	<0.01	<0.001
River	2	<0.01	0.09	<0.001		<0.01	<0.001	<0.001	<0.001	0.070	<0.01
Season * River	2				<0.006	0.06	<0.01	<0.05			
Moisture * Season	1			0.06				<0.01			
Moisture*River	2	<0.05	<0.001	<0.001	0.08	<0.01	<0.001	<0.01	<0.01	<0.01	<0.001

Exchangeable Si (Si-exc) concentration varied substantially (0 – 440 µg Si g^{-1}_{DW}) across samplings within the three rivers in the two seasons. Si-exc concentration resulted 6.6 times higher in summer (51.3 ± 12.1 µg Si g^{-1}_{DW}) compared to spring (7.7 ± 1.1 µg Si g^{-1}_{DW}) (Table 14; Figure 26) and it resulted similar between rivers even if a tendency toward an increase from Trebbia to Enza (91.0 ± 32.6 µg Si g^{-1}_{DW}) was observed in summer (Figure 26). Sediment moisture significantly affect Si-exc concentration (Figure 27), but the effect is different depending on river (Table 14). Si-exc concentration decreased with sediment drying in the Enza and partially in the Taro rivers while it increased in the Trebbia river (Figure 25). The relative importance of Si-exc slightly increased from spring (0.7 ± 0.1%) to summer (1.8 ± 0.4%).

Iron bound silica (Si-Fe) concentration varied substantially (8 – 753 µg Si g^{-1}_{DW}) across samplings within the three rivers in the two seasons. Average Si-Fe concentration increased from spring (56 ± 4 µg Si g^{-1}_{DW}) to summer (139 ± 27 µg Si g^{-1}_{DW}) (Table 14, Figure 26) and was highest in the Enza river and lowest in Trebbia river. Sediment moisture significantly influences Si-Fe

concentration (Figure 27), but the effect depends on river (Table 14). Si-Fe concentration decreased with sediment drying in Enza and Taro while it increased in Trebbia (Figure 25).

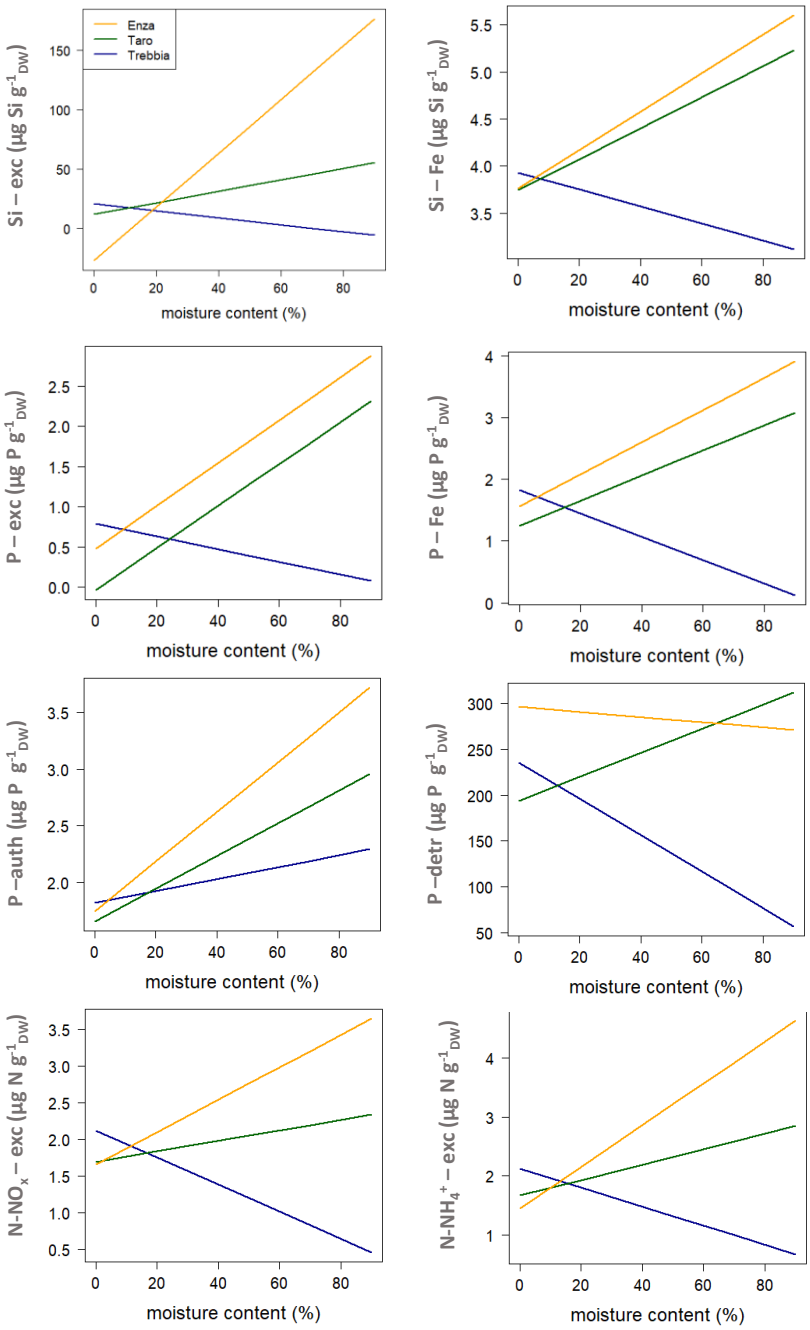

Figure 25. Graphical summary of the effects of sediment moisture on sedimentary concentrations of exchangeable silica (Si-exc), iron bound silica (Si-Fe), exchangeable phosphorus (P-exc), iron bound phosphorus (P-Fe), authigenic calcium bound phosphorus (P-auth), detritic calcium bound phosphorus (P-detr), exchangeable nitrate and nitrite (N-NO_x-exc) and exchangeable ammonium (N-NH_4^+-exc) in the three rivers.

Biogenic silica (BSi) was the most important Si pool (3652 ± 718 µg Si g^{-1}_{DW}) but the concentrations varied substantially across samplings, ranging between 22 to 44568 µg Si g^{-1}_{DW}. Average BSi concentration resulted similar in the three rivers and increased from 1335 ± 168 µg Si g^{-1}_{DW} in spring to 5971 ± 1347 µg Si g^{-1}_{DW} in summer (Figure 26, Table 14). Sediment moisture is positive related to BSi concentration (Figure 27).

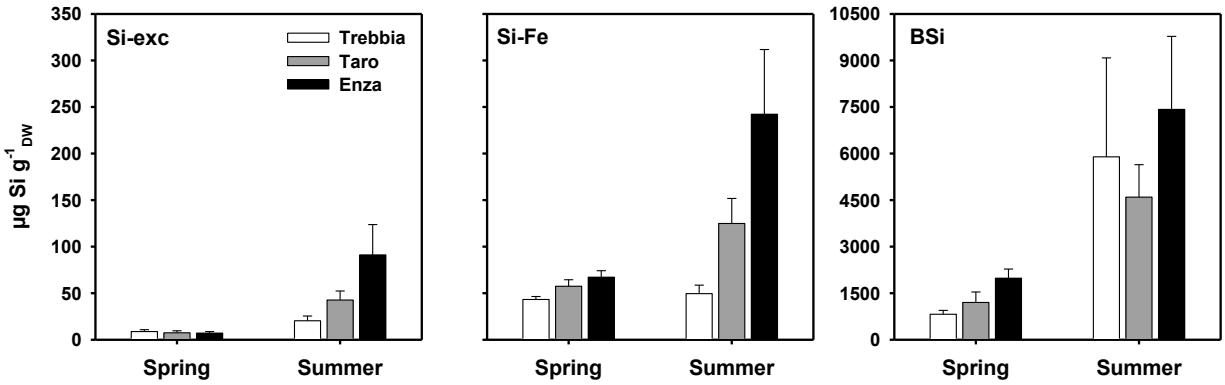

Figure 26. Sediment concentrations of exchangeable silica (Si-exc), iron bound silica (Si-Fe) and biogenic silica (BSi) measured in the three rivers in the different seasons. Error bars represent standard error (n = 15).

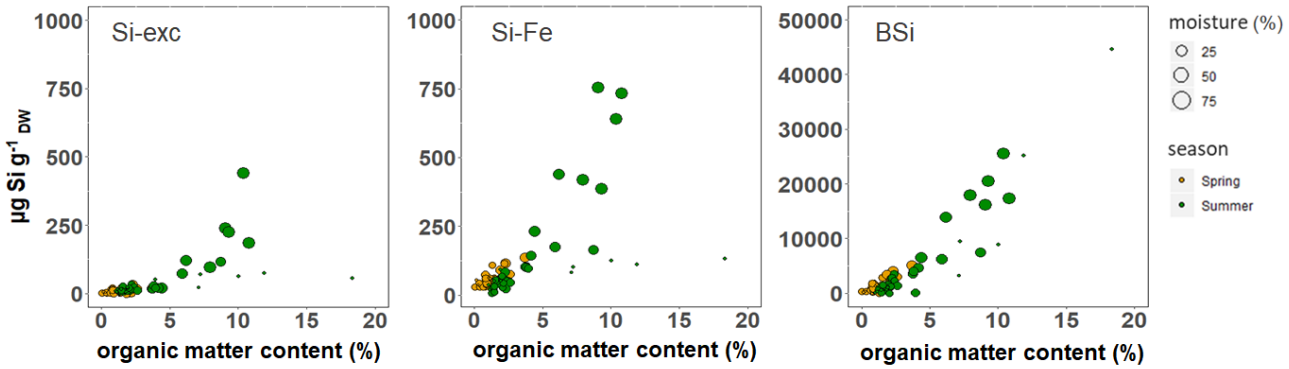

Figure 27. Concentrations of exchangeable silica (Si-exc), iron bound silica (Si-Fe) and biogenic silica (BSi) in riverbed sediments in relation to organic matter content in the three rivers. Dots are filled according to season and the size is proportional to moisture content.

Average total inorganic phosphorus (TIP = exchangeable phosphorus + iron bound phosphorus + authigenic calcium bound phosphorus + detritic calcium bound phosphorus) concentration was 268 ± 10 µg P g^{-1}_{DW} and resulted similar across rivers and seasons (data not shown). The four analyzed

P pools contributed differently to the sedimentary TIP: exchangeable phosphorus represented the lower pool (2.3 ± 0.4%), iron bound phosphorus and authigenic calcium bound phosphorus contributed respectively 3.8% (±0.4) and 4.6% (±0.5), while detritic calcium bound phosphorus was the most important pool (89.4 ± 1.2%).

Average concentration of detritic calcium bound phosphorus (P-detr) resulted different between rivers (Table 14) being highest in Enza (283.8 ± 14.6 µg P g^{-1}_{DW}) and lowest in Trebbia (195.3 ± 12.4 µg P g^{-1}_{DW}). On average P-detr concentration slightly decreased from spring (255.6 ± 11.3 µg P g^{-1}_{DW}) to summer (219.4 ± 12 µg P g^{-1}_{DW}) (Table 14, Figure 28). Sediment moisture did not influence the concentration of P-detr in Enza and Taro while a slight increase was observed in Trebbia in relation to sediment drying (Figure 25).

Exchangeable phosphorus (P-exc) concentrations varied substantially (0.2 – 88.2 µg P g^{-1}_{DW}) across samplings within the three rivers. Average P-exc concentration resulted 7 times higher in summer (11.5 ± 2.7 µg P g^{-1}_{DW}) compared to spring (1.6 ± 0.2 µg P g^{-1}_{DW}) (Table 14; Figure 28) and it increased from Trebbia (4.5 ± 1.7 µg P g^{-1}_{DW}) to Enza (11.0 ± 3.7 µg P g^{-1}_{DW}) (Figure 28). Sediment moisture affects P-exc concentration (Figure 29), but the effect depends on river (Table 14). P-exc concentration decreased with sediment drying in Enza and Taro but it increased in Trebbia (Figure 25).

Iron bound phosphorus (P-Fe) concentrations comprised between 1.4 to 56.4 µg P g^{-1}_{DW}, with the lowest average concentration measured in Trebbia (6.5 ± 1.6 µg P g^{-1}_{DW}) and the highest in Enza (17.1 ± 3.0 µg P g^{-1}_{DW}). P-Fe increased significantly from 7 ± 1 µg P g^{-1}_{DW} measured in spring to 15.0 ± 2 µg P g^{-1}_{DW} measured in summer (Table 14, Figure 28). P-Fe concentration were significantly influenced by moisture content but the effect depends on river (Table 14, Figure 29). P-Fe concentration decreased with sediment drying in Enza and Taro but it increased in Trebbia (Figure 25).

The concentration of authigenic calcium bound phosphorus (P-auth) ranged between 4 to 80 µg P g^{-1}_{DW}. Average concentration significantly increased between spring (8 ± 1 µg P g^{-1}_{DW}) to summer (18 ± 3 µg P g^{-1}_{DW}) and resulted significantly higher in the Enza river (19 ± 4 µg P g^{-1}_{DW}) (Figure 28). P-auth concentration were significantly influenced by moisture content but the effect depends on river and season (Table 14, Figure 29). P-auth concentration decreased with sediment drying and the effect resulted stronger in summer and in Enza and Taro rivers (Figure 25).

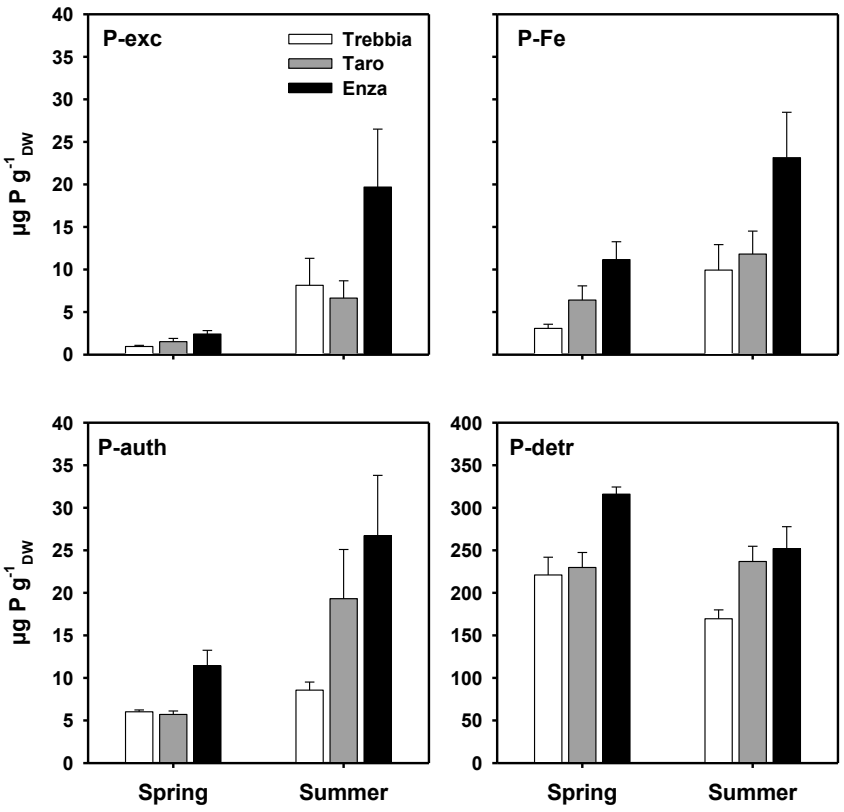

Figure 28. Sediment concentrations of exchangeable phosphorus (P-exc), iron bound phosphorus (P-Fe), authigenic calcium bound phosphorus (P-auth) and detritic calcium bound phosphorus (P-detr) measured in the three rivers at the different seasons. Error bars represent standard error (n = 15).

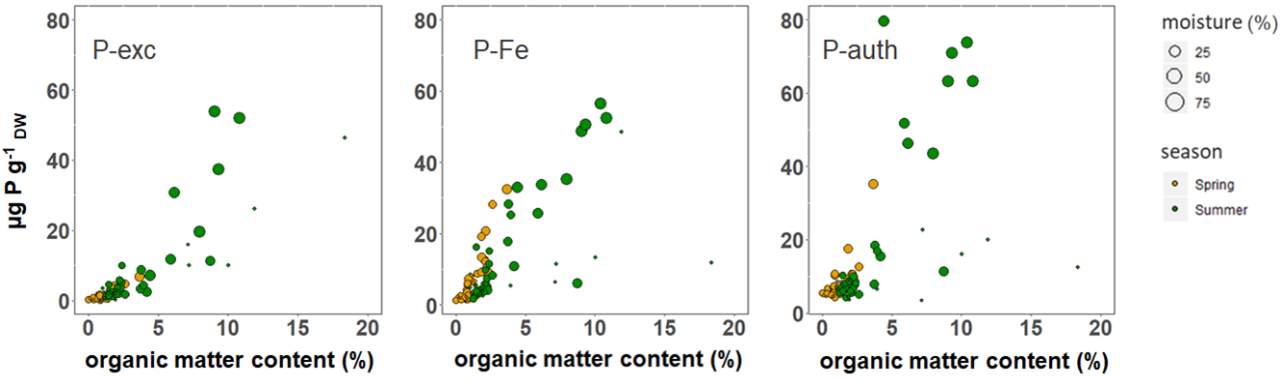

Figure 29. Concentrations of exchangeable phosphorus (P-exc), iron bound phosphorus (P-Fe) and authigenic phosphorus (P-auth) in riverbed sediments in relation to organic matter content in the three rivers. Dots are filled according to season and the size is proportional to moisture content.

Average concentration of exchangeable dissolved inorganic nitrogen (DIN-exc = exchangeable ammonium + exchangeable nitrate) resulted 32 ± 6 µg N g^{-1}_{DW} and was higher in summer

(51 ± 12 µg N g^{-1}_{DW}) than spring (14 ± 2 µg N g^{-1}_{DW}). Exchangeable ammonium (N-NH_4^+-exc) average concentration resulted significantly different between rivers being highest in the Enza river (36.4 ± 10.8 µg N g^{-1}_{DW}) and lowest in the Trebbia River (9.6 ± 2.6 µg N g^{-1}_{DW}) and increased from spring (8.3 ± 1.9 µg N g^{-1}_{DW}) to summer (29.8 ± 7.4 µg N g^{-1}_{DW}) (Table 14, Figure 30). N-NH_4^+-exc concentration resulted significantly influenced by moisture content (Table 14, Figure 31) but the effect depend on river. N-NH_4^+-exc concentration decreased with sediment drying in Enza and Taro rivers but it increased in Trebbia river (Figure 25).

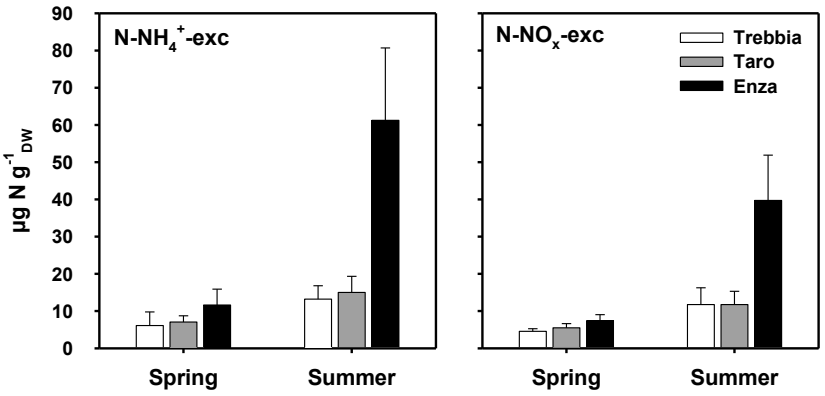

Figure 30. Sediment concentrations of exchangeable ammonium (N-NH_4^+-exc) and exchangeable nitrate and nitrite (N-NO_x-exc) measured in the three rivers at the different seasons. Error bars represent standard error (n = 15).

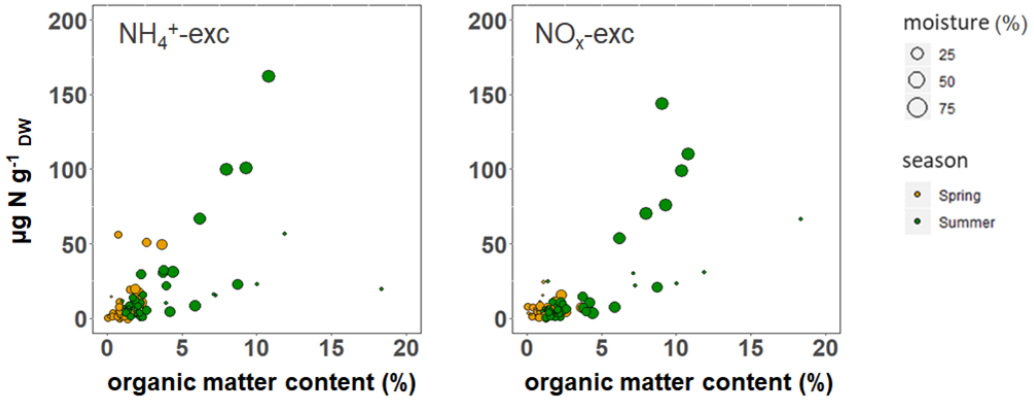

Figure 31. Concentrations of exchangeable ammonium (N-NH_4^+-exc) and nitrate (N-NO_x-exc) in riverbed sediments in relation to organic matter content in the three rivers. Dots are filled according to season and the size is proportional to moisture content.

Exchangeable nitrate (N-NO_x-exc) concentration varied substantially (0 – 144 µg N g^{-1}_{DW}) across samplings within the three rivers. N-NO_x-exc average concentration resulted different between rivers being highest in the Enza river (23.6 ± 6.7 µg N g^{-1}_{DW}) and lowest in the Trebbia River (8.1 ± 2.3 µg N g^{-1}_{DW}) and increased from spring (5.8 ± 0.7 µg N g^{-1}_{DW}) to summer (21.1 ± 4.8 µg N g^{-1}_{DW}) (Table 14, Figure 30). N-NO_x-exc concentration resulted significantly influenced by moisture content (Table 14, Figure 31) but the effect depends on river. N-NO_x-exc concentration decreased with sediment drying in Enza and Taro rivers but it increased in Trebbia river (Figure 25).

4.3.3. Quantification of Nutrients Net Exchange during Sediment Resuspension

Suspended and rewetted sediment on average released inorganic nutrients to water. The released amount was variable depending on the specific nutrient and was highest for DSi and lowest for SRP.

Released DSi (DSi-rel) varied substantially across samplings within the three rivers in the two seasons. On average DSi was released from sediment to water column (38.4 ± 10.2 µg Si g^{-1}_{DW}) and the release increased from 6.7 ± 1.4 µg Si g^{-1}_{DW} in spring to 70.0 ± 19.3 µg Si g^{-1}_{DW} in summer (Figure 32) in particular in the Enza river where a summer average release of 159 ± 47 µg Si g^{-1}_{DW} was measured. Sediment moisture was not related to DSi release (Table 15).

Table 15. Summary of the results of two-way generalized least square (GLS) models of dissolved silica (DSi), soluble reactive phosphorus (SRP), nitrate and nitrite (N-NO_x) and ammonium (N-NH_4^+) concentrations measured after the rewetting simulation. Only significant p level ($p < 0.05$) are reported.

Source of Variation	DF	DSi-rel	SRP-rel	N-NO_x-rel	N-NH_4-rel
Moisture	1			<0.05	<0.05
Season	1	<0.001	<0.001	<0.05	<0.05
River	2				<0.01
Season * River	2	<0.001			<0.05
Moisture * Season	1				<0.05
Moisture*River	2				<0.01

Released SRP (SRP-rel) from suspended and rewetted sediment ranged from 0 to 40.4 µg P g^{-1}_{DW} and increased from spring (0.4 ± 0.1 µg P g^{-1}_{DW}) to summer (2.5 ± 1.0 µg P g^{-1}_{DW})

(Table 15, Figure 32). The greatest SRP release to water column occurred in Trebbia river in summer (11.4 ± 7.6 µg P g^{-1}_{DW}) but the difference was not statistically significant (Table 15).

Ammonium released (N-NH_4^+-rel) from sediment (4.7 ± 0.7 µg N g^{-1}_{DW}) resulted different between rivers but the magnitude of the difference depends on season (Table 15). On average the highest release was measured in the Enza river (8.2 ± 1.7 µg N g^{-1}_{DW}) and the lowest in the Trebbia river (2.5 ± 0.7 µg N g^{-1}_{DW}). Sediment moisture significantly influenced N-NH_4^+-rel but the effect depends on river and season (Table 15).

N-NO_x released (N-NO_x-rel) varied substantially across samplings within the three rivers in the two seasons with an average value of 4.4 ± 1.5 µg N g^{-1}_{DW}. N-NO_x-rel increased from spring (1.1 ± 0.6 µg N g^{-1}_{DW}) to summer (7.6 ± 2.9 µg N g^{-1}_{DW}) (Table 15, Figure 32). Sediment moisture influences N-NO_x-rel with the release that increases as the sediment became drier.

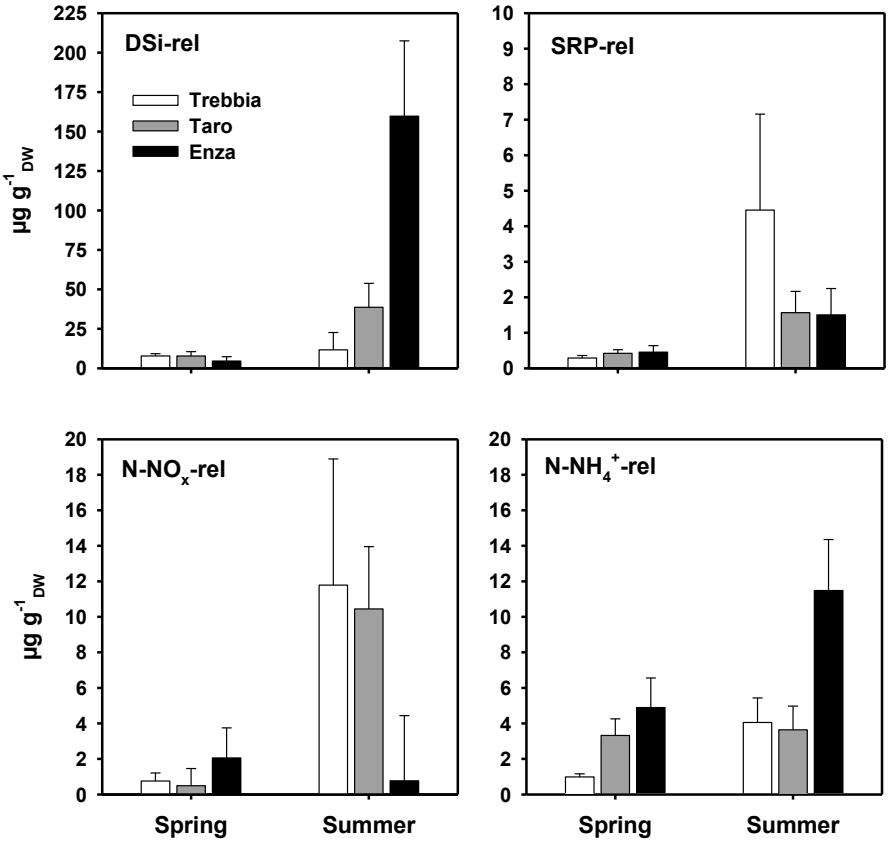

Figure 32. Sediment concentrations of dissolved silica (DSi), soluble reactive phosphorus (SRP), nitrate and nitrite (N-NO_x) and ammonium (N-NH_4^+) measured after the rewetting simulation in the three rivers water at the different seasons. Error bars represent standard error (n = 15).

4.4. Discussion

In this work spatial and temporal variation of Si, P and N concentrations in surficial riverbed sediments was analyzed in relation to different degrees of drying in three rivers characterized by a different hydrology. These are understudied but important issues in inland waters as they can provide new insights on the effect of river fragmentation and drying on benthic Si cycling and its relation to N and P. Flow reduction is in fact an increasing phenomenon worldwide and rivers that cease to flow are estimated to comprise at least half of the global fluvial network (Skoulikidis et al., 2017; Shumilova et al., 2019).

The results highlight a strong variability in nutrient concentrations and suggest that summer flow contraction and sediment drying can be key determinants of benthic biogeochemistry in the studied rivers. Si concentrations rose from spring to summer, but the magnitude of the increase depends on the Si pool and on the river and was most accentuated in sediments characterized by high moisture. Labile P and N concentrations followed a similar pattern but the degree of change was different compared to Si determining a higher accumulation of labile inorganic P and N relative to Si. A fraction of the accumulated nutrients is released to the water column as water returns and sediments are suspended. However, the amount of released nutrients does not correspond to the relative availability of the more mobile accumulated fractions.

4.4.1. Silica Content in River Sediment and Si:N:P Stoichiometry in Relation to the Degree of Flow Contraction and Sediment Drying

The BSi content in the sediment of the studied rivers (0.02 – 44 mg Si g^{-1}_{DW}) is comparable to values (1 – 50 mg Si g^{-1}_{DW}) detected in soils (Struyf et al., 2009; Clymans et al., 2011) but falls in the lower range of values (0.5 – 800 mg Si g^{-1}_{DW}) measured in freshwater environments (Carter & Colman, 1994; Struyf et al., 2007; Carey & Fulweiler, 2013a; Zhu et al., 2016). The highest concentrations measured in freshwater environments were found in deep sediments of lakes where the organic matter input is dominated by settling phytoplankton mainly composed by siliceous algae (Salmaso et al., 2018). On the contrary, shallow aquatic environments like wetlands and estuaries result more similar to river sediments. Few works have quantified the concentration of inorganic labile Si pools (Si-exc and Si-Fe fractions) that are the most mobile and reactive, using a comparable method. The Si-exc content of sediments measured in this study (0 – 0.44 mg Si g^{-1}_{DW}) is comparable but falls in the lower range of values (0 – 1.9 mg Si g^{-1}_{DW}) detected in estuarine and coastal sediments (Tallberg et al., 2009; Lehtimäki et al., 2013; Siipola et al., 2016) and in soils (0 – 3.8 mg Si g^{-1}_{DW}) (Georgiadis et al., 2013). The Si-Fe concentration measured in this study (0.01 – 0.75 mg Si g^{-1}_{DW})

falls in the upper range of values (0 – 0.4 mg Si g^{-1}_{DW}) detected in coastal sediments (Tallberg et al., 2009; Siipola et al., 2016) but in the lower range of values (0.9 – 1.3 mg Si g^{-1}_{DW}) detected in soils (Georgiadis et al., 2013).

All the three different Si fractions accumulate in the sediment of the investigated rivers during the summer season. Such changes can be the consequence of DSi uptake and storage in primary producer biomass as BSi, followed by its partial dissolution. River substrates are mainly colonized by diatoms and filamentous algae, for the most part belonging to the genus *Cladophora* that are able to accumulate Si as already observed in the littoral zone of Lake Iseo (Malkin et al., 2009, see Chapter 3). Therefore, the growth of primary producers can account for Si assimilation, explaining the spring to summer BSi accumulation in sediments. The highest and more variable concentrations of Si-exc and Si-Fe measured in the submerged sediments and the fact that driest sediment maintains a relatively constant Si concentration indicate that sediment exposure to air and subsequent drying interfere with Si biogeochemistry. Such effect can be explained considering how flow contraction influences primary production and decomposition rates of the accumulated organic matter.

Flow regime regulates both the river metabolism rates and the biomass of primary producer communities (Bernhardt et al., 2018). During flow contraction, reduction of water velocity and depth coupled with an increase of light conditions stimulate primary production of epilithic micro and macroalgae (Harvey et al., 2003; Uehlinger, 2006; Roberts et al., 2007; von Schiller et al., 2017; Ulseth et al., 2018), particularly in isolated pools (Acuña et al., 2005). Unlike mountain streams where the contribution of allochthonous material is supposed to represent a high percentage of the organic input (von Schiller et al., 2015), the contribution of allochthonous material is likely low in the studied rivers as they are characterized by a low development of riparian vegetation compared to riverbed width. Therefore, the net accumulation of organic matter content measured in the sediment and the fact that OM concentration was on average higher in Enza river and lowest in Trebbia river support the hypothesis of increased autochthonous production in pools of fragmented rivers. In the three rivers analyzed, characterized by a different extent of flow reduction, organic matter content can result patchy distributed in exposed sediments depending on the river productivity, the timing and the degree of exposure. It can be hypothesized that the accumulation of organic matter in exposed sediment is lower in river as Taro and Enza - where flow fragmentation occurs early in summer and water flow shrink faster - compared to river as Trebbia - where the water flow gradually decreases leading to an accumulation of primary producers on riverbed. At the same time, temporary pools can represent hot spots of organic matter accretion, as observed in the Enza river.

The recycling of DSi from BSi depends on dissolution rates of BSi and on the activity of the microbial community (Alfredsson et al., 2016; Lehtimäki et al., 2016), which are strongly influenced

by local environmental variables such as, temperature, pH, oxygen concentration, moisture and organic matter content that fuel microbial metabolism (Baldwin & Mitchell, 2000; Lake, 2003; Catalán et al., 2013; Abril et al., 2016). The higher labile Si concentrations measured in submerged sediments during summer can be therefore a consequence of the high mineralization rates, promoted by microbial activity. On the other hand, sediment exposure limits the decomposition of previously accumulated organic matter (Tzoraki et al., 2007; Bernal et al., 2013; Merbt et al., 2016; Arce et al., 2018). As such, under dry condition the accumulation of labile silica pools is limited likely because of low decomposition and low BSi dissolution rates.

The concentration of labile P and N pools changed in the investigated sediments following a pattern similar to Si and, similarly to Si, their general behavior can be mainly explained by accumulation in primary producer biomass, its subsequent decomposition and mineralization, and recycling of the resulting inorganic fraction. However, the degree of change was different compared to Si determining a relatively higher accumulation of labile inorganic P and N which is evident considering either the total labile pools or only the exchangeable pools (Figure 33).

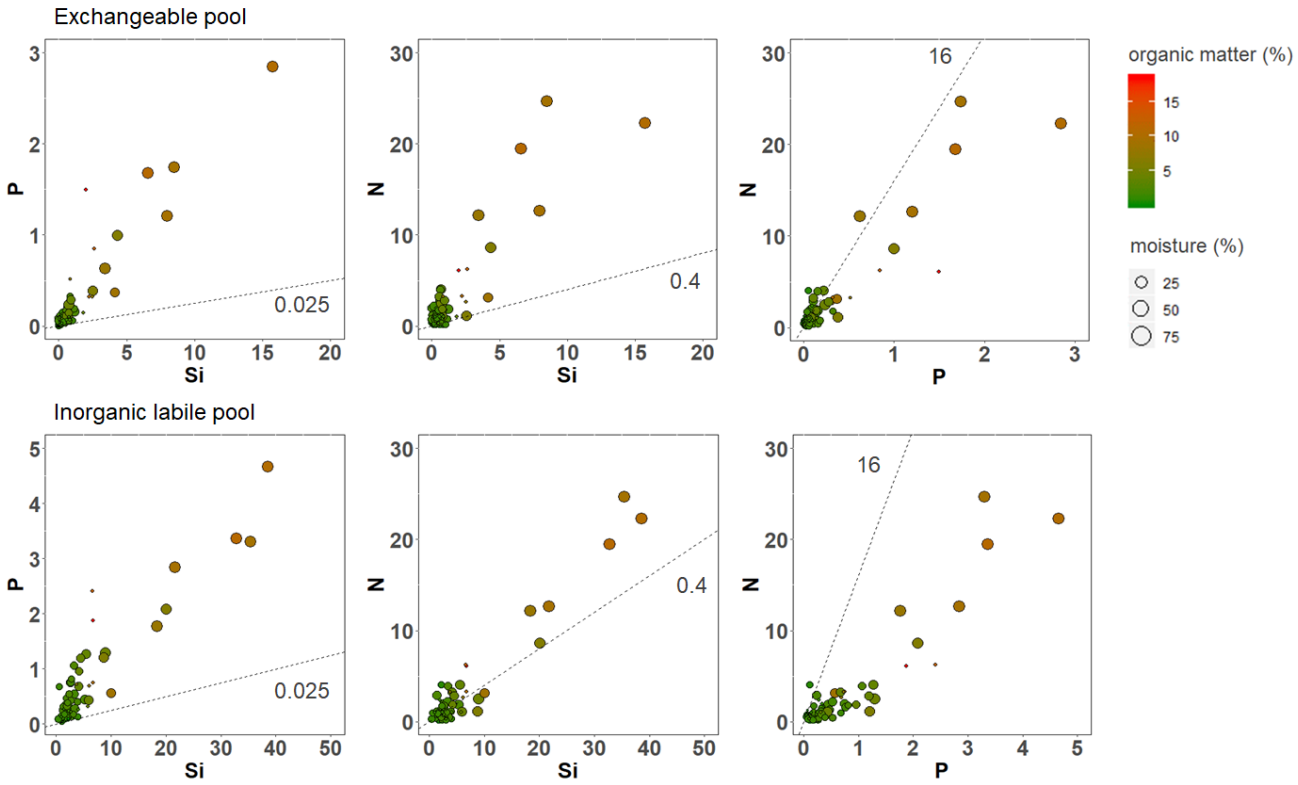

Figure 33. P:Si, N:Si and N:P molar ratios of exchangeable pools (upper panel) and labile inorganic pools (resulted by the sum of exchangeable and iron bound pool, lower panel) in superficial sediment in relation to organic matter (color scale, OM %) and humidity content (dots size, moisture %) in the three sampling sites.

The Si:N:P stoichiometry highlighted how the Si resulted always in low concentration when compared to N and P. Considering the more labile fractions, P-exc:Si-exc ratio increased from spring (0.05) to summer (0.10) while N-exc:Si-exc ratios decreased from 3.7 to 2.0 in the same period. The observed imbalance of labile Si relative to labile P and N concentrations can be the consequence of a slower dissolution of BSi compared to mineralization of organic nitrogen and phosphorus, to a lower mobility of labile P and N forms, or to a preferential accumulation of P and N in the biomass of benthic primary producers.

4.4.2. Silica, Nitrogen and Phosphorus Release after Sediment Resuspension and Rewetting

This experiment was intended to evaluate nutrient dynamics associated with sediment rewetting and resuspension due to hydrological expansion or reconnection after the dry period. Under these circumstances the lateral and longitudinal hydrological connection of rivers is re-established, exposed sediments are flooded and the sediment, both exposed and submerged, can be suspended and transported downstream depending on water speed. Previous studies demonstrate that rewetting of dry sediments during the so-called "first flush events" leads to massive pulsed releases of dissolved nutrients (Skoulikidis et al., 2017) originating from the emergent and riparian area through the leaching from accumulated debris (Ylla et al., 2010), from cells lysis in exposed sediment (Schimel et al., 2007) and through the dissolution of salts from the sediment (Baldwin & Mitchell, 2000).

The results of this experiment confirm previous findings evidencing that suspended and rewetted sediments are, on average, a source of dissolved inorganic nutrients to the water column (Skoulikidis et al., 2017; Shumilova et al., 2019). The highest release of nutrients occurred in summer in association with high OM content is in agreement with previous studies that shows a higher release of N and P from organic material compared to sediment (Shumilova et al., 2019). Conversely, sediment drying does not influences DSi release while the effect on SRP release is not clear. Oxic conditions may favor P precipitation due to complex formation with Fe and Al oxides and hydroxides, while reducing conditions in submerged sediments would favor its mobility and accumulation in pore water. However, there are contrasting results on sediment P dynamics in relation to the effect of drying, with some studies reporting an increase of P mobile forms in dry sediments compared to submerged sediment (Gilbert et al., 2014; Dieter et al., 2015; Attygalla et al., 2016), and others reporting an increase of more stable forms (De Groot & Van Wijck, 1993; de Vicente et al., 2010). The results of this study are not able to demonstrate any effect of exposure to air and drying of sediment on P mobility, because only a slightly higher release of SRP was found in sediments exposed to air but it was localized in sediments of the Trebbia river which are also characterized by high OM content. It can be hypothesized that the P mobility and the amount of P that is released to the water

column are not only a function of sediment exposure but also depends on the organic matter quantity and quality. Conversely, both N-NO_x and N-NH_4^+ release is influenced by moisture, but sediment drying has an opposite effect on the two ions. While accumulation of N-NO_x in dry riverbeds is promoted by aerobic conditions that favor nitrification over denitrification, accumulation of N-NH_4^+ is promoted under humid and submerged conditions where the microbial activity that mineralizes the organic substance favor the production and subsequent release of N-NH_4^+ from sediments and the consumption of N-NO_x under anaerobic conditions, which also contrasts nitrification (von Schiller et al., 2015; Merbt et al., 2016; Arce et al., 2018).

The released amount was variable depending on the specific nutrient and, even though labile P and labile N concentrations in sediment resulted in excess compared to labile Si, DSi release to water resulted in excess compared to both SRP (P:Si <0.025) and DIN (N:Si <0.4) (Figure 34). Similar results were observed following DSi, SRP and DIN concentrations in the water column of an intermittent river immediately after flow resumption (Skoulikidis et al., 2017). Therefore, despite a higher accumulation of labile P and N in sediments, these results suggest that the Si fraction is more mobile compared to the other two nutrients, probably due to the high mineralization of BSi under hypoxic conditions (Lehtimäki et al., 2016) and the higher accumulation of BSi pool (Figure 26, Figure 27) in comparison to N and P labile pools.

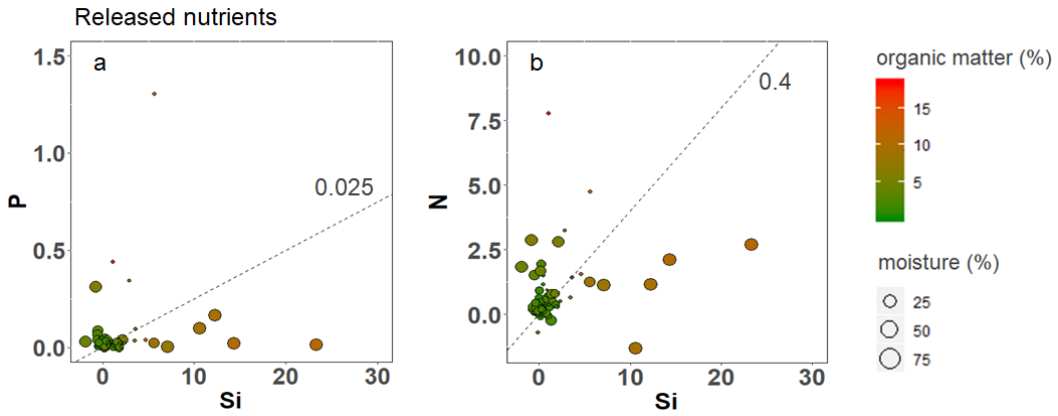

Figure 34. Si:P (a) and Si:N (b) molar ratios (in µmol g^{-1}_{DW}) of released nutrient in superficial sediment in relation to organic matter (color scale, OM %) and humidity content (dots size, moisture %) in the three sampling sites during rewetting simulation.

4.5. Conclusions

The results of this study evidence that from a biogeochemical point of view, flow contraction and sediment drying are key determinants of Si benthic biogeochemistry as already observed for N and P.

Si concentrations increase during summer, but the magnitude of the increase depends on the hydrological condition of the river and is almost restricted to submerged riverbeds. As such, sediment exposure to air and subsequent drying interfere with Si biogeochemistry and dry sediment maintains a relatively constant Si concentration. Sediment resuspension following hydrological expansion or reconnection after the dry period has the potential to determine an immediate release to the water of a fraction of the accumulated Si.

Labile P and N concentrations follow a similar pattern to that of Si but the degree of change is different determining a higher accumulation of labile inorganic P and N relative to Si in the sediment. However, the ratio of released nutrients does not correspond to the ratio in sediments suggesting that the Si fraction is more mobile compared to N and P.

Si cycle is nowadays poorly explored and river intermittency is a recent field of study in environmental sciences. Future perspectives on this subject could involve laboratory experiments in order to explore which environmental variable mostly influence Si release under contraction and fragmentation condition of riverbed, i.e. pH, temperature, light and air exposure. In addition, the regeneration of Si and dissolution of solid phases during the re-flooding processes will have to be properly follow under the different flow conditions with field samplings.

General conclusions

The aim of this thesis was to analyze how Si, N and P are processed in the hydrographic network under a climate change scenario and altered anthropogenic pressures. Specifically, transformations and accumulation, and downstream transport of these elements were analyzed in relation to hydrological discontinuities in rivers either due to the presence of natural lakes or depending on the flow alteration, i.e. hydrological intermittency.

Although the biogeochemistry of N and P have been extensively studied, there are still many aspects of the Si cycle which are insufficiently known. This is especially true for the interactions between the chemical and biological cycles of Si and processes of the Si cycle at the water sediment interface. At the same time, the knowledge of factors regulating Si biogeochemistry requires a comparison with the dynamics of other nutrients, as the ecosystem functioning depends on multiple element processes and stoichiometry.

More specifically three main questions were addressed related to the Si cycle:

a) River discontinuities due to natural lakes. Emphasis was put on how and to which extent a meromictic deep lake can act as a Si filter in the hydrographic network. In particular, Si retention and pathways were compared with those of N and P;

b) Which is the role of different primary producer communities in Si accumulation and recycling the littoral zone of a lake;

c) How the flow decrease influences Si, P and N concentration and mobilization in river sediments during the summer dry period.

The overarching hypotheses were that alteration of the hydrological characteristics of a given aquatic ecosystem, in terms of either reduced frequency of water mixing in lakes or water flow changes in rivers can deeply modify Si retention and fluxes, and that both benthic and planktonic primary producers can play an important role as Si filters and temporary sinks. Additionally, because of the differences between the biogeochemistry of Si compared to that of N and P, one also expected that these hydrological factors can also modify the stoichiometry of the three elements.

In the Oglio river-Lake Iseo hydrographic system, the lake is a biogeochemical reactor which retains and accumulates more Si (75%) and P (79%) than N (45%). As such, outflowing compared to inflowing waters are more enriched in N than Si and P. In Lake Iseo, meromixis exacerbates Si and P retention as the cycles of these two elements are mainly regulated by sedimentation of the particulate forms. The sedimented Si and P are either buried in the sediment or recycled through the water column as dissolved forms. The persistent stratification that characterize the meromixis keeps the recycled nutrients in the monimolimnion, making them unavailable to the photic zone while the stratification persists, i.e. for decades.

The littoral zone of lake Iseo also plays a potentially important role as regulator of DSi, SRP and DIN availability in the water column, but this function is strictly dependent on the structure and activity of the primary producer community. Macro- and microalgae communities on rocky substrates behave as a DSi sink and are a source of inorganic nitrogen and phosphorus to the water column. By contrast, littoral sediments colonized by submerged aquatic vegetation and microphytobenthos behave as a DSi source for the water column and as a sink for inorganic nitrogen and phosphorus. Specifically, the rooted vegetation can extract DSi from pore water, transferring it in the water column in particulate form, as phytoliths, which are easily decomposable. This pathway can be a relevant DSi source, compensating for possible Si losses due to sedimentation and segregation in the deeper water mass. This is a key issue for oligomictic and, especially, meromictic lakes, that however depends on the health status of the community. This aspect should not be ignored when considering the anthropogenic impact from watersheds and lake surroundings and should be further analyzed.

Hydrological changes in rivers flow, during summer water shortage and autumn resumption influence the Si accumulation in sediments. In particular, from a biogeochemical point of view, flow contraction and sediment drying are key determinants of Si benthic biogeochemistry as already observed for N and P. Si concentrations increase during summer, but the magnitude of the increase depends on the hydrological condition of the river and is almost restricted to submerged riverbeds. As such, sediment exposure to air and subsequent drying interfere with Si biogeochemistry and dry sediment maintains a relatively constant Si concentration. Labile P and N concentrations followed a similar pattern to that of Si, but the degree of change is different determining a higher accumulation of labile inorganic P and N relative to Si in the sediment. Hydrological expansion or reconnection phase, through sediment rewetting and resuspension, have the potential to release to the water a fraction of the Si accumulated during dry period and the ratio of released nutrients suggests that the Si fraction is more mobile compared to N and P.

In summary, the results of this research highlights that both lentic and lotic ecosystems are not only links that connect terrestrial and marine ecosystems acting as pipes, but they behave as biogeochemical regulators of Si delivery, thus modifying also its stoichiometry relative to N and P. Hydrology appears to be an important factor regulating this function by directly influencing transport processes and by indirectly shaping the activity of primary producers and microbial communities, and the chemical and physical characteristics of the environment where primary production, decomposition and ultimately mineralization take place.

Finally, the role of Si and its stoichiometry relative to N and P in regulating both growth and phenology of freshwater and marine algae and phanerogams may shape the ecosystem responses to both global and local pressures, which are still poorly understood.

Among other factors, one has to underline that in most of the deep perialpine lakes the full overturn is becoming less frequent (Salmaso et al., 2018). Moreover, many holo-oligomictic lakes are shifting towards a pronounced oligomixis and are close to turn meromictic (Zadereev et al., 2017). In such scenario, the hydrographic system of the main rivers in the alpine margin, will suffer for a nutrient filtration by deep lakes, which would enhance the ratio of DIN to both Si and P. This is a key point, nitrogen, especially nitrate, being a critical nutrient for the Po plain and similar watersheds.

Recent studies, strongly demonstrate that in southern Europe, Mediterranean conditions are expanding northwards. In other words, rivers are suffering for a relevant flow reduction, especially in summer, as well as streams are exposed to very long phases of very low to null flow (Larned et al., 2010; Datry et al., 2014). This is a key point for ecosystem processes, e.g. due to changes of either the upstream-downstream continuity or the more or less regular flow pulses, which are underpinning the river metabolism. Especially in the Po river area, where water contamination by nutrients and frequent outbreaks in the adjacent marine zone occur, there is the need of studies on nutrient cycling in rivers experiencing more and more riverbed contraction and fragmentation. This could shed more light on the complex interactions between water quality and land and water uses, in a climate change context.

5. Bibliography

Abril, M., I. Muñoz, & M. Menéndez, 2016. Heterogeneity in leaf litter decomposition in a temporary Mediterranean stream during flow fragmentation. Science of the Total Environment 553: 330–339.

Acreman, M., A. H. Arthington, M. J. Colloff, C. Couch, N. D. Crossman, F. Dyer, I. Overton, C. A. Pollino, M. J. Stewardson, & W. Young, 2014. Environmental flows for natural, hybrid, and novel riverine ecosystems in a changing world. Frontiers in Ecology and the Environment 12: 466–473.

Acuña, V., T. Datry, J. Marshall, D. Barceló, C. N. Dahm, A. Ginebreda, G. McGregor, S. Sabater, K. Tockner, & M. A. Palmer, 2014. Why should we care about temporary waterways?. Science 343: 1080–1081.

Acuña, V., I. Muñoz, A. Giorgi, M. Omella, F. Sabater, & S. Sabater, 2005. Drought and postdrought recovery cycles in an intermittent Mediterranean stream: structural and functional aspects. Journal of the North American Benthological Society 24: 919–933.

Aigars, J., R. Poik, T. Dalsgaard, E. Egl, & M. Jansons, 2015. Biogeochemistry of N, P and SI in the Gulf of Riga surface sediments: Implications of seasonally changing factors. Continental Shelf Research 105: 112–120.

Alexandre, A., J.-D. Meunier, F. Colin, & J.-M. Koud, 1997. Plant impact on the biogeochemical cycle of silicon and related weathering processes. Geochimica et Cosmochimica Acta 61: 677–682.

Alfredsson, H., W. Clymans, J. Stadmark, D. Conley, & J. Rousk, 2016. Bacterial and fungal colonization and decomposition of submerged plant litter : consequences for biogenic. FEMS Microbiology Ecology 92: fiw011.

Ambrosetti, W., & L. Barbanti, 2005. Evolution towards meromixis of Lake Iseo (Northern Italy) as revealed by its stability trend. Journal of Limnology 64: 1–11.

Ambrosetti, W., L. Barbanti, R. Mosello, & A. Pugnetti, 1992. Limnological studies on the deep southern Alpine lakes Maggiore, Lugano, Como, Iseo and Garda. In P. Guilizzoni, G. T. & G. G. (ed), Memorie dell'Istituto Italiano di Idrobiologia. Limnology in Italy: 117–146.

Anderson, L. D., & M. L. Delaney, 2000. Sequential extraction and analysis of phosphorus in marine sediments: Streamlining of the SEDEX procedure. Limnology and Oceanography 45: 509–515.

APHA, (American Public Health Association), 1998. Standard methods for the examination of water and wastewaters. Washington, DC.

Arce, M. I., C. Mendoza-Lera, M. Almagro, N. Catalán, A. M. Romaní, E. Martí, R. Gómez, S. Bernal, A. Foulquier, M. Mutz, R. Marcé, A. Zoppini, G. Gionchetta, G. Weigelhofer, R. del Campo, C. T. Robinson, A. Gilmer, M. Rulik, B. Obrador, O. Shumilova, S. Zlatanović, S. Arnon, P. Baldrian, G. Singer, T. Datry, N. Skoulikidis, B. Tietjen, & D. von Schiller, 2019. A conceptual framework for understanding the biogeochemistry of dry riverbeds through the lens of soil science. Earth-Science Reviews 188: 441–453.

Arce, M. I., M. del M. Sánchez-Montoya, M. R. Vidal-Abarca, M. L. Suárez, & R. Gómez, 2014. Implications of flow intermittency on sediment nitrogen availability and processing rates in a Mediterranean headwater stream. Aquatic Sciences 76: 173–186.

Arce, M. I., D. von Schiller, M. M. Bengtsson, C. Hinze, H. Jung, R. J. E. Alves, T. Urich, & G. Singer, 2018. Drying and rainfall shape the structure and functioning of nitrifying microbial communities in riverbed sediments. Frontiers in Microbiology 9: 1–17.

Arnell, N. W., & S. N. Gosling, 2013. The impacts of climate change on river flow regimes at the global scale. Journal of Hydrology 486: 351–364.

Aspila, K., H. Agemian, & A. S. Y. Chau, 1976. A semi-automated method for the determination of inorganic, organic and total phosphate in sediments. Analyst 101: 187–197.

Attygalla, N. W., D. S. Baldwin, E. Silvester, P. Kappen, & K. L. Whitworth, 2016. The severity of sediment desiccation affects the adsorption characteristics and speciation of phosphorus. Environmental Sciences: Processes and Impacts Royal Society of Chemistry 18: 64–71.

Azzoni, R., D. Nizzoli, M. Bartoli, & R. R. Christian, 2015. Factors controlling benthic biogeochemistry in urbanized coastal systems: an example from Venice (Italy). Estuaries and Coasts 38: 1016–1031.

Baker, D. B., R. Confesor, D. E. Ewing, L. T. Johnson, J. W. Kramer, & B. J. Merryfield, 2014. Phosphorus loading to Lake Erie from the Maumee, Sandusky and Cuyahoga rivers: The importance of bioavailability. Journal of Great Lakes Research 40: 502–517.

Baldwin, D. S., & A. M. Mitchell, 2000. The effects of drying and re-flooding on the sediment and soil nutrient dynamics of lowland river–floodplain systems: a synthesis. Regulated Rivers: Research & Management 16: 457–467.

Baron, J. S., E. K. Hall, B. T. Nolan, J. C. Finlay, E. S. Bernhardt, J. A. Harrison, F. Chan, & E. W. Boyer, 2013. The interactive effects of excess reactive nitrogen and climate change on aquatic ecosystems and water resources of the United States. Biogeochemistry 114: 71–92.

Barone, L., M. Pilotti, G. Valerio, M. Balistrocchi, L. Milanesi, S. C. Chapra, & D. Nizzoli, 2019. Analysis of the residual nutrient load from a combined sewer system in a watershed of a deep Italian lake. Journal of Hydrology 571: 202–213.

Bartoli, M., D. Nizzoli, & P. Viaroli, 2003. Microphytobenthos activity and fluxes at the sediment-water interface: interactions and spatial variability. Aquatic Ecology 37: 341–349.

Bates, B., Z. Kundzewicz, S. Wu, & J. Palutokof, 2008. Climate change and water. IPCC technical paper VI. UNEP, Geneva.

Bennett, E. M., S. R. Carpenter, & N. F. Caraco, 2001. Human Impact on Erodable Phosphorus and Eutrophication: A Global Perspective. BioScience 51: 227.

Bernal, S., D. von Schiller, F. Sabater, & E. Martí, 2013. Hydrological extremes modulate nutrient dynamics in mediterranean climate streams across different spatial scales. Hydrobiologia 719: 31–42.

Bernhardt, E. S., J. B. Heffernan, N. B. Grimm, E. H. Stanley, J. W. Harvey, M. Arroita, A. P. Appling, M. J. Cohen, W. H. McDowell, R. O. Hall, J. S. Read, B. J. Roberts, E. G. Stets, & C. B. Yackulic, 2018. The metabolic regimes of flowing waters. Limnology and Oceanography 63: S99–S118.

Billen, G., & J. Garnier, 2007. River basin nutrient delivery to the coastal sea: Assessing its potential to sustain new production of non-siliceous algae. Marine Chemistry 106: 148–160.

Bini, A., D. Corbari, P. Falletti, M. Fassina, C. R. Perotti, & A. Piccin, 2007. Morphology and geological setting of Iseo Lake (Lombardy) through multibeam bathymetry and high-resolution seismic profiles. Swiss Journal of Geosciences 100: 23–40.

Blackwell, M. S. A., A. M. Carswell, & R. Bol, 2013. Variations in concentrations of N and P forms in leachates from dried soils rewetted at different rates. Biology and Fertility of Soils 49: 79–87.

Blecker, S. W., R. L. McCulley, O. A. Chadwick, & E. F. Kelly, 2006. Biologic cycling of silica across a grassland bioclimosequence. Global Biogeochemical Cycles 20: 1–11.

Boehrer, B., C. von Rohden, & M. Schultze, 2017. Physical Features of Meromictic Lakes: Stratification and Circulation. In Gulati, R., E. Zadereev, & A. Degermendzhi (eds), Ecology of Meromictic Lakes. Ecological Studies (Analysis and Synthesis). Springer, Cham: 15–34.

Bolpagni, R., M. M. Azzella, C. Agostinelli, A. Beghi, E. Bettoni, G. Brusa, C. De Molli, R. Formenti, F. Galimberti, & B. E. L. Cerabolini, 2017. Integrating the water framework directive into the habitats directive: Analysis of distribution patterns of lacustrine EU habitats in lakes of Lombardy (Northern Italy). Journal of Limnology 76: 75–83.

Bonada, N., & V. H. Resh, 2013. Mediterranean-climate streams and rivers: Geographically separated but ecologically comparable freshwater systems. Hydrobiologia 719: 1–29.

Borrelli, N., M. Fernández, S. Maris, & M. Osterrieth, 2011. Calcium and silica biomineralizations in leaves of eleven aquatic species of the Pampean Plain , Argentina. Aquatic Botany 94: 29–

36.

Boulton, A. J., R. J. Rolls, K. L. Jaeger, & T. Datry, 2017. Hydrological Connectivity in Intermittent Rivers and Ephemeral Streams In Datry, T., B. Núria, & A. J. Boulton (eds), Intermittent Rivers and Ephemeral Streams: Ecology and Management. Elsevier Inc., Amsterdam: 79–108.

Bouwman, A. F., M. F. P. Bierkens, J. Griffioen, M. M. Hefting, J. J. Middelburg, H. Middelkoop, & C. P. Slomp, 2013. Nutrient dynamics, transfer and retention along the aquatic continuum from land to ocean: Towards integration of ecological and biogeochemical models. Biogeosciences 10: 1–23.

Braga, A., R. Azzoni, & P. Viaroli, 2014. Valutazione dei fattori che regolano il carico interno di fosforo nel lago d'Idro. Master thesis, University of Parma.

Breese, R. O. Y., 1994. Diatomite In Carr, D. D. (ed), Industrial Mineral and Rocks. Society for Mining, Metallurgy, and Exploration, Inc., Littleton: 397–412.

Broadley, M. R., P. Brown, I. Cakmak, J. F. Ma, Z. Rengel, & F. Zhao, 2012. Beneficial elements Marschner's Mineral Nutrition of Higher Plants. Academic Press: 249–269.

Bruesewitz, D. A., J. L. Tank, & S. K. Hamilton, 2012. Incorporating spatial variation of nitrification and denitrification rates into whole-lake nitrogen dynamics. Journal of geophysical research 117: 1–12.

Burgin, A. J., & S. K. Hamilton, 2007. Have we overemphasized the role of denitrification in aquatic ecosystems? A review of nitrate removal pathways. Frontiers in Ecology and the Environment 5: 89–96.

Burkholder, J. M., & R. G. Wetzel, 1989. Microbial colonization on natural and artificial macrophytes in a phosphorus-limited, hardwater lake. Journal of Phycology 25: 55–65.

Cao, Y., N. Zhang, J. Sun, & W. Li, 2019. Responses of periphyton on non-plant substrates to different macrophytes under various nitrogen concentrations: A mesocosm study. Aquatic Botany Elsevier 154: 53–59.

Carey, J. C., & R. W. Fulweiler, 2013a. Nitrogen enrichment increases net silica accumulation in a temperate salt marsh. Limnology and Oceanography 58: 99–111.

Carey, J. C., & R. W. Fulweiler, 2013b. Watershed land use alters riverine silica cycling. Biogeochemistry 113: 525–544.

Carey, J. C., & R. W. Fulweiler, 2014. Salt marsh tidal exchange increases residence time of silica in estuaries. Limnology and Oceanography 59: 1203–1212.

Carey, J. C., & R. W. Fulweiler, 2016. Human appropriation of biogenic silicon – the increasing role of agriculture. Functional Ecology 30: 1331–1339.

Carrick, H. J., & R. L. Lowe, 2007. Nutrient limitation of benthic algae in Lake Michigan: The role of silica. Journal of Phycology 43: 228–234.

Carter, S. J., & S. M. Colman, 1994. Biogenic Silica in Lake Baikal Sediments: Results From 1990–1992 American Cores. Journal of Great Lakes Research Elsevier 20: 751–760.

Catalán, N., B. Obrador, C. Alomar, & J. L. Pretus, 2013. Seasonality and landscape factors drive dissolved organic matter properties in Mediterranean ephemeral washes. Biogeochemistry 112: 261–274.

Cattaneo, A., G. Galanti, S. Gentinetta, & S. Romo, 1998. Epiphytic algae and macroinvertebrates on submerged and floating-leaved macrophytes in an Italian lake. Freshwater Biology 39: 725–740.

Clow, D. W., S. M. Stackpoole, K. L. Verdin, D. E. Butman, Z. Zhu, D. P. Krabbenhoft, & R. G. Striegl, 2015. Organic Carbon Burial in Lakes and Reservoirs of the Conterminous United States. Environmental Science and Technology 49: 7614–7622.

Clymans, W., E. Struyf, G. Govers, F. Vandevenne, & D. J. Conley, 2011. Anthropogenic impact on amorphous silica pools in temperate soils. Biogeosciences 8: 2281–2293.

Conley, D. J., 2002. Terrestrial ecosystems and the global biogeochemical silica cycle. Global Biogeochemical Cycles 16: 68-1-68–8.

Conley, D. J., M. A. Quigley, & C. L. Schelske, 1988. Silica and phosphorus flux from sediments: importance of internal recycling in Lake Michigan. Canadian Journal of Fisheries and Aquatic Sciences 45: 1030–1035.

Conley, D. J., C. L. Schelske, & E. F. Stoermer, 1993. Modification of the biogeochemical cycle of silica with eutrophication. Marine Ecology Progress Series 179–192.

Cook, P. L. M., K. T. Aldridge, S. Lamontagne, & J. D. Brookes, 2010. Retention of nitrogen, phosphorus and silicon in a large semi-arid riverine lake system. Biogeochemistry 99: 49–63.

Cooke, J., J. L. DeGabriel, & S. E. Hartley, 2016. The functional ecology of plant silicon: geoscience to genes. Functional Ecology 30: 1270–1276.

Cooper, S. D., P. S. Lake, S. Sabater, J. M. Melack, & J. L. Sabo, 2013. The effects of land use changes on streams and rivers in mediterranean climates. Hydrobiologia 719: 383–425.

Cornelis, J. T., B. Delvaux, R. B. Georg, Y. Lucas, J. Ranger, & S. Opfergelt, 2011. Tracing the origin of dissolved silicon transferred from various soil-plant systems towards rivers: A review. Biogeosciences 8: 89–112.

Coskun, D., R. Deshmukh, H. Sonah, J. G. Menzies, O. Reynolds, J. F. Ma, H. J. Kronzucker, & R. R. Bélanger, 2019. The controversies of silicon's role in plant biology. New Phytologist 221: 67–85.

Danielsson, Å., 2014. Influence of hypoxia on silicate concentrations in the Baltic Proper (Baltic Sea). Boreal Environment Research 19: 267–280.

Datry, T., A. Foulquier, R. Corti, D. von Schiller, K. Tockner, C. Mendoza-Lera, J. C. Clément, M. O. Gessner, M. Moleón, R. Stubbington, B. Gücker, R. Albarinõ, D. C. Allen, F. Altermatt, M. I. Arce, S. Arnon, D. Banas, A. Banegas-Medina, E. Beller, M. L. Blanchette, J. F. Blanco-Libreros, J. J. Blessing, I. G. Boëchat, K. S. Boersma, M. T. Bogan, N. Bonada, N. R. Bond, K. C. Brintrup Barriá, A. Bruder, R. M. Burrows, T. Cancellario, C. Canhoto, S. M. Carlson, S. Cauvy-Fraunié, N. Cid, M. Danger, B. De Freitas Terra, A. M. De Girolamo, E. De La Barra, R. Del Campo, V. D. Diaz-Villanueva, F. Dyer, A. Elosegi, E. Faye, C. Febria, B. Four, S. Gafny, S. D. Ghate, R. Gómez, L. Gómez-Gener, M. A. S. Gracą, S. Guareschi, F. Hoppeler, J. L. Hwan, J. I. Jones, S. Kubheka, A. Laini, S. D. Langhans, C. Leigh, C. J. Little, S. Lorenz, J. C. Marshall, E. Martín, A. R. McIntosh, E. I. Meyer, M. Miliša, M. C. Mlambo, M. Morais, N. Moya, P. M. Negus, D. K. Niyogi, A. Papatheodoulou, I. Pardo, P. Pařil, S. U. Pauls, V. Pešić, M. Polášek, C. T. Robinson, P. Rodríguez-Lozano, R. J. Rolls, M. M. Sánchez-Montoya, A. Savić, O. Shumilova, K. R. Sridhar, A. L. Steward, R. Storey, A. Taleb, A. Uzan, R. Vander Vorste, N. J. Waltham, C. Woelfle-Erskine, D. Zak, C. Zarfl, & A. Zoppini, 2018. A global analysis of terrestrial plant litter dynamics in non-perennial waterways. Nature Geoscience 11: 497–503.

Datry, T., S. T. Larned, & K. Tockner, 2014. Intermittent rivers: A challenge for freshwater ecology. BioScience 64: 229–235.

Datry, T., B. Núria, & A. J. Boulton, 2017a. General introduction In Datry, T., B. Núria, & A. J. Boulton (eds), Intermittent Rivers and Ephemeral Streams: Ecology and Management. Elsevier Inc., Amsterdam: 1–20.

Datry, T., G. Singer, E. Sauquet, D. Jorda-Capdevila, D. von Schiller, R. Stubbington, C. Magand, P. Pařil, M. Miliša, V. Acuña, M. H. Alves, B. Augeard, M. Brunke, N. Cid, Z. Csabai, J. England, J. Froebrich, P. Koundouri, N. Lamouroux, E. Martí, M. Morais, A. Munné, M. Mutz, V. Pesic, A. Previšić, A. Reynaud, C. Robinson, J. Sadler, N. Skoulikidis, B. Terrier, K. Tockner, D. Vesely, & A. Zoppini, 2017b. Science and Management of Intermittent Rivers and Ephemeral Streams (SMIRES). Research Ideas and Outcomes 3: 1–23.

De Groot, C. J., & C. Van Wijck, 1993. The impact of desiccation of a freshwater marsh (Garcines Nord, Camargue, France) on sediment-water-vegetation interactions. Part 1: The sediment chemistry. Hydrobiologia 252: 83–94.

de Jonge, V. N., 1980. Fluctuations in the Organic Carbon to Chlorophyll a Ratios for Estuarine Benthic Diatom Populations. Marine Ecology Progress Series 2: 345–353.

de Vicente, I., F. Ø. Andersen, H. C. B. Hansen, L. Cruz-Pizarro, & H. S. Jensen, 2010. Water level fluctuations may decrease phosphate adsorption capacity of the sediment in oligotrophic high mountain lakes. Hydrobiologia 651: 253–264.

DeMaster, D. J., 1981. The supply and accumulation of silica in the marine environment. Geochimica et Cosmochimica Acta 45: 1715–1732.

Den Heyer, C., & J. Kalff, 1998. Organic matter mineralization rates in sediments: a within- and among-lake study. Limnology and Oceanography 43: 695–705.

Dieter, D., C. Herzog, & M. Hupfer, 2015. Effects of drying on phosphorus uptake in re-flooded lake sediments. Environmental Science and Pollution Research 22: 17065–17081.

Dodds, W. K., S. A. Higgs, M. J. Spangler, J. Guinnip, J. D. Scott, S. C. Hedden, B. D. Frenette, R. Taylor, A. E. Schechner, D. J. Hoeinghaus, & M. A. Evans-White, 2018. Spatial heterogeneity and controls of ecosystem metabolism in a Great Plains river network. Hydrobiologia Springer International Publishing 813: 85–102.

Dodds, W. K., & M. R. Whiles, 2010. Freshwater Ecology: concepts and environmental applications of Limnology. Elsevier. Burlington, MA, U.S.A.

Donnermeyer, G. N., & M. M. Smart, 1985. The biomass and nutritive potential of Vallisneria americana Michx in navigation pool 9 of the upper Mississippi river. Aquatic Botany 22: 33–44.

Duarte, C. M., D. J. Conley, J. Carstensen, & M. Sánchez-Camacho, 2009. Return to Neverland: Shifting baselines affect eutrophication restoration targets. Estuaries and Coasts 32: 29–36.

Dupas, R., M. Delmas, J. M. Dorioz, J. Garnier, F. Moatar, & C. Gascuel-Odoux, 2015. Assessing the impact of agricultural pressures on N and P loads and eutrophication risk. Ecological Indicators 48: 396–407.

Dürr, H. H., M. Meybeck, J. Hartmann, G. G. Laruelle, & V. Roubeix, 2011. Global spatial distribution of natural riverine silica inputs to the coastal zone. Biogeosciences 8: 597–620.

Egge, J. K., & D. L. Aksnes, 1992. Silicate as regulating nutrient in phytoplankton competition. Marine Ecology Progress Series 83: 281–289.

Elser, J. J., & A. Hamilton, 2007. Stoichiometry and the new biology: The future is now. PLoS Biology 5: 1403–1405.

Epstein, E., 1994. The anomaly of silicon in plant biology. Proceedings of the National Academy of Sciences of the United States of America 91: 11–17.

Fenocchi, A., M. Rogora, S. Sibilla, M. Ciampittiello, & C. Dresti, 2018. Forecasting the evolution in the mixing regime of a deep subalpine lake under climate change scenarios through numerical modelling (Lake Maggiore, Northern Italy/Southern Switzerland). Climate

Dynamics 51: 3521–3536.

Fenocchi, A., M. Rogora, S. Sibilla, & C. Dresti, 2017. Relevance of inflows on the thermodynamic structure and on the modeling of a deep subalpine lake (Lake Maggiore, Northern Italy/Southern Switzerland). Limnologica 63: 42–56.

Ferris, J. A., & J. T. Lehman, 2007. Interannual variation in diatom bloom dynamics: Roles of hydrology, nutrient limitation, sinking, and whole lake manipulation. Water Research 41: 2551–2562.

Ficker, H., M. Luger, & H. Gassner, 2017. From dimictic to monomictic: Empirical evidence of thermal regime transitions in three deep alpine lakes in Austria induced by climate change. Freshwater Biology 62: 1335–1345.

Francis, T. B., D. E. Schindler, J. M. Fox, & E. Seminet-reneau, 2007. Effects of Urbanization on the Dynamics of Organic Sediments in Temperate Lakes. Ecosystems 10: 1057–1068.

Fraysse, F., O. S. Pokrovsky, J. Schott, & J. D. Meunier, 2006. Surface properties, solubility and dissolution kinetics of bamboo phytoliths. Geochimica et Cosmochimica Acta 70: 1939–1951.

Friedrich, J., C. Dinkel, E. Grieder, S. Radan, D. Secrieru, S. Steingruber, & B. Wehrli, 2003. Nutrient uptake and benthic regeneration in Danube Delta Lakes. Biogeochemistry 64: 373–398.

Frings, P. J., W. Clymans, E. Jeppesen, T. L. Lauridsen, E. Struyf, & D. J. Conley, 2014. Lack of steady-state in the global biogeochemical Si cycle: Emerging evidence from lake Si sequestration. Biogeochemistry 117: 225–277.

Galloway, J. N., J. D. Aber, J. W. Erisman, S. P. Seitzinger, R. W. Howarth, E. B. Cowling, & B. J. Cosby, 2003. The Nitrogen Cascade. BioScience 53: 341–356.

Georgiadis, A., D. Sauer, L. Herrmann, J. Breuer, M. Zarei, & K. Stahr, 2013. Development of a method for sequential Si extraction from soils. Geoderma Elsevier B.V. 209–210: 251–261.

Ghirardi, N., R. Bolpagni, M. Bresciani, G. Valerio, M. Pilotti, & C. Giardino, 2019. Spatiotemporal Dynamics of Submerged Aquatic Vegetation in a Deep Lake from Sentinel-2 Data. Water 11: 1–14.

Gilbert, J. D., F. Guerrero, & I. De Vicente, 2014. Sediment desiccation as a driver of phosphate availability in the water column of Mediterranean wetlands. Science of the Total Environment 466–467: 965–975.

Glibert, P. M., 2017. Eutrophication, harmful algae and biodiversity — Challenging paradigms in a world of complex nutrient changes. Marine Pollution Bulletin 124: 591–606.

Golterman, H. L., R. S. Clymo, & M. A. M. Ohnstand, 1978. Methods for Physical and Chemical Analysis of Freshwaters. Oxford.

Gómez, R., I. M. Arce, J. J. Sánchez, & M. del Mar Sánchez-Montoya, 2012. The effects of drying

on sediment nitrogen content in a Mediterranean intermittent stream: A microcosms study. Hydrobiologia 679: 43–59.

Gommes, R., & H. Muntau, 1981. The chemical composition of limnophytes in lake Maggiore. Memorie dell'Istituto Italiano di Idrobiologia 38: 237–307.

Grill, G., B. Lehner, M. Thieme, B. Geenen, D. Tickner, F. Antonelli, S. Babu, P. Borrelli, L. Cheng, H. Crochetiere, H. Ehalt Macedo, R. Filgueiras, M. Goichot, J. Higgins, Z. Hogan, B. Lip, M. E. McClain, J. Meng, M. Mulligan, C. Nilsson, J. D. Olden, J. J. Opperman, P. Petry, C. Reidy Liermann, L. Sáenz, S. Salinas-Rodríguez, P. Schelle, R. J. P. Schmitt, J. Snider, F. Tan, K. Tockner, P. H. Valdujo, A. van Soesbergen, & C. Zarfl, 2019. Mapping the world's free-flowing rivers. Nature 569: 215–221.

Grimshaw, H. J., M. Rosen, D. R. Swift, K. Rodberg, & J. M. Noel, 1993. Marsh phosphorus concentrations, phosphorus content and species composition of Everglades periphyton communities. Archive fur Hydrobiologie 128: 257–276.

Harrison, J. A., P. J. Frings, A. H. W. Beusen, D. J. Conley, & M. L. McCrackin, 2012. Global importance, patterns, and controls of dissolved silica retention in lakes and reservoirs. Global Biogeochemical Cycles 26: 1–12.

Harrison, J. A., R. J. Maranger, R. B. Alexander, A. E. Giblin, P. Jacinthe, E. Mayorga, S. P. Seitzinger, D. J. Sobota, & W. M. Wollheim, 2009. The regional and global significance of nitrogen removal in lakes and reservoirs. Biogeochemistry 93: 143–157.

Hartikainen, H., M. Pitkänen, T. Kairesalo, & L. Tuominen, 1996. Co-occurrence and potential chemical competition of phosphorus and silicon in lake sediment. Water Research 30: 2472–2478.

Harvey, J. W., M. H. Conklin, & R. S. Koelsch, 2003. Predicting changes in hydrologic retention in an evolving semi-arid alluvial stream. Advances in Water Resources 26: 939–950.

Havens, K. E., 2008. Cyanobacteria blooms: effects on aquatic ecosystems. In Springer (ed), Hudnell H.K. (eds) Cyanobacterial Harmful Algal Blooms: State of the Science and Research Needs. Advances in Experimental Medicine and Biology. New York, NY: 733–747.

Hecky, R. E., & P. Kilham, 1988. Nutrient limitation of phytoplankton in freshwater and marine environments: A review of recent evidence on the effects of enrichment. Limnology and Oceanography 33: 796–822.

Hillebrand, H., J. M. Cowles, A. Lewandowska, D. B. Van de Waal, & C. Plum, 2014. Think ratio! A stoichiometric view on biodiversity-ecosystem functioning research. Basic and Applied Ecology 15: 465–474.

Hillebrand, H., & U. Sommer, 1999. The nutrient stoichiometry of benthic microalgal growth:

Redfield proportions are optimal. Limnology and Oceanography 44: 440–446.

Hobbs, W. O., S. V. Lalonde, R. D. Vinebrooke, K. O. Konhauser, R. P. Weidman, M. D. Graham, & A. P. Wolfe, 2010. Algal-silica cycling and pigment diagenesis in recent alpine lake sediments: Mechanisms and paleoecological implications. Journal of Paleolimnology 44: 613–628.

Hotaling, S., D. S. Finn, J. Joseph Giersch, D. W. Weisrock, & D. Jacobsen, 2017. Climate change and alpine stream biology: progress, challenges, and opportunities for the future. Biological Reviews 92: 2024–2045.

House, W. A., F. H. Denison, M. S. Warwick, & B. V. Zhmud, 2000. Dissolution of silica and the development of concentration profiles in freshwater sediments. Applied Geochemistry 15: 425–438.

Howarth, R., F. Chan, D. J. Conley, J. Garnier, S. C. Doney, R. Marino, & G. Billen, 2011. Coupled biogeochemical cycles: Eutrophication and hypoxia in temperate estuaries and coastal marine ecosystems. Frontiers in Ecology and the Environment 9: 18–26.

Humborg, C., D. J. Conley, L. Rahm, F. Wulff, A. Cociasu, & V. Ittekkot, 2000. Silicon retention in river basins: Far-reaching effects on biogeochemistry and aquatic food webs in coastal marine environments. AMBIO: A Journal of the Human Environment 29: 45–50.

Humborg, C., V. Ittekkot, A. Cociasu, & v. B. Bodungen, 1997. Effect of Danube river dam on Black Sea biogeochemistry and ecosystem structure. Nature 386: 385–388.

ISTAT, 2010. (Italian National Institute of Statistics) 2010. Available online: http://dati. istat.it/ (accessed on 21 april 2017). .

Ittekkot, V., C. Humborg, & P. Schafer, 2000. Hydrological Alterations and Marine Biogeochemistry: A Silicate Issue?. BioScience 50: 776–782.

Jeppesen, E., S. Brucet, L. Naselli-Flores, E. Papastergiadou, K. Stefanidis, T. Nõges, P. Nõges, J. L. Attayde, T. Zohary, J. Coppens, T. Bucak, R. F. Menezes, F. R. S. Freitas, M. Kernan, M. Søndergaard, & M. Beklioğlu, 2015. Ecological impacts of global warming and water abstraction on lakes and reservoirs due to changes in water level and related changes in salinity. Hydrobiologia 750: 201–227.

Kahlert, M., 1998. C:N:P ratios of freshwater benthic algae. Archives of Hydrobiology Special Issue Advances in Limnology 51: 105–114.

Kelderman, P., H. J. Lindeboom, & J. Klein, 1988. Light dependent sediment-water exchange of dissolved reactive phosphorus and silicon in a producing microflora mat. Hydrobiologia 159: 137–147.

Koroleff, F., 1970. Direct determination of ammonia in natural waters as indophenol blue.

Information on techniques and methods for seawater analysis. I.C.E.S. Interlaboratory Rep 3: 19–22.

Kraemer, B. M., O. Anneville, S. Chandra, M. Dix, E. Kuusisto, D. M. Livingstone, A. Rimmer, S. G. Schladow, E. Silow, L. M. Sitoki, R. Tamatamah, Y. Vadeboncoeur, & P. B. McIntyre, 2015. Morphometry and average temperature affect lake stratification responses to climate change. Geophysical research letters 42: 4981–4988.

Lake, P. S., 2003. Ecological effects of perturbation by drought in flowing waters. Freshwater Biology 48: 1161–1172.

Larned, S. T., T. Datry, D. B. Arscott, & K. Tockner, 2010. Emerging concepts in temporary-river ecology. Freshwater Biology 55: 717–738.

Lehner, B., C. R. Liermann, C. Revenga, C. Vörömsmarty, B. Fekete, P. Crouzet, P. Döll, M. Endejan, K. Frenken, J. Magome, C. Nilsson, J. C. Robertson, R. Rödel, N. Sindorf, & D. Wisser, 2011. High-resolution mapping of the world's reservoirs and dams for sustainable river-flow management. Frontiers in Ecology and the Environment 9: 494–502.

Lehtimäki, M., H. Sinkko, & P. Tallberg, 2016. The role of oxygen conditions in the microbial dissolution of biogenic silica under brackish conditions. Biogeochemistry 129: 355–371.

Lehtimäki, M., P. Tallberg, & V. Siipola, 2013. Seasonal Dynamics of Amorphous Silica in Vantaa River Estuary. Silicon 5: 35–51.

Lenth, R., H. Singmann, J. Love, P. Buerkner, & M. Herve, 2018. Estimated Marginal Means, aka Least-Squares Means. R Foundation for Statistical Computing, Vienna, Austria, R Package Version 1.3.1.

Lorenzen, C. J., 1967. Determination of chlorophyll and pheo-pigments: spectrophotometric equations. Limnology and Oceanography: Methods 12: 343–346.

Maasri, A., S. Fayolle, E. Gandouin, R. Garnier, & E. Franquet, 2008. Epilithic chironomid larvae and water enrichment: is larval distribution explained by epilithon quantity or quality?. Journal of the North American Benthological Society 27: 38–51.

Maavara, T., J. L. A. Hood, R. L. North, L. E. Doig, C. T. Parsons, J. Johansson, K. Liber, J. J. Hudson, B. T. Lucas, D. M. Vandergucht, & P. Van Cappellen, 2015. Reactive silicon dynamics in a large prairie reservoir (Lake Diefenbaker, Saskatchewan). Journal of Great Lakes Research 41: 100–109.

Maher, W., F. Krikowa, D. Wruck, H. Louie, T. Nguyen, & W. Y. Huang, 2002. Determination of total phosphorus and nitrogen in turbid waters by oxidation with alkaline potassium peroxodisulfate and low pressure microwave digestion, autoclave heating or the use of closed vessels in a hot water bath: Comparison with Kjeldahl digesti. Analytica Chimica Acta 463:

283–293.

Malkin, S. Y., R. J. Sorichetti, J. A. Wiklund, & R. E. Hecky, 2009. Seasonal abundance, community composition, and silica content of diatoms epiphytic on Cladophora glomerata. Journal of Great Lakes Research 35: 199–205.

Maranger, R., S. E. Jones, & J. B. Cotner, 2018. Stoichiometry of carbon, nitrogen, and phosphorus through the freshwater pipe. Limnology and Oceanography Letters 3: 89–101.

McClain, M. E., E. W. Boyer, C. L. Dent, S. E. Gergel, N. B. Grimm, P. M. Groffman, S. C. Hart, J. W. Harvey, C. A. Johnston, E. Mayorga, W. H. McDowell, & G. Pinay, 2003. Biogeochemical Hot Spots and Hot Moments at the Interface of Terrestrial and Aquatic Ecosystems. Ecosystems 6: 301–312.

Mckeague, J. A., & M. G. Cline, 1963. Silica in soils. Advances in Agronomy 15: 339–396.

Merbt, S. N., L. Proia, J. I. Prosser, E. Marti, E. O. Casamayor, & D. von Schiller, 2016. Stream drying drives microbial ammonia oxidation and first-flush nitrate export. Ecology 97: 2192–2198.

Meybeck, M., & C. Vörösmarty, 2005. Fluvial filtering of land-to-ocean fluxes: from natural Holocene variations to Anthropocene. Comptes Rendus - Geoscience 337.1-2: 107–123.

Moore, P. A., K. R. Reddy, & M. M. Fisher, 1998. Phosphorus Flux between Sediment and Overlying Water in Lake Okeechobee, Florida: Spatial and Temporal Variations. Journal of Environmental Quality 1439: 1428–1439.

Mosello, R., W. Ambrosetti, S. Arisci, R. Bettinetti, F. Buzzi, A. Calderoni, E. Carrara, R. De Bernardi, S. Galassi, L. Garibaldi, B. Leoni, M. Manca, A. Marchetto, G. Morabito, A. Oggioni, R. Pagnotta, D. Ricci, M. Rogora, N. Salmaso, M. Simona, G. Tartari, M. Veronesi, & P. Volta, 2010. Recent evolution of water quality in the deep subalpine lakes (Maggiore, Lugano, Como, Iseo and Garda) as a response to anthropogenic pressures and climate changes. Biologia Ambientale 24(1): 167–177.

Müller, C., 1983. Uptake and accumulation of some nutrient elements in relation to the biomass of an epilithic community Periphyton of Freshwater Ecosystems. Springer Netherlands, Dordrecht: Volume 17, 147-151.

Newberry, T. L., & C. L. Schelske, 1986. Biogenic silica record in the sediments of Little Round Lake, Ontario. Hydrobiologia 143: 293–300.

Nilsson, C., C. A. Reidy, M. Dynesius, & C. Revenga, 2005. Fragmentation and flow regulation of the world's large river systems. Science 308: 405–408.

Nizzoli, D., M. Bartoli, R. Azzoni, D. Longhi, G. Castaldelli, & P. Viaroli, 2018. Denitrification in a meromictic lake and its relevance to nitrogen flows within a moderately impacted forested

catchment. Biogeochemistry 137: 143–161.

Nizzoli, D., M. Bartoli, M. Cooper, D. T. Welsh, G. J. C. Underwood, & P. Viaroli, 2007. Implications for oxygen, nutrient fluxes and denitrification rates during the early stage of sediment colonisation by the polychaete Nereis spp . in four estuaries. Estuarine, Coastal and Shelf Science 75: 125–134.

Nizzoli, D., D. T. Welsh, D. Longhi, & P. Viaroli, 2014. Influence of Potamogeton pectinatus and microphytobenthos on benthic metabolism, nutrient fluxes and denitrification in a freshwater littoral sediment in an agricultural landscape: N assimilation versus N removal. Hydrobiologia 737: 183–200.

Officer, C. B., & J. H. Ryther, 1980. The Possible Importance of Silicon in Marine Eutrophication. Marine Ecology Progress Series 3: 83–91.

Paerl, H. W., J. T. Scott, M. J. McCarthy, S. E. Newell, W. S. Gardner, K. E. Havens, D. K. Hoffman, S. W. Wilhelm, & W. A. Wurtsbaugh, 2016. It Takes Two to Tango: When and Where Dual Nutrient (N & P) Reductions Are Needed to Protect Lakes and Downstream Ecosystems. Environmental Science and Technology 50: 10805–10813.

Pansu, M., & J. Gautheyrou, 2007. Handbook of soil analysis: mineralogical, organic and inorganic methods. Springer Science & Business Media.

Pekel, J. F., A. Cottam, N. Gorelick, & A. S. Belward, 2016. High-resolution mapping of global surface water and its long-term changes. Nature 540: 418–422.

Pettit, N. E., D. P. Ward, M. F. Adame, D. Valdez, & S. E. Bunn, 2016. Influence of aquatic plant architecture on epiphyte biomass on a tropical river floodplain. Aquatic Botany 129: 35–43.

Pinardi, M., M. Bartoli, D. Longhi, U. Marzocchi, A. Laini, C. Ribaudo, & P. Viaroli, 2009. Benthic metabolism and denitrification in a river reach: a comparison between vegetated and bare sediments. Journal of Limnology 68: 133–145.

Pinheiro, J., D. Bates, S. DebRoy, D. Sarkar, & R Core Team, 2016. nlme: linear and nonlinear mixed effects models. The R package, R Package Version 3.1-126.

Quilbé, R., A. N. Rousseau, M. Duchemin, A. Poulin, G. Gangbazo, & J. P. Villeneuve, 2006. Selecting a calculation method to estimate sediment and nutrient loads in streams: Application to the Beaurivage River (Québec, Canada). Journal of Hydrology 326: 295–310.

Racchetti, E., M. Bartoli, E. Soana, D. Longhi, R. R. Christian, M. Pinardi, & P. Viaroli, 2011. Influence of hydrological connectivity of riverine wetlands on nitrogen removal via denitrification. Biogeochemistry 103: 335–354.

Redfield, A., B. H. Ketchum, & F. A. Richards, 1963. The influence of organisms of the composition of seawater In Hill, M. N. (ed), The Sea. Wiley-Interscience, New York, NY: Vol. 2., pp. 26–

77.

Reynolds, C. S., & P. S. Davies, 2001. Sources and bioavailability of phosphorus fractions in freshwaters: a British perspective. Biological Reviews 76(1): 27–64.

Riber, H. H., J. P. Sørensen, & A. Kowalczewski, 1983. Exchange of phosphorus between water, macrophytes and epiphytic periphyton in the littoral of Mikolajskie Lake, Poland Periphyton of Freshwater Ecosystems. Springer Netherlands, Dordrecht: Volume17, 235–243.

Roberts, B. J., P. J. Mulholland, & W. R. Hill, 2007. Multiple scales of temporal variability in ecosystem metabolism rates: Results from 2 years of continuous monitoring in a forested headwater stream. Ecosystems 10: 588–606.

Rogora, M., F. Buzzi, C. Dresti, B. Leoni, F. Lepori, R. Mosello, M. Patelli, & N. Salmaso, 2018. Climatic effects on vertical mixing and deep-water oxygen content in the subalpine lakes in Italy. Hydrobiologia 824: 33–50.

Ruban, V., J. F. López-Sánchez, P. Pardo, G. Rauret, H. Muntau, & P. Quevauviller, 1999. Selection and evaluation of sequential extraction procedures for the determination of phosphorus forms in lake sediment. Journal of Environmental Monitoring 1: 51–56.

Rubel, F., K. Brugger, K. Haslinger, & I. Auer, 2017. The climate of the European Alps: Shift of very high resolution Köppen-Geiger climate zones 1800-2100. Meteorologische Zeitschrift 26: 115–125.

Ruttenberg, K. C., 1992. Development of a sequential extraction method for different forms of phosphorus in marine sediments. Limnology and Oceanography 37: 1460–1482.

Ruttenberg, K. C., 2003. The global phosphorus cycle. Treatise on geochemistry 8: 682.

Sala, O. E., F. S. Chapin, J. J. Armesto, E. Berlow, J. Bloomfield, R. Dirzo, E. Huber-Sanwald, L. F. Huenneke, R. B. Jackson, A. Kinzig, R. Leemans, D. M. Lodge, H. A. Mooney, M. Oesterheld, N. L. R. Poff, M. T. Sykes, B. H. Walker, M. Walker, & D. H. Wall, 2000. Global biodiversity scenarios for the year 2100. Science 287: 1770–1774.

Salmaso, N., O. Anneville, & D. Straile, 2018. European large perialpine lakes under anthropogenic pressures and climate change: present status , research gaps and future challenges. Hydrobiologia Springer International Publishing 824:1: 1–32.

Salmaso, N., F. Buzzi, L. Cerasino, L. Garibaldi, B. Leoni, G. Morabito, M. Rogora, & M. Simona, 2014. Influence of atmospheric modes of variability on the limnological characteristics of large lakes south of the Alps: A new emerging paradigm. Hydrobiologia 731: 31–48.

Salmaso, N., & R. Mosello, 2010. Limnological research in the deep southern subalpine lakes: synthesis, directions and perspectives. Advances in Oceanography and Limnology 1:1: 29–66.

Sangster, A. G., 1970. Intracellular Silica Deposition in Immature Leaves in Three Species of the Gramineae. Annals of Botany 34: 245–257.

Saunders, D. L., & J. Kalff, 2001. Nitrogen retention in wetlands, lakes and rivers. Hydrobiologia 443: 205–212.

Schaller, J., J. Schoelynck, E. Struyf, & P. Meire, 2016. Silicon affects nutrient content and ratios of wetland plants. Silicon 8: 479–485.

Scheffer, M., 1997. Ecology of Shallow Lakes. Population and Community Biology Series. Springer Netherlands, Dordrecht.

Schelske, C. L., & E. F. Stoermer, 1971. Eutrophication, silica depletion, and predicted changes in algal quality in Lake Michigan. Science 173: 423–424.

Schelske, C. L., E. F. Stoermer, & W. F. Kenney, 2006. Historic low-level phosphorus enrichment in the Great Lakes inferred from biogenic silica accumulation in sediments. Limnology and Oceanography 51: 728–748.

Schimel, J., T. C. Balser, & M. Wallenstein, 2007. Microbial stress-response physiology and its implications for ecosystem function. Ecology 88: 1386–1394.

Schlesinger, W. H., 1997. Biogeochemistry: an analysis ofglobal change. Academic Press, San Diego.

Schoelynck, J., K. Bal, H. Backx, T. Okruszko, P. Meire, & E. Struyf, 2010. Silica uptake in aquatic and wetland macrophytes: a strategic choice between silica, lignin and cellulose?. New Phytologist 186: 385–391.

Schoelynck, J., K. Bal, S. Puijalon, P. Meire, & E. Struyf, 2012. Hydrodynamically mediated macrophyte silica dynamics. Plant Biology 14: 997–1005.

Schoelynck, J., & E. Struyf, 2016. Silicon in aquatic vegetation. Functional Ecology 30: 1323–1330.

Scibona, A., R. Azzoni, E. Soana, & P. Viaroli, 2015. Flussi e speciazione di fosforo nel fiume Po e nei suoi principali affluenti. Master thesis, University of Parma.

Seitzinger, S., J. A. Harrison, J. K. Böhlke, A. F. Bouwman, R. Lowrance, B. Peterson, C. Tobias, & G. Van Drecht, 2006. Denitrification across landscapes and waterscapes: A synthesis. Ecological Applications 16: 2064–2090.

Seitzinger, S. P., E. Mayorga, A. F. Bouwman, C. Kroeze, A. H. W. Beusen, G. Billen, G. Van Drecht, E. Dumont, B. M. Fekete, J. Garnier, & J. A. Harrison, 2010. Global river nutrient export: A scenario analysis of past and future trends. Global Biogeochemical Cycles 24: 1–16.

Serediak, N. A., E. E. Prepas, & G. J. Putz, 2014. Eutrophication of freshwater systems. Environmental Geochemistry 11: 305–323.

Sferratore, A., J. Garnier, G. Billen, D. Conley, & S. Pinault, 2006. Diffuse and Point Sources of Silica in the Seine River Watershed. Environmental Science and Technology 40: 6630–6635.

Shumilova, O., D. Zak, T. Datry, D. von Schiller, R. Corti, A. Foulquier, B. Obrador, K. Tockner, D. C. Allan, F. Altermatt, M. I. Arce, S. Arnon, D. Banas, A. Banegas-Medina, E. Beller, M. L. Blanchette, J. F. Blanco-Libreros, J. Blessing, I. G. Boëchat, K. Boersma, M. T. Bogan, N. Bonada, N. R. Bond, K. Brintrup, A. Bruder, R. Burrows, T. Cancellario, S. M. Carlson, S. Cauvy-Fraunié, N. Cid, M. Danger, B. de Freitas Terra, A. M. De Girolamo, R. del Campo, F. Dyer, A. Elosegi, E. Faye, C. Febria, R. Figueroa, B. Four, M. O. Gessner, P. Gnohossou, R. G. Cerezo, L. Gomez-Gener, M. A. S. Graça, S. Guareschi, B. Gücker, J. L. Hwan, S. Kubheka, S. D. Langhans, C. Leigh, C. J. Little, S. Lorenz, J. Marshall, A. McIntosh, C. Mendoza-Lera, E. I. Meyer, M. Miliša, M. C. Mlambo, M. Moleón, P. Negus, D. Niyogi, A. Papatheodoulou, I. Pardo, P. Paril, V. Pešić, P. Rodriguez-Lozano, R. J. Rolls, M. M. Sanchez-Montoya, A. Savić, A. Steward, R. Stubbington, A. Taleb, R. Vander Vorste, N. Waltham, A. Zoppini, & C. Zarfl, 2019. Simulating rewetting events in intermittent rivers and ephemeral streams: A global analysis of leached nutrients and organic matter. Global Change Biology 25: 1591–1611.

Sigmon, D. E., & L. B. Cahoon, 1997. Comparative effects of benthic microalgae and phytoplankton on dissolved silica fluxes. Aquatic microbial ecology 13: 275–284.

Siipola, V., M. Lehtimäki, & P. Tallberg, 2016. The effects of anoxia on Si dynamics in sediments. J Soils Sediments 16: 266–279.

Skoulikidis, N., & Y. Amaxidis, 2009. Origin and dynamics of dissolved and particulate nutrients in a minimally disturbed Mediterranean river with intermittent flow. Journal of Hydrology 373: 218–229.

Skoulikidis, N. T., L. Vardakas, Y. Amaxidis, & P. Michalopoulos, 2017. Biogeochemical processes controlling aquatic quality during drying and rewetting events in a Mediterranean non-perennial river reach. Science of the Total Environment 575: 378–389.

Soana, E., M. Naldi, S. Bonaglia, E. Racchetti, G. Castaldelli, V. Bruchert, P. Viaroli, & M. Bartoli, 2015. Benthic nitrogen metabolism in a macrophyte meadow (Vallisneria spiralis L.) under increasing sedimentary organic matter loads. Biogeochemistry 124: 387–404.

Sommer, M., D. Kaczorek, Y. Kuzyakov, & J. Breuer, 2006. Silicon pools and fluxes in soils and landscapes - A review. Journal of Plant Nutrition and Soil Science 169: 310–329.

Spears, B. M., L. Carvalho, R. Perkins, & D. M. Paterson, 2008. Effects of light on sediment nutrient flux and water column nutrient stoichiometry in a shallow lake. Water research 42: 977–986.

Stanley, E. H., S. G. Fisher, & N. B. Grimm, 1997. Ecosystem expansion and contraction in streams: Desert streams vary in both space and time and fluctuate dramatically in size. BioScience 47: 427–435.

Steward, A. L., D. von Schiller, K. Tockner, J. C. Marshall, & S. E. Bunn, 2012. When the river runs dry: Human and ecological values of dry riverbeds. Frontiers in Ecology and the Environment 10: 202–209.

Strayer, D. L., & S. E. G. Findlay, 2010. Ecology of freshwater shore zones. Aquatic Sciences 72: 127–163.

Street-Perrott, F. A., & P. A. Barker, 2008. Biogenic silica: A neglected component of the coupled global continental biogeochemical cycles of carbon and silicon. Earth Surface Processes and Landforms 33: 1436–1457.

Struyf, E., & D. J. Conley, 2009. Silica: An essential nutrient in wetland biogeochemistry. Frontiers in Ecology and the Environment 7: 88–94.

Struyf, E., & D. J. Conley, 2012. Emerging understanding of the ecosystem silica filter. Biogeochemistry 107: 9–18.

Struyf, E., S. Van Damme, B. Gribsholt, J. J. Middelburg, & P. Meire, 2005. Biogenic silica in tidal freshwater marsh sediments and vegetation (Schelde estuary, Belgium). Mar Ecol Prog Ser 303: 51–60.

Struyf, E., A. Smis, S. Van Damme, J. Garnier, G. Govers, B. Van Wesemael, D. J. Conley, O. Batelaan, E. Frot, W. Clymans, F. Vandevenne, C. Lancelot, P. Goos, & P. Meire, 2010. Historical land use change has lowered terrestrial silica mobilization. Nature Communications 1: 1–7.

Struyf, E., A. Smis, S. van Damme, P. Meire, & D. J. Conley, 2009. The global biogeochemical silicon cycle. Silicon 1: 207–213.

Struyf, E., S. Van Damme, B. Gribsholt, K. Bal, O. Beauchard, J. J. Middelburg, & P. Meire, 2007. Phragmites australis and silica cycling in tidal wetlands. Aquatic Botany 87: 134–140.

Sundback, K., A. Miles, & E. Goransson, 2000. Nitrogen fluxes, denitrification and the role of microphytobenthos in microtidal shallow-water sediments: an annual study. Marine Ecology Progress Series 200: 59–76.

Swift, D., & R. Nicholas, 1987. Periphyton and water quality relationships in the Everglades Water Conservation Areas, 1978-1982 South Florida Water Management District Tech. Pub., West Palm Beach, FL, USA: Volume 87-2, 44.

Tallberg, P., A. S. Heiskanen, J. Niemistö, P. O. J. Hall, & J. Lehtoranta, 2017. Are benthic fluxes important for the availability of Si in the Gulf of Finland?. Journal of Marine Systems 171: 89–100.

Tallberg, P., J. Lehtoranta, & S. Hietanen, 2013. Silicate Release from Sand-Manipulated Sediment Cores: Biogenic or Adsorbed Si?. Silicon 5: 67–74.

Tallberg, P., K. Lukkari, A. Räike, J. Lehtoranta, & M. Leivuori, 2009. Applicability of a sequential P fractionation procedure to Si in sediment. Journal of Soils and Sediments 9: 594–603.

Teodoru, C., A. Dimopoulos, & B. Wehrli, 2006. Biogenic silica accumulation in the sediments of Iron Gate I Reservoir on the Danube River. Aquatic Sciences 68: 469–481.

The R Core Team, 2019. R: A language and environment for statistical computing. R Foundation for Statistical Computing, Vienna, Austria.

Tonkin, J. D., D. M. Merritt, J. D. Olden, L. V. Reynolds, & D. A. Lytle, 2018. Flow regime alteration degrades ecological networks in riparian ecosystems. Nature Ecology and Evolution 2: 86–93.

Toporowska, M., B. Pawlik-Skowrońska, & A. Z. Wojtal, 2008. Epiphytic algae on Stratiotes aloides L., Potamogeton lucens L., Ceratophyllum demersum L. and Chara spp. in a macrophyte-dominated lake. Oceanological and Hydrobiological Studies 37: 51–63.

Trachsel, M., M. Grosjean, I. Larocque-tobler, M. Schwikowski, A. Blass, & M. Sturm, 2010. Quantitative summer temperature reconstruction derived from a combined biogenic Si and chironomid record from varved sediments of Lake Silvaplana (south-eastern Swiss Alps) back to AD 1177. Quaternary Science Reviews 29: 2719–2730.

Tréguer, P. J., & C. L. De La Rocha, 2013. The World Ocean Silica Cycle. Annual Review of Marine Science 5: 477–501.

Turner, R. E., N. Qureshi, N. N. Rabalais, Q. Dortch, D. Justic, R. F. Shaw, & J. Cope, 1998. Fluctuating Silicate : Nitrate Ratios and Coastal Plankton Food Webs. Proceedings of the National Academy of Sciences of the United States of America 95: 13048–13051.

Tzoraki, O., N. P. Nikolaidis, Y. Amaxidis, & N. T. Skoulikidis, 2007. In-stream biogeochemical processes of a temporary river. Environmental Science and Technology 41: 1225–1231.

Uehlinger, U., 2006. Annual cycle and inter-annual variability of gross primary production and ecosystem respiration in a floodprone river during a 15-year period. Freshwater Biology 51: 938–950.

Ulseth, A. J., E. Bertuzzo, G. A. Singer, J. Schelker, & T. J. Battin, 2018. Climate-Induced Changes in Spring Snowmelt Impact Ecosystem Metabolism and Carbon Fluxes in an Alpine Stream Network. Ecosystems 21: 373–390.

Vadeboncoeur, Y., & A. D. Steinman, 2002. Periphyton Function in Lake Ecosystems. The Scientific World JOURNAL 2: 1449–1468.

Valderrama, J. C., 1981. The simultaneous analysis of total nitrogen and total phosphorus in natural waters. Marine Chemistry 10: 109–122.

Valerio, G., M. Pilotti, S. Barontini, & B. Leoni, 2015. Sensitivity of the multiannual thermal

dynamics of a deep pre-alpine lake to climatic change. Hydrological Processes 29: 767–779.

Van Cappellen, P., 2003. Biomineralization and Global Biogeochemical Cycles. Reviews in Mineralogy and Geochemistry 54: 357–381.

Van Damme, S., D. Frank, T. Micky, B. Olivier, S. Eric, G. Britta, V. C. Oswald, & M. Patrick, 2009. Tidal exchange between a freshwater tidal marsh and an impacted estuary: the Scheldt estuary, Belgium. Estuarine, Coastal and Shelf Science 85: 197–207.

Van Dokkum, H. P., J. H. J. Hulskotte, K. J. M. Kramer, & J. Wilmot, 2004. Emission, Fate and Effects of Soluble Silicates (Waterglass) in the Aquatic Environment. Environmental Science and Technology 38: 515–521.

Vandevenne, F., E. Struyf, W. Clymans, & P. Meire, 2012. Agricultural silica harvest: have human created a new loop in the global silica cycle?. Front Ecol Environ 10(5): 243–248.

Verburg, P., J. Horrox, E. Chaney, J. C. Rutherford, J. M. Quinn, & R. J. Wilcock, 2013. Nutrient ratios, differential retention, and the effect on nutrient limitation in a deep oligotrophic lake. Hydrobiologia 718: 119–130.

Viaroli, P., 2017. I corsi d'acqua nell'Antropocene: processi e servizi ecosistemici, deterioramento e riqualificazione. Biologia Ambientale 31: 1–8.

Viaroli, P., R. Azzoni, M. Bartoli, P. Iacumin, N. Salmaso, & D. Nizzoli, 2018. Persistence of meromixis and its effects on redox conditions and trophic status in Lake Idro (Southern Alps, Italy). Hydrobiologia 824: 51–69.

Viaroli, P., M. Bartoli, C. Bondavalli, R. R. Christian, G. Giordani, & M. Naldi, 1996. Macrophyte communities and their impact on benthic fluxes of oxygen, sulphide and nutrients in shallow eutrophic environments. Hydrobiologia 329: 105–119.

Viaroli, P., M. Bartoli, G. Giordani, M. Naldi, S. Orfanidis, & J. M. Zaldivar, 2008. Community shifts, alternative stable states, biogeochemical controls and feedbacks in eutrophic coastal lagoons: a brief overview. Aquatic Conservation: Marine and Freshwater Ecosystems 18: S105–S117.

Viaroli, P., D. Nizzoli, M. Pinardi, G. Rossetti, & M. Bartoli, 2013. Factors Affecting Dissolved Silica Concentrations, and DSi and DIN Stoichiometry in a Human Impacted Watershed (Po River, Italy). Silicon 5: 101–114.

Vollenweider, R. A., & J. J. Kerekes, 1982. Eutrophication of Waters: Monitoring, Assessment and Control. OECD, Paris.

von Schiller, D., V. Acuña, D. Graeber, E. Martí, M. Ribot, S. Sabater, X. Timoner, & K. Tockner, 2011. Contraction, fragmentation and expansion dynamics determine nutrient availability in a Mediterranean forest stream. Aquatic Sciences 73: 485–497.

von Schiller, D., S. Bernal, C. N. Dahm, & E. Martí, 2017. Nutrient and Organic Matter Dynamics in Intermittent Rivers and Ephemeral Streams. Intermittent Rivers and Ephemeral Streams. Academic Press: 135–160.

von Schiller, D., D. Graeber, M. Ribot, X. Timoner, V. Acuña, E. Martí, S. Sabater, & K. Tockner, 2015. Hydrological transitions drive dissolved organic matter quantity and composition in a temporary Mediterranean stream. Biogeochemistry 123: 429–446.

Wagener, S. M., M. W. Oswood, & J. P. Schimel, 1998. Rivers and Soils: Parallels in Carbon and Nutrient Processing. BioScience 48: 104–108.

Wedepohl, K. H., 1995. The composition of the continental crust. Geochimica et Cosmochimica Acta 59: 1217–1232.

Wetzel, R. G., & G. E. Likens, 1991. Limnological Analyses. Lakes and Reservoirs: Research and Management. New York.

White, A. F., & A. E. Blum, 1995. Effects of climate on chemical weathering in watersheds. Water-rock interaction. Proc. symposium, Vladivostok, 1995 59: 57–60.

Xing, W., H. Wu, B. Hao, & G. Liu, 2013. Stoichiometric characteristics and responses of submerged macrophytes to eutrophication in lakes along the middle and lower reaches of the Yangtze River. Ecological Engineering 54: 16–21.

Ylla, I., I. Sanpera-Calbet, E. Vázquez, A. M. Romaní, I. Muñoz, A. Butturini, & S. Sabater, 2010. Organic matter availability during pre- and post-drought periods in a Mediterranean stream In Stevenson, R. J., & S. Sabater (eds), Global Change and River Ecosystems—Implications for Structure, Function and Ecosystem Services. Springer, Dordrecht: 217–232.

Zadereev, E. S., B. Boehrer, & R. D. Gulati, 2017. Introduction: Meromictic Lakes, Their Terminology and Geographic Distribution In Gulati, R., E. Zadereev, & A. Degermendzhi (eds), Ecology of Meromictic Lakes. Ecological Studies. Springer, Cham: 1–11.

Zhu, H., C. Wang, P. Wang, J. Hou, J. Qian, Y. Ao, & C. Liu, 2016. Speciation of potentially mobile Si in Yangtze Estuary surface sediments: estimates using a modified sequential extraction technique. Environmental Science and Pollution Research 23: 18928–18941.

Zohary, T., & I. Ostrovsky, 2011. Ecological impacts of excessive water level fluctuations in stratified freshwater lakes. Inland Waters 1:1: 47–59.

6. Acknowledgements

This study was conducted at the University of Parma, Department of Chemistry, Life Sciences and Environmental Sustainability. Chapter 2 and 3 have been supported by the CARIPLO 2015 grant "ISEO: Improving the lake Status from Eutrophy towards Oligotrophy". In this project I had the pleasure to collaborate with Dr. Michael Hupfer (IGB, Leibniz-Institute of Freshwater Ecology and Inland Fisheries), who deployed and handled sediment traps, quantified P and N of the settled material and kindly provided dried materials for further analyses of BSi. In addition, Dr. Hupfer made possible the sampling of deep sediment cores I used to estimate the nutrient budgets in Lake Iseo. The collaboration with Dr. Marco Pilotti and Dr. Giulia Valerio (DICATAM, University of Brescia, Italy) was profitable and pleasant, in particular I'm grateful for the provision of information and data on the Lake Iseo physics. Chapter 4 has been supported by the PRIN 2015 grant "NOACQUA – responses of communities and processes in intermittent rivers". I would like to express my gratitude to Professor Pierluigi Viaroli for making this thesis possible and to be a wise guide as supervisor of this journey. I would like to express my deepest gratitude to my PhD co-supervisor Prof. Daniele Nizzoli, who patiently and friendly guided me (almost daily) over the last three years. Working with him has been easy and he taught me a lot about aquatic biogeochemistry.

Big thanks to all the colleagues and friends in the department, who created an atmosphere where it was easy and fun to work.

Finally, the deepest gratitude to my family and my girlfriend, who never lost hope and gave me the best support I could have ever hoped for.